CONF-7906180

Proceedings of the Workshop on the Modification of the Upper Atmosphere by Satellite Power System (SPS) Propulsion Effluents

La Jolla Institute
La Jolla, California
June 25-27, 1979

Sponsored by:
U.S. Department of Energy
Office of Energy Research
Satellite Power System Project Division

Under Contract 31-109-38-5033

June 1980

DOE/NASA
Satellite Power System
Concept Development
and
Evaluation Program

DISCLAIMER

NOTICE

This report was prepared as an account of work sponsored by the United States Government. Neither the United States nor the United States Department of Energy, nor any of their employees, makes any warranty, express or implied, or assumes any legal liability or responsibility for the accuracy, completeness, or usefulness of any information, apparatus, product, or process disclosed, or represents that its use would not infringe privately owned rights. Reference herein to any specific commercial product, process, or service by trade name, mark, manufacturer, or otherwise, does not necessarily constitute or imply its endorsement, recommendation, or favoring by the United States Government or any agency thereof. The views and opinions of authors expressed herein do not necessarily state or reflect those of the United States Government or any agency thereof.

Available from:

National Technical Information Service (NTIS)
U.S. Department of Commerce
5285 Port Royal Road
Springfield, Virginia 22161

Price: Printed Copy: $10.00
Microfiche: $4.00

CONF-7906180
Dist Category UC-13

Proceedings of the Workshop on the Modification of the Upper Atmosphere by Satellite Power System (SPS) Propulsion Effluents

La Jolla Institute
La Jolla, California
June 25-27, 1979

Master

Prepared for:
U.S. Department of Energy
Office of Energy Research
Satellite Power System Project Division
Washington, D.C. 20585

Prepared by:
Ernest Bauer
La Jolla Institute
La Jolla, California
Under Contract 31-109-38-5033

June 1980

DOE/NASA
Satellite Power System
Concept Development
and
Evaluation Program

THIS PAGE

WAS INTENTIONALLY

LEFT BLANK

FOREWORD

The Satellite Power System (SPS) is a concept for obtaining baseload, i. e., continuous, electric power from the sun. It involves placing large arrays of photovoltaic cells in geostationary earth orbit, where they would receive continuous illumination by the sun, except for periods of as much as 40 minutes per night near the equinoxes, when the arrays would be in the earth's shadow. The power would be transmitted to the ground using microwave beams, according to the reference system concept.

The scale of the reference system is very large, involving 5-GW power units in space (by comparison, a present day nuclear power reactor produces about 1 GW). One 5-GW power satellite would have a solar collector array of area 5 x 10 km and a mass of 37,000 - 50,000 metric tons in orbit; the microwave receiving antenna on the ground would cover a 10 x 13 km ellipse. The reference concept presumes that two satellites would be built each year between 2000 and 2030 to provide some 25% of total U. S. electric power needs at that time.

Environmental impact studies are divided into five major tasks, namely:

1 - Health and ecological effects of microwave radiation

2 - Other effects on health and the environment

3 - Effects on the atmosphere

4 - Effects on communication systems that use the ionosphere

5 - Electromagnetic compatibility and radio frequency interference.

The present study is part of Task III. The main effects considered result from space transportation operations -- in particular the injection by rocket engines of water and hydrogen between 70 km altitude and geostationary earth orbit (36,000 km radius) -- and with the injection of argon ion beams into the plasmasphere at the higher altitudes. The object of the present study is to identify atmospheric research needs, including both theory and experiment, for the evaluation of upper atmospheric environmental effects due to SPS construction and deployment. A list of participants in the workshop is given in Appendix A.

THIS PAGE

WAS INTENTIONALLY

LEFT BLANK

TABLE OF CONTENTS

LIST OF FIGURES

LIST OF TABLES

ABSTRACT

This report presents results of a workshop held in June, 1979, to identify research needs for evaluating environmental impacts on the upper atmosphere (here defined as greater than 70 km) due to Satellite Power System (SPS) transport, i.e., propulsion and reentry. The substantial injections of water and hydrogen therefrom may lead to global-scale regions of reduced ionization in the ionospheric F-Region that may have a serious impact on worldwide HF radio communications; and the resulting possibly significant increases in mesospheric humidity and probable cloudiness could affect climate and remote sensing from satellites. The large injections of argon ions of kilovolt energy between low earth orbit and geostationary orbit may alter substantially the trapped radiation environment of the magnetosphere and thus the hazard for personnel and electronic equipment.

During the workshop it became clear that the highest priority for SPS environmental assessment goes to theoretical studies needed before acceptable atmospheric experiments can be designed.

Problems to be addressed include: the extent, magnitude, and variability of the predicted depletion in F-region ionization together with descriptions of water and hydrogen injections into the atmosphere characteristic of SPS vehicles and flight profiles; the long-term variations in mesospheric humidity and cloudiness with and without SPS operations; and the description of condensation and evaporation processes of water exhausted from high-altitude rockets in order to predict mesospheric contrail formation and dissipation. Furthermore, in considering argon ion rocket transport to geosynchronous orbit, the stopping and lifetime of the argon ion beams and consequent changes in the radiation belts, especially as they affect spacecraft, should also be addressed.

ACKNOWLEDGEMENT

It gives me great pleasure to thank everybody who participated in this workshop for their enthusiastic and effective work. The participants not only cooperated during the initial telephone phase of the study and put in the long hours needed during the workshop but also provided a better than 90% response to the review draft which was circulated to them.

SUMMARY

In the context of reviewing the potential environmental impact of SPS construction and deployment on the upper atmosphere, the present study was designed to identify particular atmospheric experiments and theoretical studies which should be given high priority for support; it also served as a follow-up to the initial environmental impact workshops held at Argonne National Laboratory in August and September of 1978 (Brubaker, 1979; and Rote, 1978)*. The present study deals only with effects above 70 km where worldwide rather than localized effects are anticipated. The study was conducted by a panel of 27 scientists and engineers who met in La Jolla, CA, on 25-27 June 1979; the membership is listed in Appendix A. The approach used was to identify the injectants in different altitude regions and to review the anticipated impact of each (see Table S.1) in order to identify critical research requirements (see Table S.2). While emphasis was originally placed on the design of atmospheric experiments, it quickly became apparent that considerable theoretical study effort is needed before one designs dedicated atmospheric experiments.

The single most critical problem identified in the present study is the impact on global HF** radio propagation of a band of permanently depleted ionization in the F-region as a result of launch operations. Some of the hydrogen and water emitted from the exhaust of the second stage of the HLLV rocket in the 70-120 km altitude region diffuses upward and leads to the replacement of atomic O^+ ions with molecular ions H_2O^+ and OH^+. Molecular ions recombine with electrons much more rapidly than do atomic ions, and thus replacing atomic with molecular ions leads to a reduction in effective ionization. This effect is significant above 160-180 km only, as at lower altitudes the main natural atmospheric ions are molecular, NO^+ and O_2^+. The physical extent of the region could cover a band at the latitude of launch (28.5° for Cape Canaveral) of north-south extent of several thousand kilometers, extending around the globe at the latitude of injection. The effective ionization may be reduced by a factor of two at night and by 10-20% in the daytime.

The critical consequence of such a reduction in ionization is that it drastically reduces the available HF band that can be used for long-range radio communication at a time when this frequency band is already heavily overcommitted internationally (see Section 3.2.6 for a discussion, Section 5.2 for research recommendations, and item F.3 of Appendix F for a brief account of this problem).

Other problems associated with water and hydrogen releases involve the general enhancement in mesopheric humidity and cloudiness with, as opposed to without, SPS operations, including the possible production of long-lasting contrails. These changes may have some climatic impact and could impact

---

*References are listed in the bibliography, Appendix E.

**See Appendix C for a definition of abbreviations, acronyms, and specific technical terms used here.

Table S.1 Propulsion Injectants into the Upper Atmosphere

Injectant	Altitude Range	Effect	Impact
H_2O and H_2 from HLLV,2nd stage	70-120 km	1) Material diffusing upward produces a permanent "ionospheric hole" in F-region	a. Deleterious to global HF communications b. Ionospheric irregularities may affect SatCom?
		2) Enhances ambient water vapor and clouds; possibility of long-lasting contrails	a. Climatic effects? b. Deleterious to remote sensing?
		3) Increases density of upper atmosphere	Increases satellite drag?
NO due to reentry heating	70-90 km	4) Together with H_2O & H_2 may enhance airglow	?
		5) Together with H_2O & H_2 may affect VLF/ELF propagation	?
H_2O & H_2 from circularization deorbit etc burns of HLLV and POTV	500 km(LEO) also 36,000 km (GEO)	6) Some local density enhancement	?
		7) Local regions of reduced ionization	?
Ar ions of kev energy	LEO to GEO	8) Very large enhancement of ambient Ar can affect radiation belts, in particular radiation environment for personnel and electronics	Possible hazard?

Table S.2 Recommendations for Research.

1. F-Region Depletion.

1.1 Upward transport and photochemistry of H_2O and H_2: rate of transport and chemistry, relative significance of H_2O vs H_2

1.2 Laboratory study of dissociative recombination of H_2O^+ and OH^+

1.3 Spreading of tracers in the mesophere

1.4 Overall estimate of reduction in ionization:day/night variation, geometric extent of affected region, atmospheric variability; verify adequacy of prediction by comparison with observations (Skylab, LAGOPEDO, HEAO-C)

1.5 Ionospheric irregularities

2. H_2O,H_2,NO.

2.1 Water vapor in the mesosphere-long term trends

2.2 High-altitude clouds and contrails

2.3 Fate of injected H_2O and H_2 in different altitude ranges

2.4 Environmental effects of H_2O and H_2 injections (other than 1 above)

(2.5 Heterogeneous chemistry on ice crystals)

(2.6 NO production on reentry)

(2.7 Effects of H_2O, H_2, NO on lower ionosphere)

3. Ar^+ Injections.

3.1 Fate of Ar^+

3.2 Ion energization and HZEs

3.3 Alteration of trapped radiation: effects on radiation environment of spacecraft

remote sensing from satellites. Studies called for in this context include long-term measurements of water vapor concentrations and cloudiness in the mesosphere, and the description of condensation and evaporation of water vapor emitted in high-altitude rocket exhausts.

The injection of water and hydrogen, as well as that of nitric oxide (NO) due to atmospheric heating from reentering spacecraft, may enhance the airglow and may also affect the long-range propagation of relatively low frequency radio waves (VLF and ELF) by changing the ion chemistry in the ionospheric D-region.

Enhancing the hydrogen concentration in the upper atmosphere will increase the drag on low-altitude orbiting satellites; the significance of this effect is not yet established.

In going from a low-altitude parking orbit to geosynchronous orbit, the current SPS concept calls for the use of argon ion engines. The quantity of argon injected into the atmosphere above 500 km is very large indeed, relative to the ambient atmospheric mass, and it is not yet established how rapidly the ion beams will be stopped or what the lifetime and energy loss and gain processes of the ions are. The injection could lead to significant changes in the earth's radiation belts, possible changing the radiation environment of spacecraft in orbit.

The structure of the report is the following. Section 1 reviews the injections of different materials in different altitude ranges, amplifying Table S.1 and attempting a quantitative estimate of the relative significance of the different injectants. It also reviews how the study was conducted. Section 2 treats problems due to the very large propulsion injections in the 70-120 km altitude region. Section 3 discusses the general problem of hydrogen and water injections due to SPS in the ionosphere. Section 4 reviews effects on the magnetosphere in the passage from the parking orbit (LEO = Low Earth Orbit, at 500 km) to geosynchronous orbit (GEO at 36,000-km altitude, or 6.5 earth radii away). Section 5 presents the conclusions and recommendations of the study. Appendix A lists the membership of the present workshop, Appendix B gives a brief summary of the SPS transportation system, Appendix C defines abbreviations and acronyms used here, and other appendices furnish various technical details.

1 INTRODUCTION

1.1 THE CONTEXT OF THE PRESENT STUDY

The Satellite Power System (SPS) implies a very large space construction project, involving the annual construction in orbit over a 30-year period of two arrays of solar cells, each roughly 5 x 10 km in dimension and weighing 35,000-50,000 metric tons. Each array would provide 5 GW of baseload electric power, which would be beamed to the ground, using 2.45 GHz microwaves. Over a 30-year construction period this effort would provide 60 such satellites, supplying some 20-25% of U.S. anticipated electric power needs by the year 2030. The total propulsion effluents injected into the upper atmosphere per year would include 140,000 metric tons of hydrogen, 800,000 of oxygen and 25,000 of argon, and 6 x 10^{16} joules of energy.

In the context of reviewing environmental impacts on the upper atmosphere, the present study is designed to identify research needs, in particular for atmospheric experiments as a part of currently ongoing research, and to follow up on workshops held at Argonne National Laboratory in August and September, 1978 (Rote, 1978, and Brubaker, 1979). Effects of microwaves, effects due to launch and construction operations on the surface, and effects on communication systems are not addressed here.

It became apparent during the workshop that under the constraints of present understanding and the time requirements for the current SPS assessment program, certain critical questions in phenomenology must be analyzed in more detail, which will require a lot of time and funds, before one can design and execute useful atmospheric experiments. Thus the orientation of the study changed to emphasize these analytical requirements.

1.2 THE SIGNIFICANCE OF DIFFERENT INJECTIONS

The atmospheric disturbances considered cover a wide range of materials and of altitudes; see Table 1* for the injection due to each element of the system and Appendix B for more details of the scenario; also RSR, 1978. The principal material injectants in the upper atmosphere are H_2O and H_2 from chemical rocket exhausts, NO due to reentry heating of air, and argon ions in the keV energy range with their neutralizing electrons from electrical propulsion. Material injections, but not necessarily their atmospheric effects, occur in three general atmospheric domains that are described in Table 2. Domain A, 70-120 km, corresponds to the main burn of the Heavy Lift Launch Vehicle (HLLV) second stage, and to reentry heating. Domain B corresponds to Low Earth Orbit (LEO), approximately 500 km, the circularization and deorbit burns of the HLLV, while Domain C corresponds to transport from LEO to Geostationary Earth Orbit (GEO), at approximately 36,000

*Tables appear consecutively at the end of this section.

km from the surface of the earth. Figure 1 shows the altitude distribution of injectants from HLLV, and Table 3 gives the overall injection rates in each domain.

To estimate the importance of a given injectant in a specific domain requires not just the injection rate and the ambient burden in the domain but also a characteristic residence time for the different injectants in the various domains. Some initial estimates of residence times are listed in Table 2. For water they are typically characteristic times for transport out of the domain (note the large effects of condensation!), while for NO where photochemical destruction of odd nitrogen (N, NO, NO_2) is more rapid than transport, this sets the limit. In Domain C the energy equilibration time may be used, but here in particular there are large uncertainties because the phenomenology is not well understood (see Sections 4.3 and 4.4). Both the concepts and the numerical values must be examined and modified as necessary (see also Kellogg, 1964).

Table 4 represents an initial attempt to describe the loading of the atmospheric injections in each domain in terms of a dimensionless "Perturbation Factor" or PF which is defined as

$$PF = \frac{\text{(expected concentration change)}}{\text{(ambient concentration)}} \qquad (1)$$

In order to estimate a numerical value for the PF, some estimate of the expected concentration change resulting from the specified injection must be made. To lowest order, the concentration change may be estimated by the expression: (injection rate) x (residence time), in which the injection rate is given in units of mass/unit volume/unit time. An equivalent expression for the lowest-order PF is easily seen to be (total mass injection rate into domain) x (residence time in domain)/(total ambient loading in domain); this latter expression is used throughout the remainder of this report.

The concept of a PF is useful in the limited context of suggesting the general areas in which problems may be expected. (Thus the same methodology shows that at altitudes below 70 km or so, only local rather than global effects may be expected; see Brubaker, 1979). Values of PF as large as a few percent indicate that effects of a given injection should be looked for, while PF values in excess of unity raise a warning flag. The detailed numerical values are generally not significant, partly because the numerical value of the characteristic or residence time is generally not well known and partly because details of the chemistry, etc., limit the applicability of the concept. (Thus we do not list separate PF values for H_2O and H_2.)

The following points should be noted in connection with Tables 1-4:

(a) The ambient loadings of injectants as used here are presented in Appendix D.

(b) The atmospheric injections are large on an absolute scale because of the overall scale of a 5-GW SPS unit system, which corresponds to an orbital mass of 35,000-50,000 metric tons. Note that the overall effect of injectants tends to be significant on a global, rather than on a regional or local scale only above 75 km because of the very large mass of the lower atmosphere.

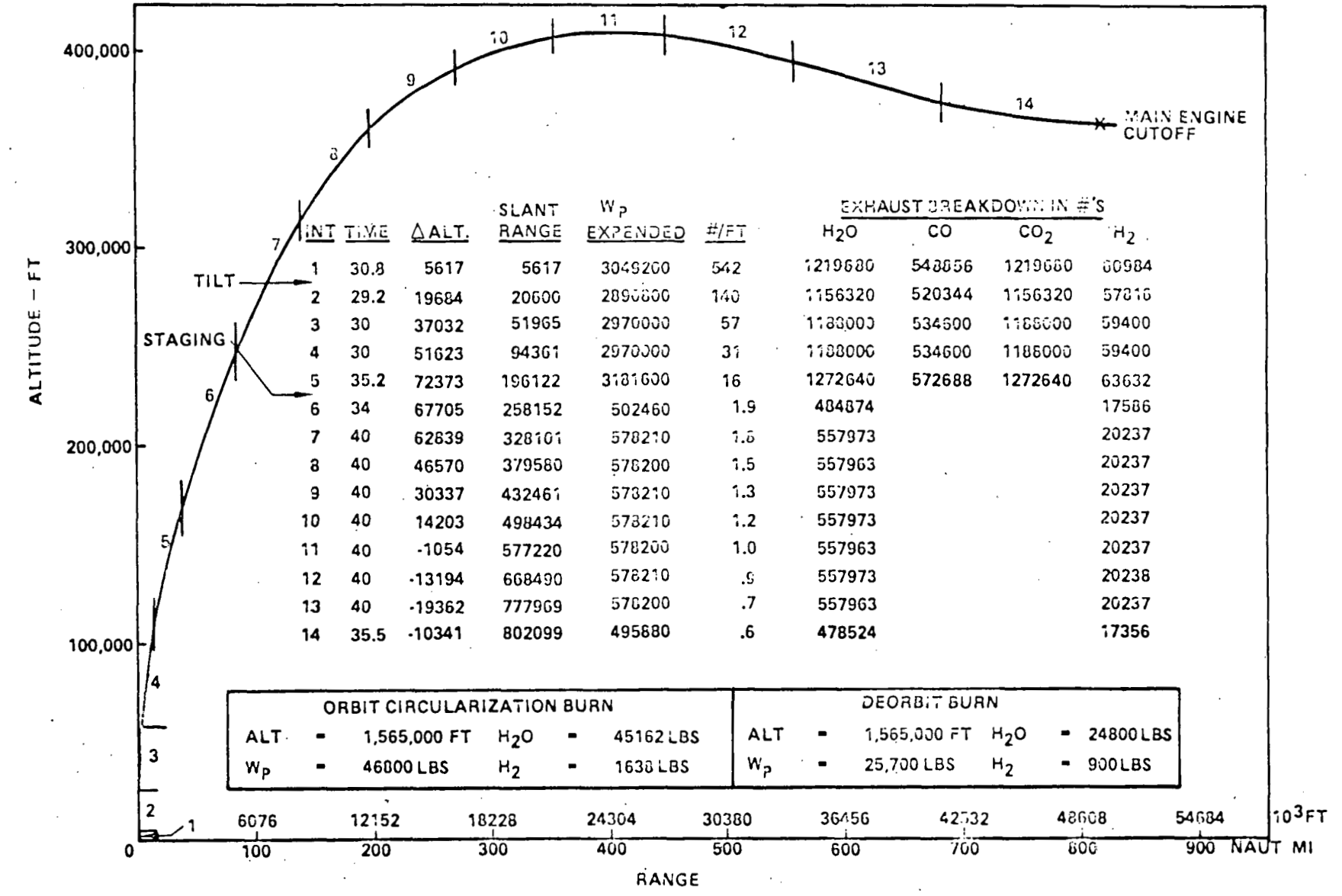

INT	TIME	ΔALT.	SLANT RANGE	W_P EXPENDED	#/FT	EXHAUST BREAKDOWN IN #'S H_2O	CO	CO_2	H_2
1	30.8	5617	5617	3049200	542	1219680	548856	1219680	60984
2	29.2	19684	20600	2896800	140	1156320	520344	1156320	57816
3	30	37032	51965	2970000	57	1188000	534600	1188000	59400
4	30	51623	94361	2970000	31	1188000	534600	1188000	59400
5	35.2	72373	196122	3181600	16	1272640	572688	1272640	63632
6	34	67705	258152	502460	1.9	484874			17586
7	40	62839	328101	578210	1.8	557973			20237
8	40	46570	379580	578200	1.5	557963			20237
9	40	30337	432461	578210	1.3	557973			20237
10	40	14203	498434	578210	1.2	557973			20237
11	40	-1054	577220	578200	1.0	557963			20237
12	40	-13194	668490	578210	.9	557973			20238
13	40	-19362	777969	578200	.7	557963			20237
14	35.5	-10341	802099	495680	.6	478524			17356

ORBIT CIRCULARIZATION BURN						DEORBIT BURN					
ALT	=	1,565,000 FT	H_2O	=	45162 LBS	ALT	=	1,565,000 FT	H_2O	=	24800 LBS
W_P	=	46000 LBS	H_2	=	1638 LBS	W_P	=	25,700 LBS	H_2	=	900 LBS

ALTERNATE TRAJECTORIES CAN BE CONSIDERED WITH LOWER INSERTION ALTITUDES IF ENVIRONMENTAL CONSIDERATIONS DEEM NECESSARY

Figure 1. SPS Heavy Lift Launch Vehicle Trajectory and Exhaust Products Data
[Source: RSR, 1978]

(c) The HLLV is approximately five times the size of the Space Shuttle, or comparable to a Boeing 747 airplane. The other vehicles are comparable or even larger in scale. Thus the (electrically propelled) Cargo Orbital Transfer Vehicle (COTV) is roughly 1 km in linear dimension and carries a 4000-ton payload from Low Earth Orbit (LEO) into Geostationary Earth Orbit (GEO). The Personnel Orbital Transfer Vehicle (POTV) carries some 160 passengers plus priority cargo from LEO to GEO; see Appendix B for details of the scenario.

(d) The reference system design of RSR, 1978, as considered here has two options, based on the use of Si and GaAℓAs solar (photovoltaic) cells, developed by Boeing and Rockwell, respectively. The Boeing/Si technology is more conservative and heavier than the Rockwell/GaAℓAs concept.

(e) The injection of H_2O and H_2 into the upper ionosphere can be very significant because these molecules produce molecular ions by charge transfer, or ion-molecule reactions with the ambient atmospheric O^+ ions, and molecular ions recombine with electrons very much faster than atomic ions, by a factor 10^4-10^5. The reason for this phenomenon is that dissociative recombination is very much faster than radiative recombination, or than three-body recombination at the low densities in question. Below 160 km the predominant atmospheric ions are O_2^+ and NO^+, which themselves recombine dissociatively with electrons, so that at these lower altitudes the change is not so obvious. However, the total electron content of the global ionosphere is of order 10^{32}, and thus the injection of 10^{32}-10^{33} H atoms, as H_2O and H_2 (see Table 3), could have very significant effects on the ionosphere, depending on the rate of removal of the injected molecules and on how fast the ionosphere responds to such perturbations (see e.g., Mendillo, et al., 1975a, b, 1979; and Zinn, et al., 1978, 1979).

(f) It is evident that the numerical values of the perturbation factor PF as quoted in Table 4 are not necessarily correct; however, the relative magnitudes are significant. The injection of water in Domain A is certainly important, and the potential importance of condensation in removing water from the ionsphere is evident. The characteristic time used in Domain C may not be appropriate, but the injection of hydrogen-containing species and of argon must be considered in this altitude region.

(g) From Table 4 we see that even the very large energy deposition due to the kinetic energy of argon ions in the magnetosphere is not important on a global scale in that the PF is very much less than one. However, local effects can be important in a variety of altitude ranges. Some possible effects due to the HLLV second stage are examined briefly in Section 2.7. (Note that the ionospheric effects of microwaves, including ionospheric heating, are being considered elsewhere, under Task IV.)

(h) Reference should be made to the early study of Kellogg, 1964.

1.3 APPROACH

The approach adopted in the present study was the following. Technically, we began by identifying injectants in the different domains and characterizing their significance (see Section 1.2, especially Tables 1, 3, and 4). Then we outlined the relevant phenomenology to pinpoint areas needing

further study in order to reduce uncertainties in the environmental impact of the SPS transportation system to acceptable levels. The initial object was to identify atmospheric experiments in this context, but many current questions first need theoretical answers before one goes to the complication of atmospheric experiments.

The organizational plan was the following, designed to produce results quickly and with optimum input from a wide range of experts. A strawman draft (Bauer, 1979) was prepared to set up the structure of the study and to define questions to be addressed. The document was circulated to the panel a month before the workshop, and during the workshop the various experts were asked to revise specific sections of the draft. Immediately afterwards a review draft was prepared and sent to the participants and to the other people listed in Appendix A. The final report was based on the responses received, which include a number of additional contributions. Table 5 lists the final task assignments as they were carried out, and Table 6 outlines the overall schedule of the study.

TABLE 1

SPS INJECTIONS INTO THE UPPER ATMOSPHERE[1,2]

Source	Number of flights per year (GA)	(Si)	Injection Height (km)	Magnitude/unit source (in 10^3 kg)	Data Source
HLLV, second stage main burn	225	375	76-120 ("Domain A")	2210 (H_2O) + 80 (H_2)	RSR,1978,p.52,74
HHLV, circularization and de-orbit burns	225	375	Low Earth Orbit (LEO, $\sim$ 500 km) ("Domain B")	32 (H_2O) + 1.1 (H_2)	"
HHLV, reentry	225	375	mesosphere	300 (NO)	Park, private communication
POTV	17	12	LEO to GEO-synchronous orbit (GEO) ("Domain C")	440 (H_2O) + 16 (H_2)	RSR,1978,p.55
COTV	22	30	LEO to GEO	(Ga): I_{sp} = 13000 sec (3.5 keV Ar^+) 140 (Ar) + 1.2 x 10^{15} joule+ 68 (H_2O) + 2.4 (H_2)	RSR,1978,pp.56-58, B-100
				(S_i): I_{sp} = 7000 sec (1 keV Ar^+) 660 (Ar) + 1.6 x 10^{15} joule+ 300 (H_2O) + 11 (H_2)	"

TABLE 1 - SPS INJECTIONS - Continued.

Structural debris: if 1% of total mass brought into GEO is lost per year, either from LEO or from GEO, taking the amount and proportions from RSR,1978,p.59, some 4×10^5 kg/year will result from reentry burnup and presumably be deposited in the mesosphere. This is small compared with the natural meteoroid infall of order 4×10^7 kg/year.

Microwaves. 2% increase in heating rate in the mesosphere and 3% in the stratosphere, both locally over the rectenna (Brubaker & Rote, Oct. 1978). Small on a global basis. Ionospheric heating being studied under Task IV.

---

[1] See Appendix B for more details of the scenario.

[2] Note that the figures in this scenario are slightly different from the Boeing/Si scenario used in Table 4. The present Si (heavy) scenario of COTV + POTV flights calls for annual use of 2400 metric tons of hydrogen (vs 2100 for Boeing) and 20,000 metric tons of argon (vs 25,000).

COTV = Cargo Orbital Transfer Vehicle; keV Ar^+ ion engine, H_2-O_2 attitude control system. LEO to GEO.

GEO = Geosynchronous Orbit ($\sim 6.6\ R_e$ from center of earth, 36,000 km from surface of earth).

HHLV = Heavy Lift Launch Vehicle (surface to LEO).

POTV = Personnel Orbital Transfer Vehicle (H_2-O_2 engine; LEO to GEO).

TABLE 2

ATMOSPHERIC DOMAINS

Domain	Altitude Range (km)	Transport Time (out of domain) Deorbit delays not included - see Section 3.1.3		Injection	Physics of Domain
A	70 - 120	10 days for H_2O or H_2[1]; 3 days for NO (photochemistry		HHLV second stage main burn-H_2O/H_2; HHLV reentry-NO	Mesosphere and lower Thermo-
B	450 - 500	ice crystals: 5 minutes[2] water vapor: 2 hours[2] H_2 gas : 6 hours[2]		LEO:HLLV circularization and de-orbit	Thermosphere/ F-region
C-1	500 - 1000	1-10 days[3]	POTV[5] (H_2O/H_2) 70%	COTV (Ar^+ & H_2O/H_2)-10% of total burn	Upper Thermosphere.
C-2	1000 - plasmapause (L=4 to 4.5)		0%	COTV & POTV-70% of total burn	Plasmasphere[6]
C-3	plasmapause to GEO		30%	COTV & POTV-20%[4]	Outer Magneto-sphere

[1] Diffusion time from 95-70 km, assuming K = 2×10^6 cm^2/sec.

[2] Estimates of J. Zinn, April 1979, from a diffusion calculation: downward transport to 120 km.

[3] Very uncertain. Values up to 100 days are possible. Also, values for H, Ar, and energy are not necessarily the same.

[4] For COTV it is assumed that the emissions of H_2O/H_2 (for attitude control) are distributed in the same way as the main propulsion emissions of Ar and energy.

[5] See Section 3.1.3 for POTV.

[6] We may assume a number density of 10^3-10^4/cm^3 in the plasmasphere, with a mean kinetic energy per particle of 0.1-1 eV.

[7] The outer magnetosphere is filled with a very diffuse plasma, with perhaps 1 proton/cm^3 of energy 1-10 keV per particle and neutralizing electrons of mean kinetic energy 0.5-5 keV per particle.

TABLE 3

ATMOSPHERIC INJECTION RATES FOR EACH DOMAIN[1]

Domain	Injectant	Injection Rate (kg/yr)	Injection Rate atoms/yr	Ambient Loading of Material (see Appendix C for an explanation of how the numbers are obtained)
A (70-120 km)	$H(H_2O/H_2)$ (75% as H_2O)	1.2×10^{8}	7.4×10^{34} (H-atoms)	3.3×10^{34} (H-atoms, present mainly as H_2O
	NO	1×10^{8}	2×10^{33}	3.5×10^{33}
B	$H(H_2O/H_2)$	1.8×10^{6}	1.06×10^{33} (H-atoms)	1.05×10^{30} (present mainly as atomic H)
C (500-35,000 km)	$H(H_2O/H_2)$	2.1×10^{6}	1.3×10^{33} (H-atoms)	1.6×10^{32} H-atoms, 500-1000 km 1.2×10^{32} H-atoms, 1000 km to plasmapause (L=4) 3×10^{29} H-atoms, L=4 to L=7
	$Ar(=Ar^{+}+e^{-})$	2.5×10^{7}	3.7×10^{32}	4.4×10^{25}
	Energy 1 keV/Ar^{+}	6.1×10^{16} joules/year		3×10^{20} joule total geomagnetic field energy: the annual dissipation in substorms is (10^{-4}-10^{-3}) times this. (see Appendix D, Item D.5)

[1]The Boeing/Si scenario is used here, with the annual injection rates from RSR, 1978, p. B-100. The Rockwell/Ga scenario calls for smaller mass and energy injection rates (about 2/3).

TABLE 4

PERTURBATION FACTOR, PF OF EQ. 1, FOR EACH DOMAIN[2]

Domain[2]	Injectant	Injection Rate (mol/yr)[3]	Residence Time[2]	Ambient Loading (mol)[4]	PF[1]
A (70-120 km)	H_2O/H_2	7.4×10^{34} (H-atoms)	10 days	3.3×10^{34} (H-atoms)	.07
	NO	2×10^{33}	4 days	3.5×10^{32}	.05
B (450-600 km)	H_2O/H_2	1×10^{33} (H-atoms)	ice: 5 minutes	1×10^{30}	.01
			water: 2 hours		.02
C LEO TO GEO	H_2O/H_2	1.3×10^{33} (H-atoms)	1 - 10 days	4.4×10^{32}	.01-0.1
	Ar^+	3.7×10^{32}		4.4×10^{25}	>> 1 ($\sim 10^5$)
	Energy	6.1×10^{16} joule/yr		3×10^{20} joule	<< 1

[1]Perturbation Factor, PF = (Injection Rate)x(Residence Time)/(Ambient Loading). This is a dimensionless quantity which gives a measure of the significance of an injectant in a given domain. The numbers are only suggestive because the concept of "Residence Time" is not always well defined - see text below Eq. 1 in Section 1.2.

[2]See Table 2 for more details.

[3]See Table 3 for more details.

[4]See Appendix D for details.

TABLE 5

TASK ASSIGNMENTS FOR THE WORKSHOP

2.2.2	NO Production on Reentry	Park*, Whitten
2.2.3	Construction Debris	Whitten*, Park, Vondrak
2.3	Water Vapor in the Mesosphere and Lower Thermosphere	Ellsaesser*, Sundararaman
2.4	High-Altitude Clouds	Ellsaesser*, Sundararaman, Turco
2.4.1	Noctilucent Clouds	Ellsaesser*, Sundararaman, Turco
2.4.2	Nacreous Clouds	Ellsaesser*, Sundararaman, Turco
2.5	Condensation in Rocket Exhausts	Mendillo*, Park, Bernhardt, Zinn
2.6	Spreading of Exhaust Clouds: Local, Regional, Zonal, Global Effects	Bernhardt*, Brubaker, Forbes, Bauer
2.7	Energy & Momentum Transfer due to Rocket Plumes	Forbes*, Brubaker, Sundararaman
2.8	Photochemical Effects	Turco*, Prasad, Garrett
2.9	Atmospheric Electricity: Conductivity in the Lower Ionosphere	Vondrak*, Fedder, Garrett
2.10	Listing of Potentially Important Phenomena	Vondrak*, Rote, Aikin, Whitten
2.11	Atmospheric Experiments:	
	A. Water Vapor in the Mesosphere	Sundararaman*, Ellsaesser, Turco
	B. Noctilucent Clouds	Sundararaman*, Ellsaesser, Turco
	C. NO Production on Reentry	Whitten*, Park
	D. Rocket Observations	Mendillo*, Pongratz
	E. Airglow	Zinn*, Turco, Prasad
	F. Cloud Dispersion	Bernhardt*, Brubaker, Forbes

TABLE 5 - TASK ASSIGNMENTS FOR THE WORKSHOP - Continued

	G. Mesospheric NO	Turco*, Prasad, Park
	H. Electric Conductivity	Vondrak*, Fedder, Garrett
	I. Other Experiments	Aikin*, Whitten, Forbes, Rote
3.1	Phenomenology of Hydrogen in the Upper Atmosphere	Zinn*, Aikin, Rote, McCormac
3.1.2	Fate of H_2O/H_2 injected in the Thermosphere	Zinn*, Aikin, Rote
3.1.3	Some Details of the Distribution of Propulsion Effluents	Park, Bauer (prepared after the workshop)
3.1.4	Effect of H_2O/H_2 Injections on Geocoronally Scattered Lyman -α and Lyman -β Radiation	Prasad, Forbes
3.2	Morphology of Perturbed Ionospheric Regions	Fedder*, Richmond, McCormac, Zinn
3.3	Effects on Satellite Drag	Curtis*, Forbes, Garrett
3.4	Other Phenomenology:	
3.4.1	Airglow	Turco*, Forbes, Zinn, Prasad
3.4.2	Condensation and Re-evaporation in Rocket Exhausts	Pongratz*, Mendillo, Prasad
3.5	Listing of Potentially Important Phenomena	Vondrak*, Rote, Mendillo, Zinn
3.6	Atmospheric Experiments:	
	A. Rocket Observations	Pongratz*, Mendillo, Simmons, Prasad
	B. Lagopedo-Type Releases	Fedder*, Pongratz, Bernhardt, McCormac
	C. Ionospheric Irregularities	Bernhardt*, Mendillo, Palmadesso, Richmond
	D. Other Experiments	Aikin*, Whitten, Forbes, Rote
4.2	Phenomenology of H_2O/H_2	Zinn*, Aikin, Chiu, Rote McCormac, Carlson

TABLE 5 - TASK ASSIGNMENTS FOR THE WORKSHOP - Continued

4.3	Injection of a kev Argon Plasma	Palmadesso*, Chiu, Curtis, Garrett, Cladis
4.4	Some Possible Effects	
4.4.1	Enhancement of Trapped Radiation	Chiu*, Carlson, Vondrak, Palmadesso , Cladis
4.4.2	Dumping of the Radiation Belts	Aikin*, Curtis, Fedder, Carlson
4.4.3	Depletion vs. Enhancement of the Radiation Belts	Curtis
4.4.4	Phenomenology associated with large space structures	Vondrak*, Garrett
4.5	Synthesis of Effects, and Possibly Important Phenomena	Chiu*, Vondrak, Rote, Richmond
4.6	Conceivable Atmospheric Experiments:	
	A. Injection of Gases, Plasmas and Beams	Pongratz*, Fedder
	B. The Relevance of SCATHA to SPS	Chiu*, Garrett, Carlson, Palmadesso , Pongratz, Cladis
	C. Firewheel and other relevant Experiments	Chiu*, Carlson, Garrett
	D. Starfish, and other past nuclear explosions	Palmadesso*, Zinn, McCormac
5.	Recommendations	Bauer, Carlson, Vondrak

Note: 1)The person whose name comes first with an * was the chairman with responsibility for coordinating the discussion, for making an oral presentation at the workshop, and for providing a revised writeup of the relevant section at the end of the workshop.

2)All the sections in Table 5 are found in the present report, but there has been some rearrangement, and some new material has been added.

TABLE 6

TIME SCHEDULE FOR STUDY

A. Overall Schedule

1 April 1979	-	Work began
1 May 1979	-	Panel established
1 June 1979	-	Straw man draft report to Panel Members
25-27 June 1979	-	3-day Workshop
30 July 1979	-	Revised Report to Panel Members
30 August 1979	-	Comments received from Panel Members by this date
4 September	-	Final report preparation begun
14 September	-	Report to Reviewers (very quick turnaround needed)
30 November 1979	-	Final Report due at Argonne National Laboratory

B. Outline of Workshop

1/2 day	-	General Introduction
1 day	-	Working groups (see Table 5) met separately to prepare their briefings to the panel as a whole, and their revised write-ups
3/4 day	-	Working group chairmen reported to the group as a whole (since there were some 30 separate presentations, this part of the program was very tight and over-ran its allocated time)
1/4 day	-	Summary of conclusions and recommendations

2 EFFECTS OF INJECTANTS IN THE 70-120-km ALTITUDE RANGE

2.1 INTRODUCTION

The injectants are discussed in Section 2.2. The ambient levels of water vapor and of noctilucent clouds are reviewed in Sections 2.3 and 2.4, respectively, since the predicted enhancement as described by PF = 0.07 (see Table 4) is so large that possible changes in both water vapor and clouds must be evaluated. We must know both the mean levels of these quantities and also their fluctuations, so as to be able to evaluate potential impacts. Condensation has been observed in rocket exhausts in this altitude range (see Benech and Dessens, 1974) as well as at high altitudes, which could give rise to a significant enhancement in mesospheric cloudiness, as discussed in Section 2.5.

The whole issue of condensation and re-evaporation in rocket exhausts is important from the standpoint of the absorption and, in particular, scattering of sunlight and earth shine, which affects the global climatology as well as optical remote sensing. Additionally, the issue is also critical for the overall effect of water injections, especially at the higher altitudes, near LEO; reference to Table 4 shows that water sediments out of Domain B much more rapidly if deposited in the atmosphere as an aerosol than as a gas, giving rise to a very much smaller perturbation factor or PF. The problem of condensation and re-evaporation was addressed by two groups (see items 2.5 and 3.4.1 of Table 5). A discussion also was given by P. Bernhardt after the workshop. These three discussions are presented verbatim as Section 2.5.

Section 2.6 treats the spreading of rocket exhausts, on various scales, which could be very important both as far as the impact and the experimental simulation of an injection are concerned. Rocket exhausts deposit a large amount of energy in the atmosphere: Would this activity be expected to produce any observable effects? This question is raised in Section 2.7. Photochemical effects, including enhancement or reduction in ionization, possible changes in ozone and other neutral species, and changes in airglow, are reviewed in Section 2.8, and changes in atmospheric conductivity related to these changes in ionization are treated in Section 2.9.

One very important effect of H_2 injections from the HLLV second stage burn is the ionospheric depletion associated with the formation of H_2O^+ and OH^+ ions in the F-region as a consequence of the upward diffusion of hydrogen from the 70-120-km altitude region. This problem is discussed in Sections 3.1 and, especially, 3.2.

The topics discussed above relate to phenomenology. The overall significance of these possible changes is reviewed in Section 2.10, and in the light of the phenomenology and of the significance of the effects a listing of atmospheric experiments that merit consideration is given in Section 2.11.

2.2 INJECTANTS

2.2.1 H_2O/H_2 Injections

The amounts and altitude profiles of injections are shown in Fig. 1 (see also Appendix B, Table B.2) and also in Tables 1, 3, and 4. To maximize the thrust per unit propellant from a rocket engine, many rocket engines are run fuel rich so that the effective molecular weight of the exhaust is relatively low. In the present case, approximately 30% of the hydrogen atoms in the exhaust are emitted as H_2 rather than as H_2O.

2.2.2 NO Production on Reentry (Park)

Every object reentering the earth's atmosphere is slowed down by friction, and the kinetic energy lost by the reentering body goes to heat up air to rather high temperatures. The amount of air heated depends upon the projected area of the body, its speed, the reentry time, and the ambient air density. Temperatures in excess of 2000 K are achieved, and at these temperatures some nitric oxide is produced, and "freezes in" as the air cools. For an entry vehicle of the size, mass, and shape of the HLLV, the amount of nitric oxide expected to be produced is approximately 22% of the mass of the vehicle. The NO produced will be distributed between 55 and 100 km in altitude, the peak being around 70 km (Rakich, Bailey, and Park, 1975; Park, 1979, to be published).

2.2.3 Construction Debris (Whitten)

During construction of the SPS satellites in space, there will certainly be some waste material or lost items. Even though a serious effort will be made to minimize any losses, yet, presumably, some of this material will reenter the earth's atmosphere. Small pieces will burn up on reentry, producing fine (micron or submicron sized) particles analogous to meteoritic dust, as well as a small amount of NO due to reentry heating. Large objects, such as Cosmos 954 or Skylab, may maintain their integrity during reentry, producing NO and a possible ground-level hazard. Other objects, such as large, light sheets of material with appropriate aerodynamic characteristics, could be expected to reach the earth's surface *without* ablation, giving rise to troublesome effects.

The structural material for the satellites will be largely graphite composite (see RSR, 1978, p. 58ff), which will burn up on reentry, but there will be a certain amount of Al and Si/SiO_2 that will presumably form small oxide particles. Regarding the quantity of material involved, lacking other information, it will be assumed here that 1% of the total mass of a 5-GW system is lost each year. From RSR, 1978, p. 59, this loss gives a mass injection rate of (3-5) x 10^5 kg/yr, perhaps half metal (Fe, Cu, etc.) and half stony (SiO_2, Al_2O_3). This quantity is small compared with the annual mass injection of meteoritic material, which is of the order of 4 x 10^7 kg/yr (see Park and Menees, 1978, p. 4033); thus the effect of such structural debris is probably negligible unless some exotic material such as teflon,

which is present in the debris but not in meteors, is deposited in the ablation region. The probable deposition of such materials and their possible effects are not known.

A recent paper (Kessler and Cour-Palais, 1978) estimated the potential for the formation of a permanent belt of satellite debris around the earth. As visualized in their study, it is highly probable that debris fragments may strike a large satellite in the next decade) some evidence indicates that this may already have occurred). Such an impact would produce many more fragments in a variety of orbital inclinations. According to their calculations, given the present launch rate and estimated population of existing satellites and debris, the near-earth orbital environment could be approaching a critical point around the year 2000 wherein such debris collisions would lead to a chain reaction type of process. The end result would be the creation of an artificial debris cloud around the earth. Not only would such a belt be a very real threat to an SPS and other satellites, but an SPS could exacerbate the situation. Although the conclusions of Kessler and Cour-Palais are somewhat tentative, they must be taken seriously as a possible environmental effect of global significance.

2.3 WATER VAPOR IN THE MESOSPHERE AND LOWER THERMOSPHERE (Ellsaesser)

At present there are very few measurements of the water vapor concentration in the mesosphere, most of which are rocket measurements at high latitudes (Arnold and Krankowsky, 1977; Rogers et al., 1977; and data from the AFGL SPIRE flight [J. S. Garing, AFGL, private communication]), suggesting a water vapor mixing ratio of 5 ppmv. Radford et al. (1977) using groundbased microwave radiometry, obtained a mixing ratio as high as 15 ppmv, but this seems much too high to understand on physical grounds. Figure 2 shows all presently available data.

The longest and most generally accepted series of H_2O observations above the tropopause are those of the MRF (British Meteorological Research Flights) and of Mastenbrook (1968, 1971, 1974). These indicate a decrease in mixing ratio for the first 1-3 km above the tropopause, both polar and tropical, to values of 3-5 ppmv (parts per million by volume, i.e., molecular rather than mass mixing ratio) near 19-20 km. Above 20 km there is a fairly consistent tendency toward both higher mixing ratios and greater uncertainty in the data. Mastenbrook (1974), Harries (1976), and Penndorf (1978) have all interpreted these and other observations as showing a constant mixing ratio from the lower stratosphere up to 28-35 km, with the suggestion of an increase at higher levels.

Below 20 km these two series of observations show seasonal cycles decreasing in amplitude with distance above tropopause, and a tendency for a biomodal distribution. Most soundings are of the "dry" type showing mixing ratios $\lesssim$ 3 ppmv, while perhaps 20% of the soundings are of the "wet" type showing mixing ratios above 10 ppmv. These series also support a long-term trend with almost a doubling between 1952 and 1973 and a decrease since then of at least twice the rate of the earlier increase. Beyond these variations, these data series show remarkably little variability.

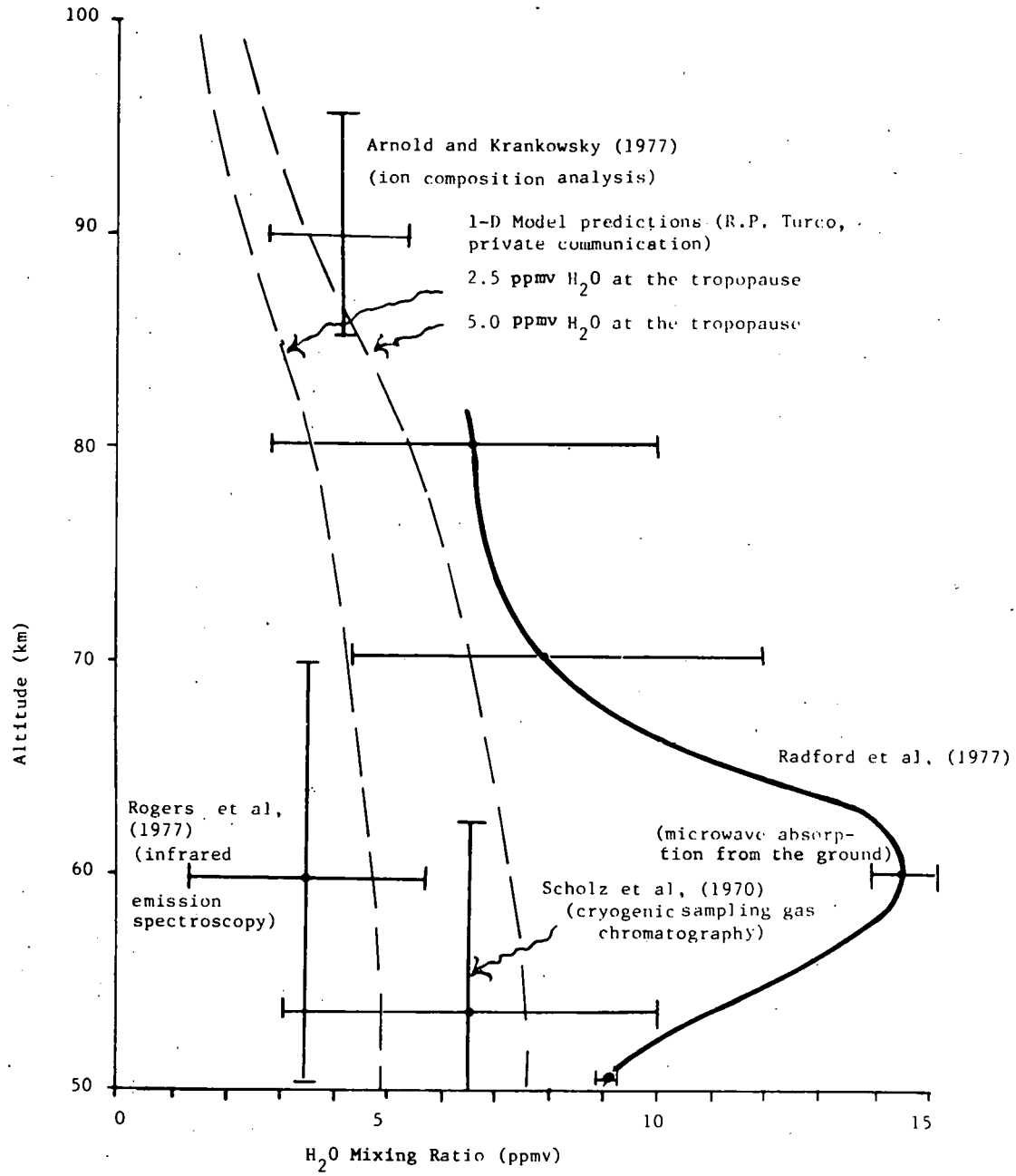

Figure 2. Mesospheric Water Vapor Measurements

(Source: R. Turco)

Current theory suggests that the only variation in H_2O mixing ratio to be expected above 20 km is that due to oxidation of CH_4, methane. Since CH_4 probably enters the stratosphere through the tropical tropopause at a mixing ratio of approximately 1.6 ppmv, it could at most add 3.2 ppmv to the H_2O mixing ratio passing through the tropical tropopause "cold trap." At -80°C and 100 mb this is 5.5 ppmv and would lead to ~ 9 ppmv as a maximum possible H_2O mixing ratio in the upper stratosphere.

However, as indicated above, current data indicates a decrease in mixing ratio from the tropical tropopause to a value near 4.5 ppmv, near 19-20 km. This decrease suggests a stratospheric sink for H_2O, but in the absence of an identified sink it must be regarded as currently unexplained. Since the methane concentration also decreases between the tropopause and 20 km, it can no longer add as much as 3.2 ppmv of H_2O by oxidation at higher levels. Thus one can arrive at a value of ~ 8 ppmv as a maximum possible mixing ratio for water at any level above 20 km. Similarly, from the minimum temperatures observed over the winter poles at 25-30 km and over the summer poles at the mesopause, one can arrive at a minimum possible water mixing ratio for the upper atmosphere. The numbers obtained from this exercise are near 3 ppmv. Any observations of upper atmospheric water vapor concentrations outside the range of 3-8 ppmv must be regarded as due to observational error or to unknown H_2O sources, sinks, or redistribution mechanisms.

During the last year (1978), limited satellite measurements of water vapor have been made with an earth limb scanner on Nimbus VI (Gille and Russell) and with a pressure-modulated radiometer (PMR) on Nimbus VII (Houghton). Both of these measurements (neither of which has yet been reported fully) have been made in the infrared at 6.3 micron wavelength. For the 1980s, there are plans to measure atmospheric water vapor using a variety of instruments, and thus it is hoped that ten years from now the situation will be much better than it is at present, when not even an adequate global mean value exists for mesopheric water vapor, to say nothing of variations with time and latitude.

2.4 HIGH-ALTITUDE CLOUDS

2.4.1 Noctilucent Clouds (Ellsaesser, Turco)

These are thin clouds observed occasionally at the high latitude summer (cold) mesopause, where the temperature drops so low (below 150 K) that condensation can occur even though water vapor mixing ratios are no greater than several ppmv. These mesopheric clouds have been the subject of scientific investigation for nearly a century. Noctilucent clouds (NLCs) have been observed from the ground (Fogle and Haurwitz, 1966), from satellites (Donahue et al., 1972), and have been sampled in situ (Hemenway et al., 1964). Current theories favor a crystalline ice composition (Reid, 1975) covering a meteoritic dust nucleus, although hydrated metallic ions have also been suggested as the nucleating agent (Goldberg and Witt, 1977). D'Angelo and Ungstrup (1976) recently reported an anticorrelation between NLCs and ionospheric electric fields (which lead to ohmic heating of the mesosphere), suggesting that NLCs are composed of a condensible substance such as H_2O. This theory tends to confirm the idea that the conditions necessary for NLC

formation are an extremely cold mesopause (Theon et al., 1967) and sufficient ambient water vapor and numerous condensation nuclei (Witt, 1969). If these conditions are met anywhere in the upper atmosphere, it is at the high latitude summer mesopause where they would be expected to be most likely. And it is here that NLCs were observed by satellite (Donahue et al., 1972). By contrast, NLCs are not seen at latitudes below 45° except for artificial NLCs correlated with SCOUT missile launches from Pt. Mugu (Meinel et al., 1963) and with French sounding rockets (Benech and Dessens, 1974). A detailed discussion of NLC sightings and morphology can be found in Fogle and Haurwitz (1966).

By depositing water vapor and exhaust particles near the mesopause and thereby enhancing two of the three conditions believed necessary for NLC formation, rockets can apparently form artificial mesospheric clouds (Meinel et al, 1963; Benech and Dessens, 1974) and might presumably increase the frequency or extent of natural NLCs. Rocket injections of water vapor may also lower the temperature at or near the mesopause. Chenurnoy and Charina (1977) studied variations in hydroxyl (OH) band emissions before, during, and after an NLC display. As a result they suggested that higher concentrations of H_2O before formation lead to enhanced OH emission causing local cooling; after formation of the NLC, H_2O vapor is condensed into cloud particles leading to reduced emission.

Despite the observed production of artificial mesospheric clouds following rocket launches, as cited above, two direct mesospheric releases each of 2 kg H_2O over Ft. Greeley, Alaska, on 5 and 8 August 1964, failed to produce observable cloud (Fogle et al., 1965). However, since the water was released in bulk at heights that could not be clearly determined, these failures may not be significant. Liquid water would not have much time to evaporate and condense into particles of sufficient size to make a visible cloud. (See also the discussion of Section 2.5.3 concerning several additional high altitude water release experiments, and the discussion in item F.2 of Appendix F on the specific enthalpy of different water releases).

Novozhilov (1979) has suggested that the formation of NLCs is probably facilitated by the presence of a deep cyclonic vortex in the mesosphere, and Scott (1974) reports that NLC sighting occur earlier in summers following major sudden stratospheric warmings.

2.4.2 Nacreous Clouds (Ellsaesser)

Nacreous clouds form in the stratosphere (~ 25 to 30 km) in the region of temperatures below -80°C that develop within the polar winter vortices, particularly over Antarctica. As such they are indicative of (high) stratospheric water vapor mixing ratios and (low) temperatures, and of year-to-year variations in atmospheric circulation. In view of the dearth of information of this type, they offer an additional source of information for interpreting or inferring conditions at high levels in the atmosphere.

The catalog of sighting by Stanford and Davis (1974) shows periods of maximum frequency in the 1880s to 1890s and in the 1930s to 1940s. There was also a 30-year period from 1895 to 1926 during which almost no sighting were done. These data suggest long-period cycles of variation in stratospheric

water vapor mixing ratios and/or temperatures that exceed anything we have seen since observations of stratospheric water vapor and temperature were begun. Stratospheric cycles of such long periods must also have an impact on the mesosphere.

2.5 CONDENSATION AND RE-EVAPORATION IN ROCKET EXHAUSTS

2.5.1 Prefatory Comments (Bauer)

The problem of condensation and re-evaporation of water vapor is significant for rocket exhausts in all altitude ranges considered here, and for a variety of applications. Two subpanels, chaired respectively by M. Mendillo and M. Pongratz (see items 2.5 and 3.4 in Table 5) addressed the problem at the workshop, and P. Bernhardt wrote a discussion afterwards. These three contributions are all presented here. There is, of course, some redundancy, but it seems preferable to present the whole of the discussion in view of the importance of the problem. Mendillo reviews the problem as a whole, Pongratz makes specific suggestions for experiments, and Bernhardt summarizes the problem as it appeared after the workshop (he participated in both Mendillo's and Pongratz' subpanels).

2.5.2 The Overall Problem (Mendillo)

A. Introduction

The exhaust gases from a rocket cool adiabatically on expanding through the nozzle and into the low-density ambient environment. At high altitudes, temperatures below the saturated vapor temperature of H_2O are reached and thus condensation and the formation of ice crystals are expected to occur. Ample evidence exists from laboratory experiment to show that under a wide variety of conditions condensation occurs rapidly once supersaturation is reached. However, the condensation mechanism is not always well defined or understood. Thus Wegener (H. G. Wolfhard, private communication) demonstrated that the concept of homogeneous condensation did not explain the Apollo-8 lunar injection effects, but Castleman (private communication, June 1979) points out that hydrated protons lead to the formation of clathrate structures involving some 20 H_2O molecules that form nuclei for condensation.

The mass fraction of the condensed phase is not well known. However, laboratory experiments indicate that under many conditions at least half the water condenses. Since condensation is enhanced by longer residence time in the rocket nozzle, there is a tendency for more condensation to occur as the size of the rocket engine increases.

Condensation in the exhaust of a hydrogen-oxygen rocket was observed in the Apollo-8 lunar orbit injection burn. Molander and Wolfhard (1969) analyzed the observations made by Smithsonian Astrophysical Observatory personnel at Mt. Haleakala of a "cloud as bright as the moon" photographed during the

injection burn. The illumination was presumably caused by sunlight scattered from ice crystals in the exhaust cloud (see also Aviation Week, 6 January 1969).

It is not known how large the ice crystals formed in a liquid fuel (H_2-O_2) rocket are, but they are probably smaller than those observed in aluminized solid propellant rocket, i.e., submicron.

Note also that various components of rocket exhausts such as atomic and molecular ions, small ice crystals and various contaminants may induce the condensation of supercooled water vapor in the ambient atmosphere to form a contrail. Such phenomena are thought to be responsible for the "noctilucent cloudlike" formation observed in some past rocket launches (see Benech and Dessens, 1974). Note also the observations of Meinel et al., 1963 of several contrails (seven over six months) observed at an altitude of order 70 km from Arizona following launches of Scout solid propellant rockets from Vandenberg Air Force Base.

B. Summary of Water-Dump Experiments

Several water-dump experiments have been decribed that address the condensation issues raised by rocket exhausts. These are:

(1) Wallops Island High Water Test. On 2 March 1962, a Nike-Cajun rocket released 18 kg of water at an altitude of approximately 100 km over Wallops Island, Virginia. The time of the release was 05:47 E.S.T., corresponding to dawn twilight. The main objective of the experiment was to provide background data for a proposed release of water from the second and third stage of a vehicle designed to test the Saturn booster (the Saturn High Water Experiments described below). The ground-based optical diagnostics led to three main conclusions (Edwards, 1962):

(a) Upon release of the water from the canister a small portion (2 kg) was perhaps vaporized and the remainder formed ice particles that continued to follow the ballistic trajectory established by the Nike-Cajun rocket.

(b) The ice crystals probably had a random size distribution with diameters from a few to several hundred microns.

(c) The vaporized water, if present, was too faint to be seen or photographed, whereas the ice crystal cloud was visible by means of scattered sunlight and could be photographed (e.g., at t = 60 seconds after the release, the diameter of the cloud was aproximately 6 km).

(2) Saturn High Water Experiments. The largest known "chemical release" experiments yet performed were the Saturn water dumps of April and November 1962. These experiments were a secondary objective of the Saturn test flight program (Debus et al., 1964). On two occasions, over 86,000 kg of water, carried as ballast in the upper stages of the Saturn vehicle, were

released by an explosive rupture of the storage tanks in the lower ionosphere. A large amount of material exists on thee experiments, almost all of it in the form of contractor reports, in-house memoranda, and partially reduced data (Lundquist, private communication, 1979). A preliminary examination of that information suggests that the major result of interest to the ionspheric hole question concerns the degree of condensation experienced by the released water. Debus et al. (1964) estimated that approximately 85% of the water formed a cloud of fine ice crystals. Photographic records exist of the early development of the resultant ice cloud. Similar records of various fuel dump scenarios carried out during several Apollo missions (Lundquist, 1970) document cases of substantial condensation percentages at higher altitudes.

As an ionospheric modification experiment, the Saturn High Water dumps were of little value. This shortcoming is due both to the altitudes of the releases and to the lack of appropriate ionospheric diagnostics. If the injections had occurred at F-region heights, the 15% of water vapor produced would have caused a large-scale ionospheric hole comparable to the Skylab effect. At 105 km and 165 km, no ill effects were produced as predicted in the preliminary planning document (Debus et al., 1964).

It is possible that a more detailed examination of the photographic record of the ice cloud could lead to a better understanding of the condensation problem or to such atmospheric questions as the formation of high altitude noctilucent clouds. These were in fact considered at the time and, as described by Debus et al. (1964), "Noctilucent clouds were not observed, or if observed, went unrecognized."

C. Current Status

Participants in the June, 1979, SPS workshop re-examined the question of condensation in rocket exhausts in the light of past experiments and new theoretical calculations. Evidence taken from the High Water experiments of 1963 and the LAGOPEDO experiments of 1977 suggest that 80-100% of water deposited in the upper atmosphere (via explosives or ruptured storage tanks) quickly condenses. The water vapor resulting from a rocket exhaust plume, which has a significantly higher specific enthalpy (see item F.2 in Appendix F), may experience a significantly lower fraction of condensation, but uncertainties in this area suggest that 50-100% may still be the range of possibilities.

Since the condensation process occurs very close to or in the rocket nozzle (in a time much less than 1 second), the degree of condensation would not be expected to exhibit appreciable diurnal or altitude dependence. Thus little difference should occur between Domains A, B, and C with respect to condensation.

While the molecules that escape condensation are available for immediate aeronomic processes, the frozen component must still be considered. Translational processes (diffusion, gravitational settling, suborbital and/or orbital motions, and atmospheric escape) will obviously transport the

condensed water from the localized point(s) of injection. Since the size of the crystals is probably in the 0.1 μm range, with perhaps 10^8-10^9 molecules, current estimates point to relatively rapid fall (speeds on the order of kilometers per second above several hundred kilometer altitude). In the lower atmosphere (Domain A) winds would be the main source of ice cloud transport.

Theoretical studies of condensation usually assume that the ice crystals can be replaced by equivalent spheres. This assumption may be too restrictive for the present application. For example, in trying to infer the degree of condensation from optical measurements, as was done in LAGOPEDO for instance, the conclusions may have a strong dependence on the shape as well as size of the ice crystals, especially if the longest dimension essentially determines the scattering properties.

An important aspect of the water injection problem deals with the subsequent sublimation of the ice crystals. In Domain A, collisions with the neutral atmosphere are probably the main source of sublimation; at higher altitudes collisional heating is no longer effective. The role of sunlight in the sublimation process is not fully understood at this time. Estimates of a half-life of ice crystals in the 2-10 minute range (see e.g., Molander and Wolfhard, 1969) may be too short (Zinn and Bernhardt, private communication; also Sharma and Buffalano, 1971, Table 1, who estimate from 20 minutes near 640 km and over a day in cislunar space).

Additional areas that need to be investigated are:

(1) The role of multi-constituent exhaust clouds in which the individual species may influence each other's tendency to condense (e.g., the Space Shuttle OMS engines, used in its circularization burn, emit H_2O, CO_2, H_2, N_2, and other minor species). In addition, any particulates or ionic species in the exhaust may enhance the condensation procss.

(2) The possible chemical interaction between ice and a plasma need to be examined.

(3) Past and current studies of comets should be examined in the context of the sublimation and plasma chemistry questions.

(4) Any archived data on rocket exhaust condensation and subsequent sublimation should be reviewed.

(5) The feeling that possible laboratory experiments (with the possible exception of Castleman's work on condensation on ions) are probably not directly relevant to rocket exhaust effects suggests that only rocket observations (via experiments of opportunity) should be planned.

(6) The use of LIDAR to address the condensation/sublimation question needs to be examined, as well as any nonvisual optical detection technique.

2.5.3 Experimental Studies, Mainly in Domain B (Pongratz)

Our current understanding of the phenomenology of the water in rocket exhausts indicates that a fraction ranging between 0.2 and 1.0 condenses and freezes into ice crystals. The characteristic ice crystal dimensions are generally considered to be in the range of 0.01-0.3 μm. Indeed, the size distribution may be dominated by large numbers of very small particles.

While a reasonable consensus exists regarding condensation, the evaporation picture changes "by the hour." Early calculations by Bernhardt indicated that in the absence of sunlight only a small amount of sublimation occurs. Sublimation in sunlight depends on whether or not the ice crystals can absorb sunlight. Bernhard (1976), Zinn et al., (1979), and Wolfhard (1969) have made calculations assuming that sunlight is absorbed, which give sublimation time constraints of about minutes.

The LAGOPEDO UNO experiment probably represents the only quantitative unclassified data on sublimation. Two instruments measured the spectrum of the reflected sunlight, which can be used to determine a characteristic size for the ice crystals. Two other cameras recorded images of the ice cloud. One imaging camera used EKIR film (3 layers, 500-900 nm) and the other camera was electrostatically intensified and filtered at 455 nm. These imaging data can give ice crystal inventories as a function of time. Preliminary data indicate that a large fraction of the H_2O froze and gave a sublimation time constant of about 10 seconds.

Experiments should be conducted to verify codes used to predict the fraction of the water vapor that condenses, based upon its specific enthalpy. Experiments are preferred that closely match the temperature, pressure, and density values anticipated for SPS rockets; however, a verification of the condensation codes using initial values of temperature, pressure, and density is a necessary minimum first step. Because of the disparate ideas regarding sublimation, experimental input is vital. Because of the rapid expansion of the ice cloud in Domain B, optical techniques using scattered sunlight can probably detect sublimation if the relevant time constant does not exceed 500 seconds; otherwise the cloud will become tenuous and the signal will fall below background before significant sublimation can be observed.

Lest it be omitted elsewhere, the issue of heterogeneous chemistry involving small ice crystals with a relatively large surface area should be raised and that of ions and electrons attaching themselves to these crystals (see Castleman, 1979). Such reactions would produce significantly different neutral chemistry and airglow compared to the charge exchange and dissociative recombination reactions.

Unfortunately, the upcoming Atlas-Centaur launch will not be useful for studying condensation and sublimation in Domain B because of the local time of the launch. The launch occurs several hours before sunrise and the ice crystals will disperse and fall long before sunlight can hit them. The Canadian National Research Council (Dr. Brian Whalen) and Los Alamos Scientific Laboratory (Dr. Gordon Smith) are proposing a LAGOPEDO-type release called Project

Waterhole that should provide an opportunity for optical ice cloud diagnostics. This experiment will be conducted in March/April 1980 and may be useful for the future.

The ideal Domain B experiment would involve a rocket exhaust simulator making releases with varying speeds above and below the terminator for the ice crystals. The rocket exhaust simulator should produce H_2O vapor with the same specific enthalpy as the SPS rockets used for the circularization, deorbit, and POTV burns) see Item F.2 in Appendix F). From a single sounding rocket launch during sunrise, many of the sublimation parameters could be varied, and the ice crystal size and inventory determined. Because of the critical impact of the sublimation question on the issue of ionospheric depletion, we would recommend that such an experiment be conducted.

2.5.4 The Current Status (Bernhardt -- prepared after the workshop)

Rapid vapor expansion produces cooling that may lead to condensation. The amount of condensation will depend on (1) the initial specific enthalpy (i.e., c_pT/ρ) of the vapor, (2) the expansion geometry (such as a spherical versus a rocket plume release), and (3) the constituents of the exhaust. The amount of condensation also depends on whether condensation nuclei are formed by the vapor molecules themselves or by some foreign particles such as smoke, dust, salt, ions, etc. With these factors in mind, several vapor releases which have produced (or will produce) ionospheric modification are considered.

The first release is the Saturn V/Skylab burn that produced the ionospheric depletions measured by Mendillo et al. (1975a,b). There seem to be good theories and measurements of the condensation in these rockets. The Saturn V ionospheric hole was produced by the second-stage burn. The second-stage propulsion systems consist of five J-2 LO_2/LH_2 rocket engines. This type of engine (J-2) was the same that is used by the Saturn IVB. The translunar injection burn of the Saturn IVB during the Apollo 8 mission produced a visible plume that was attributed to scattering of sunlight off of ice clusters. Analysis of photographs of the plume indicate that 5-10% of the exhaust condensed (Kung, Cianciolo, and Myer, 1975). The particle radius is estimated to be 70-100 Å. The visible cloud lasted for more than two hours (Lundquist, 1970). A purely theoretical calculation of this effect by Wu (1975), using nonequilibrium condensation theory, gives 10.5% condensation with 17 Å (radius) clusters. Using a simple model described in Bernhardt (1976), with modifications for rocket plumes, we calculate 12.2% condensation with a final cluster temperature of 200 K. Based on this research, it seems that the Saturn V condensation should be taken as 10%. Cluster size should be 70-100 Å and the cluster lifetime is greater than 2 hours.

The second release of interest is LAGOPEDO. Much more water vapor is expected to condense because of the high initial density of the Lagopedo release. For instance, the Lagopedo vapor density is 526 kg/m^3 at 1000 K temperature, while its Saturn V density is only 0.0146 kg/m^3 at that temperature. Our calculations indicate that 54% of this H_2O vapor will be nucleated. The heat of vaporization released for H_2O ice will prevent any of the CO_2 from freezing.

The third release of interest is the OMS engine burn during the Skylab II mission. This engine produced exhaust at a temperature of 921 K with a density of 0.0028 kg/m^3. The low density of the exhaust indicates that the degree of condensation will be even less than during the Apollo 8 (or the Skylab I) mission. Our calculations indicate that no more than 6% of the exhaust should condense.

Our modeling of condensation assumes nonequilibrium, steady-state nucleation theory. As such, it tends to overestimate the amount of condensation. Time-dependent (nonsteady-state) homogeneous nucleation has been investigated by Draine and Salpeter (1975). We are attempting to use their theory for the rocket-plume and explosive-release condensation problem.

Besides theoretical calculations and experiments in space, laboratory measurements of rocket exhaust condensation should be considered. Measurements of condensation in a vacuum chamber, however, may be prohibitive. Chamber measurements have been made of the composition of a rocket plume by McCay, Powell, and Busby (1970). Condensation measurements were not feasible because their chamber size was too small by at least a factor of two. The condensation from the Saturn IVB was calculated to start at 41 to 55 meters from the nozzle (Wu, 1975).

In summary, from the condensation calculations we conclude that nucleation is important for Lagopedo-type releases but may not be significant for rocket-plume releases. This is because of the low initial density of the vapor leaving the rocket nozzles. We are left inquiring: Does condensation seem to be necessary to explain the Skylab I ionospheric depletions (e.g., Zinn et al., 1979)?

2.6 SPREADING OF ROCKET EXHAUST CLOUDS: LOCAL, REGIONAL, ZONAL, AND GLOBAL EFFECTS (Bernhardt)

Domain A lies generally below the "turbopause" (which normally lies at 110 $\pm$ 10 km) so that turbulent diffusion dominates over molecular diffusion. In this region the mean free path is one meter or less and the rocket exhaust relaxes to collisional equilibrium with the background atmosphere. The effective atmospheric diffusion coefficient may be as much as a factor of ten greater than the molecular diffusivity at the lower altitudes.

Mesospheric winds may contain shears as large as 120 m/sec per km in altitude, which elongate and so disperse the exhaust cloud. Table 7 sketches cloud dispersion in the mesosphere, which indicates that 1-10 days after release the cloud from a point injection has spread to regional dimensions (300-3000 km). Since HLLV launches average approximately one per day, one would expect to find a zonal band of 1000-3000 km width (south to north) spread around the globe near the latitude of launch (28°N). The various chemical and photochemical reactions have different time constants, so that it is possible that rather different phenomena may be observed on a local scale, as in a point release or rocket plume, than on a regional, zonal, or global scale.

The numerical values of cloud width shown in Table 7 are schematic only, being based on the very limited data set shown in Fig. 3. At higher

TABLE 7

SKETCH OF CLOUD DISPERSION IN THE MESOSPHERE

(Lagrangian Picture, Numbers Schematic Only)

Time from Point Release:	3 Seconds	1 Minute	1 Hour	1 Day	1 Week
Horizontal Cloud Width, σ_h(km)	.01	.2	80	(300)	(1000)
Vertical Cloud Width, σ_v(km)	.01	.06	.8	6	8
Dilution Factor, $1/(\sigma_h^2 \sigma_v)$ relative to volume at t = 1 minute	10^6	1	5×10^{-7}	5×10^{-9}	3×10^{-10}
Scale:		LOCAL		REGIONAL	GLOBAL

Values for σ_h come from Figure 3 here; for σ_v see Bauer, 1974.

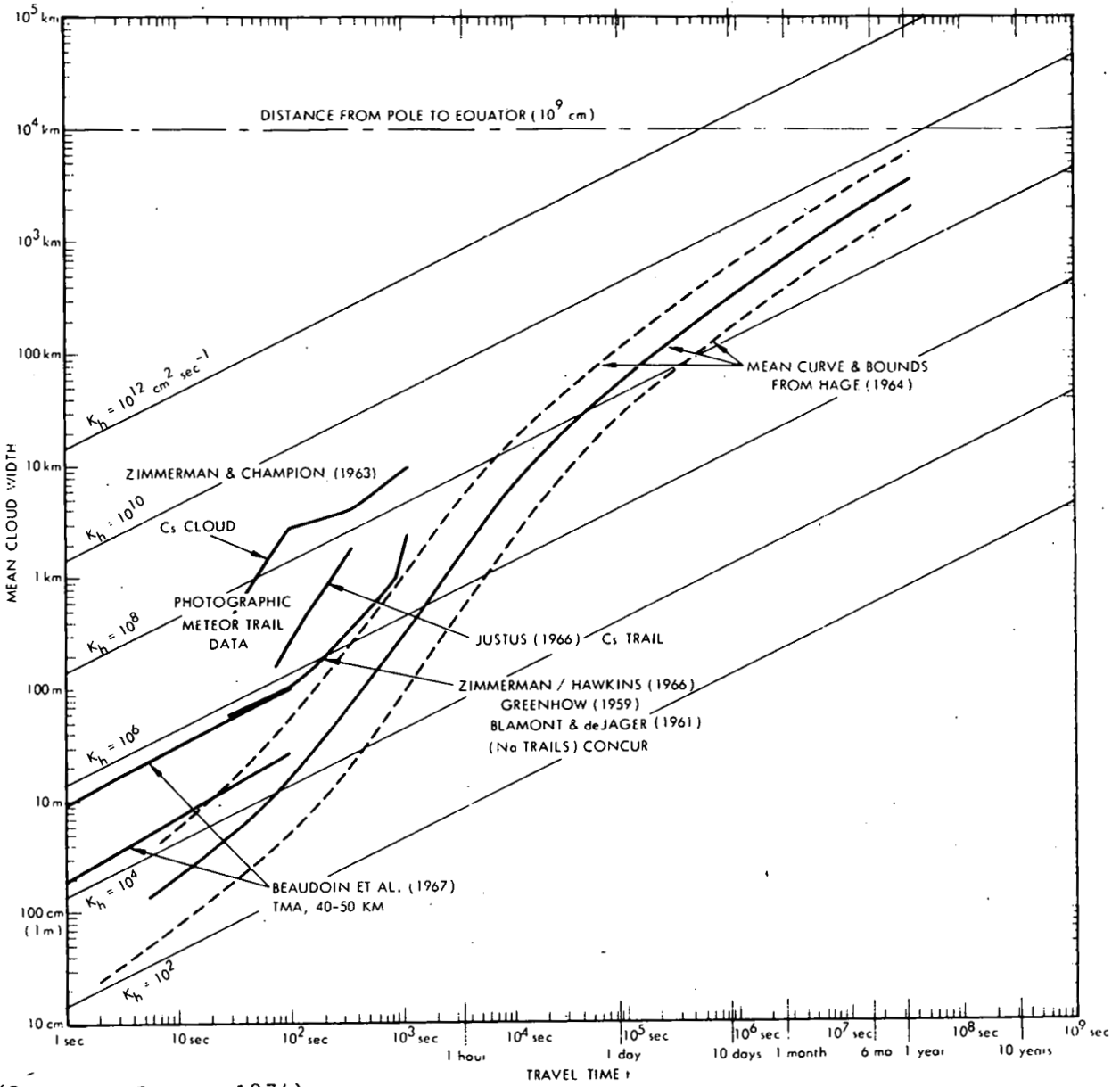

(Source: Bauer, 1974)

Figure 3. Horizontal Dispersion as a Function of Travel Time -- Data for the Upper Stratosphere and Mesosphere

Note: 1. Data in this altitude range only exists for times up to a few minutes.

2. The mean curve and bounds from Hage, 1964, were obtained for altitudes below 30 km; they are shown on this figure merely to indicate that transport is faster at these high altitudes (see Bauer, 1974, for a discussion of this point).

altitudes (100 km and above) one would expect more rapid spreading, and in any case east-west dispersion is more rapid than north-south spreading because of the zonal winds associated with the rotation of the earth.

2.7 ENERGY AND MOMENTUM TRANSFER DUE TO ROCKET EXHAUST PLUMES (Forbes)

The HLLV second stage has a mass flow of 6500 kg/sec, of which 6300 kg/sec is H_2O and 200 kg/sec H_2 (see Fig. 1). The heat of combustion of H_2 and O_2 is approximately 58 Kcal/mole, and thus the total rate of thermal energy production is 90 GW. At 95 km altitude the mean speed of the HLLV is 4 km/sec and the temperature is 200 K, so that the thermal energy in the exhaust is equal to the thermal energy of the air molecules contained in a cylinder of radius 6 km, which is approximately equal to one scale height. Thus for a distance of this order around the trajectory one would expect to find noticeable disturbances, with the possible production of shocks and gravity waves that would tend to propagate upwards with increasing amplitude as the density falls. In fact, during the ascent of Apollo 15, 16, and 17, signals were detected on a microbarograph on the ground from the plume in the 30-150 km altitude range (see Hilton et al. (1972), Henderson and Hilton (1974a,b, and Gardner and Rogers (1979), who analyzed the Concorde "hyperboom."

Dissipation of energy in the rocket plume is expected to occur via both radiative cooling and the excitation of acoustic and/or gravity waves. Oscillations with periods on the order of minutes in the bottomside F-region ionization were observed 1000 km away from the launches of Apollo 14 and 15 (Arendt, 1971, 1972). Depending on the value of the Brunt-Vaisala frequency N, which is equal to about 1.9×10^{-2} sec^{-1} at 110 km, the oscillations can be interpreted as acoustic wave modes if their frequency $f > N/2\pi$, or as gravity wave modes if $f < N/2\pi$. It is possible that these waves could act to cause Sporadic E in the vicinity of the rocket launch. By studying archived data and future launches of opportunity, the generation of wave disturbances in the ionosphere and related effects should be confirmed. The magnitude of the HLLV effect would of course be much greater, so some understanding of the physics involved would be necessary to extrapolate these results.

2.8 PHOTOCHEMICAL EFFECTS (Turco)

SPS rocket injection of large quantities of H_2O/H_2 and NO into Domain A (the mesosphere and lower thermosphere) may cause important local and global scale effects, such as:

(1) Enhanced airglow, particularly from vibrationally excited OH (infrared bands) produced by the reaction of H with O_3, and singlet oxygen atoms (^1D at 630 nm and ^1S at 557.7 nm) generated by OH^+ and O_2^+ recombination with electrons. The increase in OH emission should roughly parallel the increase in total hydrogen in the upper mesosphere (~ 90 km). The intensity of singlet oxygen emission will depend on the fraction of injected H_2O/H_2 molecules that react with atomic ions in the thermosphere. Nitric oxide chemiluminesence, due to the reactions, NO + O and NO_2 + O, may be prominent during rocket reentry.

(2) Reduction in ozone due to catalytic reaction cycles involving injected HO_x and NO_x. In the mesosphere, the major HO_x catalytic cycles involve the reactions,

$$\begin{array}{r} H + O_3 \rightarrow OH + O_2 \\ OH + O \rightarrow H + O_2 \\ \hline O + O_3 \rightarrow O_2 + O_2 \end{array} \quad \text{(net)}$$

$$\begin{array}{rl} H + O_2 + M \rightarrow & HO_2 + M \\ HO_2 + O \rightarrow & OH + O_2 \\ OH + O \rightarrow & H + O_2 \\ \hline \text{Net: } O + O \rightarrow & O_2 \end{array}$$

Ozone chemical loss in the upper mesosphere is controlled largely by HO_x reactions, and the ozone concentration will vary inversely with the HO_x concentration. Nevertheless, the total column abundance of ozone, which is dominated by the ozone layer between 10 and 30 km, would not be affected significantly by a mesospheric depletion.

However, a change in mesospheric ozone might lead to a change in mesopause temperature since ozone cools the mesospohere by infrared emission. The projected change in the average stratospheric water vapor content due to SPS rocket launch activity is only of the order of 1%; such a change would have negligible photochemical consequences.

NO produced above 70 km by reentering SPS rockets will have little effect on mesospheric ozone because the reactions of $NO + O_3$ and $NO_2 + O$ are very slow at these heights. Moreover, the expected rate of SPS NO production is too small on a global scale to affect stratospheric NO_x levels significantly.

(3) Ionospheric alterations, including:

(a) Additional hydration of ions, most importantly in the lower E-region where water vapor is not usually present in large quantities.

(b) Electron concentration decreases in regions of enhanced ion hydration, because electrons can recombine up to ten times faster with clustered positive ions than with ambient molecular ions (i.e., NO^+, O_2^+).

(3) Electron concentration increases in the vicinity of reentering spacecraft, caused by solar Lyman-α photoionization of heat-generated NO.

(d) Ionizing Lyman-β flux reductions in the vicinity of the launch plume, due to absorption by injected water vapor.

(e) Scattered Lyman-α and Lyman-β enhancements due to augmentation of the hydrogen geocorona, leading to greater nighttime ionization in the D- and lower E-regions.

(f) Atmospheric conductivity profile alterations resulting from changes in ion and elctron concentration and composition.

(4) Thermal and dynamical perturbations near the mesopause following large H_2O/H_2 injections. The major thermal effects are probably related to direct infrared radiation transfer in the water vapor bands (between 6.3 and 2.7 μm), OH infrared emission in the Meinel bands (between about 0.6 and 3.0 μm), and chemical energy release by hydrogen-catalyzed oxygen atom recombination. Note that the OH Meinel band emissions can represent up to 20% of the ambient cooling rate of the mesopause region. It is not possible to estimate the dynamical implications of small rocket-induced temperature changes because the dynamics of the mesosphere are only poorly understood at present.

Although the effects outlined above will probably be small on a global scale, locally (i.e., within 5-10° latitude of the injection) the effects may be large enough to cause noticeable (and possibly detrimental), changes. Accordingly, it is important to consider both the short-term local, and long-term global, impacts of SPS rocket activities.

2.9 IONOSPHERIC CONDUCTIVITY AND ATMOSPHERIC ELECTRICITY (Vondrak)

The electrical conductivity of the ionosphere and middle atmosphere is directly proportional to the electron and ion concentration. The injection of H_2O and H_2 by the SPS transportation system will cause both localized and widespread reduction in ionization density and in conductivity. On the other hand, the NO produced during reentry is expected to increase the D-region electron density, resulting in a localized conductivity enhancement. A global increase in nightttime D- and E-region ionization might also result from Lyman-α and Lyman-β scattering from an enhanced hydrogen geocorona (see Section 3.1.4). Another possible source of conductivity change is an alteration of charged particle precipitation at high latitudes if the SPS transportation system alters the radiation belts or magnetospheric structure (see Sections 4.3-4.5). Particle precipitation is the main source of the high-latitude night time ionosphere and, if the particles are energetic, it may enhance the conductivity of the middle atmosphere.

An alteration of the ionospheric conductivity will affect the pattern of the ionospheric currents and electric fields. In particular, the intensitv of the equatorial and low latitude electric field is influenced by the ionospheric conductivity distribution at high latitudes. An alteration of the equatorial electric field may strongly affect the occurrence of equatorial Spread F. At higher latitudes the ionospheric electric currents are part of the electric current circuit that includes the Birkeland currents coupling the ionosphere to the magnetosphere. Thus modifying the high-latitude conductivity may alter the magnetospheric structure.

The conductivity in the middle atmosphere is important for communication systems, particularly VLF. Also, changes in electrical conductivity in

this region may perturb both the electric current and electric field patterns of the global atmospheric electricity circuit that is established mainly by thunderstorms. If these perturbations affect thunderstorm characteristics, they may alter tropospheric weather and climate.

H.C. Carlson pointed out (after the meeting) that it is unlikely that changes in conductivity of the D- and E-regions of the ionosphere might have much global impact on the global electric circuit, at least as long as the altered conductivity is confined to sub-auroral latitudes. The reason for this is that only 10% of the total columnar resistance and ionospheric potential occurs above an altitude of 10 km (see, e.g., Roble and Hays, 1979; Vonnegut, 1979).

2.10 POTENTIALLY IMPORTANT PHENOMENA (Vondrak)

Following the practice in PEA (1978), each item in Sections 2.10, 3.5, and 4.5 will be given a two-index rating (A,B), where A = probability of occurrence, and B = importance of potential impact. Each index will be assigned the value H (high), L (low), or U (unknown).

The following issues appear to be most relevant to the terrestrial environment and to users of present operational systems:

1. Formation of high-altitude clouds (NLC and nacreous clouds). This could result from a cooling of the mesopause due to the increased humidity in the mesosphere or due to the addition of nucleation centers from ablated reentry material. Such cloud formation may have the following user impact:

   (a) Atmospheric albedo change that may alter the tropospheric weather and climate (see e.g., Herman and Goldberg, 1978, p. 243f). (H, U/L)

   (b) Reduced effectiveness of satellite-borne system for surveillance and remote sensing. (H,U)

2. Alteration of mesospheric temperature structure and dynamics. This is principally due to the increased water vapor concentration in the mesosphere, which may alter the reflectivity of planetary waves of the mesopause. Changing the mode of planetary wave propagation has been suggested (Hines, 1974) as a factor that modulates the tropospheric weather and climate. (U,U)

3. Alteration of electric conductivity in the lower ionosphere and mesosphere. The global distribution of ionospheric conductivity affects the propagation of high-latitude electric fields to low latitudes and the location and intensity of high-latitude currents (auroral electrojet). These high-latitude currents are important elements of the current system that includes the Birkeland (field-aligned) currents that couple the ionosphere to the magnetosphere. These electrojet currents also affect power transmission lines, long communication (telephone) lines, and terrestrial magnetic surveys. The global distribution of total conductivity (mesospheric and ionospheric) is an element of the global atmosphereic electricity circuit.

User effects may be:

(a) Alteration of high-latitude electric fields and currents that interfere with communication systems by altering ionospheric morphology and in particular the formation of equatorial Spread F. (U,H)

(b) Alteration of location and magnitude of auroral current systems that adversely affect power transmission networks and longline telephone systems. (U,H)

(c) Alteration of global atmospheric electricity circuit modifies tropospheric weather and climate. (U/L,U)

2.11 ATMOSPHERIC EXPERIMENTS

2.11.1 Water Vapor in the Mesosphere (Sundararaman)

We need to know the variability and trend profiles for water vapor. At present there is essentially no information above 70 km; what little is available (see Figure 2) has errors of about ± 50% between 30 and 70 km.

Some satellite measurements (e.g., Nimbus VII) exist, and more are planned, which raises the question of how good these measurements are. We clearly need a few good profiles in the short term. In the long term, satellite measurements will be available, and they must be verified against ground truth observations.

Thus in the short term we make the following recommendations:

1. Evaluate how good ground-based systems (e.g., microwave spectrometry) are in obtaining profile information in the mesosphere, noting that at present the microwave measurements are about a factor of 2 or 3 greater than available rocket measurements.

2. Develop new instruments or adapt existing ones (such as the NOAA Lyman-α instrument) for rocket platforms so that a systematic program of measurements can be undertaken to determine the water vapor content above 20 km altitude, and also that a "ground truth" verification of forthcoming satellite measurements can be undertaken. (This is a midterm recommendation, to be carried out over the next 2-5 years).

2.11.2 Noctilucent Clouds (Sundararaman, Turco)

In the context of natural noctilucent clouds, the following studies should be made:

1. Examine archived pictures of NLCs to determine if possible their spatial extent, latitudinal/longitudinal distribution, day-to-day and seasonal variabilities and the seasonal duration of occurrences.

2. Undertake model calculations to assess the importance of NLCs such as sensitivity studies on climate (see e.g., Herman & Goldberg, 1978, p. 243f, in particular the study of Hummel and Olivero (1976) referenced therein).

3. Examine the feasibility of NLC observations by satellites during time of rocket launches, such as the recent Atlas-Centaur launch.

If the results of item 2 above show that NLCs have some significance, it is reasonable to consider a broader program, including the following items.

4. Studies of (natural NLCs to determine their origin, composition, microphysics and spatial/temporal characteristics.

5. Investigate ambient mesospheric water vapor concentrations from the standpoint of global morphology and variability, and also the mesospheric circulation, both from the standpoint of correlating or predicting with natural NLCs.

In addition, several classes of experiments can be designed relative to the formation of long-lasting contrails or artificial noctilucent clouds:

6. Monitor rocket launches of opportunity for high-altitude cloud formation, contrails, and related phenomena.

7. Execute a mesospheric water release to generate an artificial noctilucent cloud for study.

8. Investigate water vapor condensation in adiabatically expanding rocket plumes, to deduce eventual particle concentrations, size, and momentum.

The experimental tools that might be utilized in these studies may be divided into the following categories:

1. Cloud detection and characterization

   (a) Twilight photography/photometry from the ground.

   (b) Limb scanning photometry from satellites in place.

   (c) High resolution spectral and polarization measurement of reflected light (from the ground or from rockets).

   (d) Rocket sampling of clouds using various collection surfaces/filters to detect solid and volatile materials.

   (e) Electron microscopy/chemical analysis of NLC samples.

   (f) In situ optical sizing instruments and condensation nuclei counters.

2. Related atmospheric parameters

   (a) Air temperatures using rocket grenades (or infrared emissions).

(b) Wind patterns via cloud motions, or movement of injected tracers.

(c) Mass spectrometer ion composition measurements.

3. Airglow observations

(a) OH emission photometry in selected bands, both wide and narrow view.

(b) OH rotational spectroscopy.

(c) H_2O 6.3 μm emission spectroscopy from rockets.

All of the above instruments and techniques have been used in earlier cloud/aerosol/aeronomy studies. What remains to be done is to address the following practical and technical problems: Which of experiments 1-8, if any, will yield new information relevant to an environmental assessment of the proposed SPS rocket program? Are such experiments feasible, given the time and funds available? What instrument modifications or development will be needed? Will there be ample opportunity to make the required observations?

2.11.3 NO Production on Reentry (Whitten) (Priority: U,M)

The quantity of nitric oxide produced by a reentering Space Shuttle has been calculated by Park (1976), but the computations have never been validated by observation. The following experiment is suggested for that purpose, using simple scaling to extend the results to HLLV reentry.

We envisage two sets of airborne observations, one to measure the emission spectrum in the wake arising from the NO + O chemiluminescence in the 0.6-1.1 μm spectral region, and a second to measure the intensities in the 5.3 μm (fundamental) and 2.7 μm (first overtone) bands of NO. The 0.6-1.1 μm emissions will occur in the wake so that about 10 minutes are available for the measurement of intensities. The second observation must be made above the tropopause so that atmospheric water vapor interference does not prevent observation of the NO bands (Traub and Stier, 1976). Furthermore, a relatively high resolution spectrograph must be employed.

The computer model used to calculate the NO production during reentry can be modified to yield the predicted infrared band intensities as well as the intensities for the NO + O chemiluminescence reaction. These theoretical results would then be compared with measured intensities at corresponding points along the wake.

2.11.4 Rocket Observations (Mendillo)

Given the enormous costs involved with rocket launches, every effort should be made to support investigators wishing to monitor various effects associated with planned rocket programs, if these "experiments of opportunity" are likely to be of value for the SPS assessment. There are several types of such experiments of opportunity:

1. Pre-Shuttle, large rocket launches. The HEAO-C launch of an Atlas-Centaur scheduled for late August/early September, 1979, is a particularly striking example of thermospheric (Domain B) injection. Questions of condensation and sublimation, airglow, and radio propagation effects near the F-region ionospheric hole could be investigated from this event.

2. Note that most rocket launches terminate their main engine burns in Domain A and thus ample opportunities exist for work in that region addressing the problem of contrails (condensation and sublimation, noctilucent clouds) and D-region electron density reductions.

3. Atmospheric experiments using small rockets. Various "routine" rocket-borne scientific payloads carried by sounding rockets could be used to study vehicle-induced ionospheric disturbances. The small amounts of exhaust involved would limit effects to small-scale and localized phenomena in Domains A and B.

4. Rocket-borne payloads designed to study ionospheric modification effects directly. Such a LAGOPEDO-type experiment is planned by Los Alamos Scientific Laboratory (LASL) for Ft. Churchill, Canada, in March 1980.

5. Early space Shuttle Mission engine burns. These experiments of opportunity offer insertion, circularization, and deorbit burns at low latitudes that are of direct relevance to possible HLLV-induced effects in Domain A and can be scaled to Domain B (note that most parking orbits are at 200-300 km altitude rather than 500 km as for SPS, the latter choice being determined by the high drag of the large SPS arrays of solar panels). It would be particularly valuable to request that mission-required or dedicated engine burns be made over atmospheric observatories.

6. Spacelab-2 type ionospheric modification experiments. Seven OMS engine burns are planned over five ionospheric and radio astronomical observatories as part of the Spacelab-2 mission, which is currently scheduled for January 1982. These will address a full range of ionospheric disturbances capable of being created by rocket emission.

7. AMPS (Atmospheric & Magnetospheric Plasmas in Space), CRM (Chemical Release Module) and "Getaway Special" cannisters can be used to carry out chemical releases from the Space Shuttle for studies of specific atmospheric perturbations.

2.11.5 Airglow (Zinn)

Airglow emissions arising from chemical interactions of rocket exhaust products with the ionosphere may be substantial; however, they are unpredictable at the present time. Likely emissions are the red and green oxygen lines at 630, 636.4, and 557.7 nm. If the exhaust gases consist entirely of H_2O and H_2, then the main reactions producing the OI emissions are

$$O^+ + H_2O \rightarrow H_2O^+ + O \ , \qquad (1)$$

$$H_2O^+ + e^- \rightarrow O(^1D) + H_2 \ , \qquad (2a)$$

$$\rightarrow O(^1S) + H_2. \qquad (2b)$$

The $O(^1D)$ atoms give rise to the 630 and 636.4 nm emissions; the $O(^1S)$ gives rise to the green 557.7 nm line. However, reactions (2a,b) are improbable paths for the reaction of H_2O^+ with electrons. The most likely path is

$$H_2O^+ + e^- \rightarrow OH(^2\pi) + H \qquad (2c)$$

(Wadt, et al., 1977). The rates of (2a) and (2b) together are expected to be less than 10% as large as the rate of (2c).

The OH radicals produced in (2c) may be vibrationally excited, giving rise to some OH band emission. However, most of the 7.5 eV of energy released in the reaction is expected to go into translation of the H atoms, (Wadt et al., 1977). If this is the case, it should result in some local heating of the ionosphere and generation of gravity waves.

An additional source of $O(^1D)$ and $O(^1S)$ atoms is the reaction sequence

$$O^+ + H_2 \rightarrow OH^+ + H\ , \qquad (3)$$

$$OH^+ + e^- \rightarrow O(^1D) + H\ , \qquad (4a)$$

$$\rightarrow O(^1S) + H\ . \qquad (4b)$$

However, reactions (4a,b) are expected to be improbable relative to

$$OH^+ + e^- \rightarrow O(^3P) + H\ . \qquad (4c)$$

The ground state $O(^3P)$ atoms do not radiate. The energy released in the reaction is expected to go mainly into translation of the H atoms (Wadt et al., 1977). The branching ratio for the $O(^1D)$-producing reaction (4a) is expected to be 10 to 15%, relative to (4a) + (4b) + (4c).

Thus, something of the order of 10% of the energy released in the recombination reactions may go into OI airglow emissions. Another unknown fraction, between 0 and 50%, goes into OH emissions. The remainder goes into heating, gravity waves, and H atoms that escape to space.

The above statements are based on theory alone. Branching ratios for the $H_2O^+ + e^-$ and $OH^+ + e^-$ reactions have never been measured. It would be of great interest to obtain some experimental data, perhaps on the September 1979 HEAO-C launch.

Airglow measurements were made in the 1977 Lagopedo experiments. The equipment included several narrow-band-filtered photometers, some filtered, image-intensified cameras, and an intensified spectrograph. Quantitative measurements were made at 630 nm ($O(^1D)$), 557.7 nm (O^1S)), 666 nm (OH*(10-4, R-branch)), 623.4 nm (OH*(9-3)), 772 and 786 nm (OH*(9-4)), and 455.5 nm (continuum). Of these the only bands that showed enhancements attributable to airglow were 630, 557.7, and 666 nm. (Horak et al., 1978).

The observed strong 630 and 557.7 nm emissions in LAGOPEDO were produced mainly in a reaction sequence involving CO_2, namely

$$O^+ + CO_2 \rightarrow O_2^+ + CO$$
$$O_2^+ + e^- \rightarrow O(^1D) + O$$
$$\rightarrow O(^1S) + O$$

Therefore, the data shed no light on the unknown branching ratios for the $H_2O^+ + e^-$ and $OH^+ + e^-$ reactions. The OH* channels at 623.4, 772, and 786 nm recorded only background signals attributable to the normal twilight-sky emission. The OH*(10-4, R-branch) channel at 666 nm was chosen for the Lagopedo experiments because there is no normal twilight radiation at that wavelength, whereas emission from the $v' = 10$ level is energetically possible from the $H_2O^+ + e^-$ reaction (2c). The 666 nm channel recorded a weak, but nonetheless definite signal in LAGOPEDO I, but that signal was due to scattering of sunlight from ice particles. (LAGOPEDO I occurred before local sunset; LAGOPEDO II occurred after local sunset on the following night).

It would be of great interest to obtain airglow measurements during the scheduled Atlas-Centaur (HEAO-C) launch, coordinated with measurements of electron density distributions, total electron content, ionospheric winds, and TIDs. A minimum set of wavelengths should include 557.7, 630, and 666 nm. The signals at all three of those wavelengths can be expected to be weak. However, measurements of their intensities would shed light on two matters, namely:

1. the branching ratios for Reactions (2a,b,c) and (4a,b,c) and

2. the percentage of water vapor that condenses out of the rocket exhaust plume and falls out of the F layer.

The calculated probable minimum airglow intensity at 630 nm, as viewed from Cape Canaveral 30 minutes after launch, is 150 Rayleighs. This value, which is well above night-sky background, is based on the assumptions that

1. half of the rocket-exhaust water vapor condenses,

2. the pre-launch F2 peak electron concentration is 10^5 cm^{-3}, and

3. the branching ratios for Reactions (2a) and (4a) are 5 and 10%, respectively.

The intensity at 666 nm could be in the kilorayleigh range. We base this statement on the fact that measure intensity in LAGOPEDO II was 90 R above background. There are several reasons for supposing that the OH production rate will be much larger in the Atlas Centaur event. We should definitely measure the 666 emission. To confirm the identification of the 666 nm as being due to OH(10-4), it would be desirable to measure one or more related bands, such as the (10-3) at 552.7 nm, the (11-5) at 714 nm, or the (11-4) at 591.3 nm. The relative intensities are, to a limited extent, predictable from the behavior of the normal OH airglow. Thus, the (11-4) band should be more intense than the (10-3) band and less intense than the (11-5)

band. The (11-5) band should be stronger than the (10-4) band, the one observed in LAGOPEDO II. There is enough energy in the $H_2O^+ + e^-$ reaction to populate all possible vibrational levels of OH. If, as seems likely, the OH band intensitities are in the kilorayleigh range, then it may be worthwhile to attempt to record spectra.

It is possible that some of the infrared OH airglow is formed by reaction between H and O_3, and some from the NaD emissions that are correlated with the OH emissions. Simultaneous observations of the OH and NaD emissions could provide valuable diagnostics of mesospheric conditions (Takahashi et al., 1979, and other references cited therein).

It seems quite possible that SPS rocket activities may give rise to noticeable airglow. Whether or not this is of environmental concern depends on its intensity, which is not predictable at the present time. It is important to field a set of airglow experiments for the September, 1979, HEAO-C launch.

2.11.6 Cloud Dispersion (Bernhardt)

Only very limited data is available on the spreading of tracers in the mesosphere, and that is limited to relatively short times or small distances, see Fig. 3. In view of the potential importance of H_2 diffusing upward from the mesosphere, this deficiency may be significant, and should be re-examined.

2.11.7 Mesopheric NO (Turco)

Ambient Nitric Oxide. NO concentrations have been measured in the mesosphere, mainly with rocket-borne instruments, and some of the recent values are shown in Fig. 4. Based on this data, there seems to be general agreement that an NO concentration minimum exists near 85 km at mid and low altitudes (although some data, e.g., Barth (1966) and Tisone (1973), do not show this minimum). Such a minimum can be understood in terms of the well-known photochemical reactions of NO:

$$NO + h\nu \rightarrow N + O$$

$$N + NO \rightarrow N_2 + O$$

$$N + O_2 \rightarrow NO + O \ ,$$

where the last reaction acts to conserve NO in competition with the second reaction. The natural sources of mesospheric NO include: upward transport from the middle stratosphere (30-40 km), where N_2O reacts with $O(^1D)$ to form NO; downward transport from the thermosphere (above 90 km), where solar EUV and X-ray radiation ionizes and dissociates air molecules (Strobel, 1971); and meridional transport of NO from high latitudes, where it is produced by auroral activity and solar particle precipitation (Bauer, 1978). In addition, there is a worldwide source of mesospheric NO due to high velocity meteor ablation in the atmosphere (Park and Menees, 1978). For comparison, the

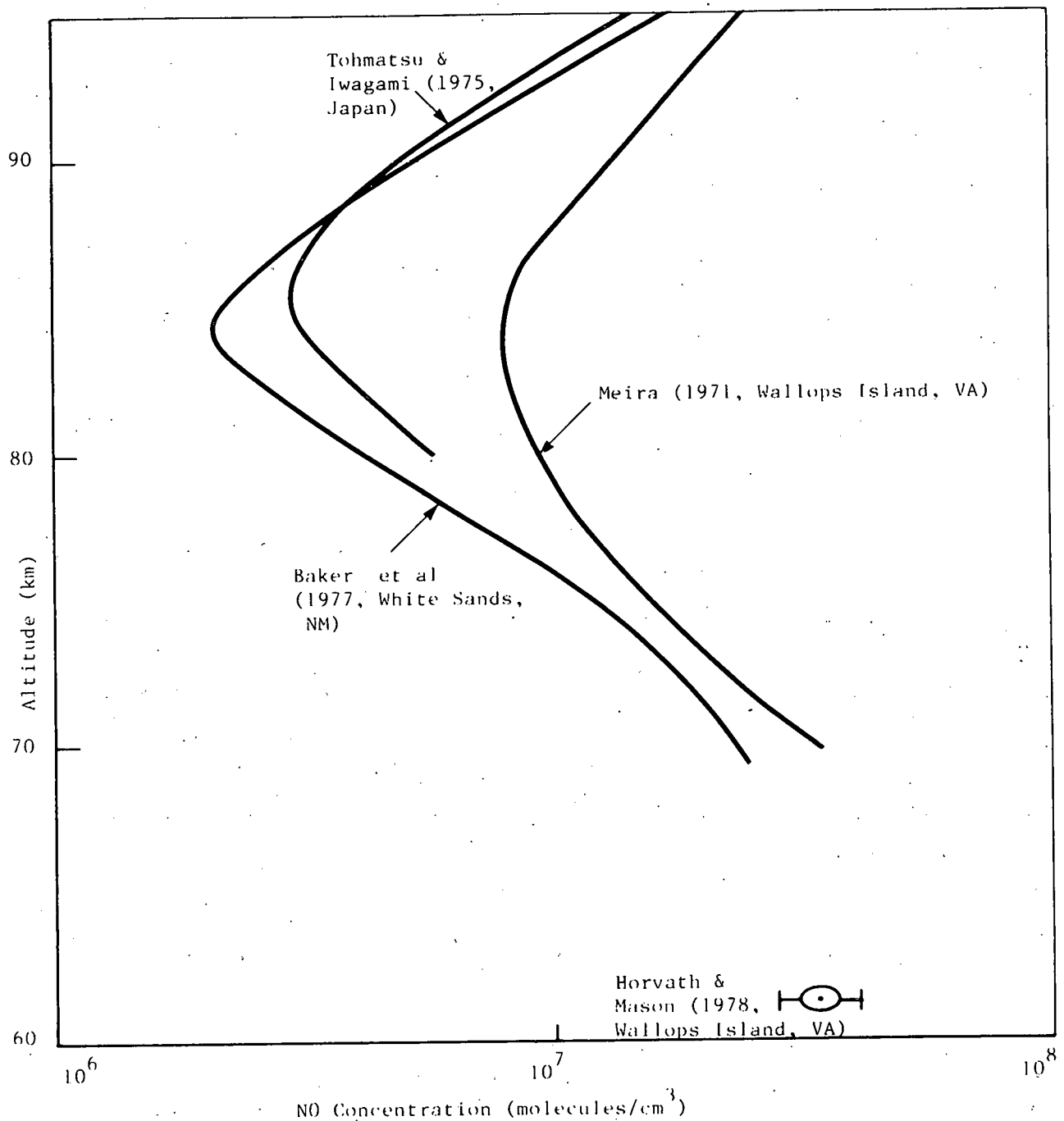

Figure 4. Mesospheric Nitric Oxide Measurements

(Source: R. Turco)

integrated global NO source strengths are roughly: 3 tg/yr* in the stratosphere from N_2O decomposition; 2 tg/yr transported from the thermosphere to the mesosphere; 1-8 tg/yr between 70 and 90 km due to aurora; and 0.05 tg/yr between 70 and 100 km from meteors.

The global morphology and variability of thermospheric nitric oxide (above 100 km) have been defined in detail by extensive satellite observations (Rusch and Barth, 1975; Stewart and Cravens, 1978; Cravens and Stewart, 1978). Thermospheric morphology should be reflected, to some degree, in mesospheric NO concentrations. In the case of mesospheric nitric oxide at mid and low altitudes, Rusch (1973) found typically less than 25% variability in NO concentrations at all altitudes between 65 and 105 km over a wide latitude range (from 40°N to 40°S) for the months of his observations (December, March, and July). By contrast, nitric oxide below 105 km in the polar region is found to be significantly more abundant and highly variable (Rusch and Barth, 1975).

Large local variations may occur in mesospheric nitric oxide even at mid-latitudes. For example, the winter anomaly in D-region radiowave absorption at mid-latitudes is probably related to the transport of large quantities of NO from the auroral zone (Sechrist, 1977). Rusch (1973) reports one occasion of a sudden threefold increase in mesospheric NO between 10°N and 40°N observed by satellite. Basically, however, we expect SPS rocket-generated NO to be super-imposed on a background mid-latitude concentration profile similar to that in Fig. 4.

Nitric Oxide Experiments. Nitric oxide generated in rocket reentry plumes can affect D- and E-region ionization and, as a result, high frequency (HF) communication links and dynamo region conductances. Hence, it is important to evaluate the potential impact on the lower ionosphere of heavy SPS rocket activity. Nitric oxide produced by reentering spacecraft may be detected in several ways: by enhanced resonant scattering of ultraviolet sunlight; by enhanced infrared emission at 5.3 μm; by induced chemiluminescence (NO + O, NO_2 + O, NO + O_3); by changes caused in D-region electron concentrations and ion composition; or, least directly, by alterations in radiowave propagation characteristics. All of the above measurements are difficult enough to carry out in the ambient atmosphere, and would be more difficult in the wake of a rentering rocket. Major problems could involve the identification and tracking of the reentry plume and the deployment of instruments to favorable viewing sites. Nevertheless, several atmospheric experiments relevant to SPS activities could be proposed:

1. Studies of ambient mesospheric NO to determine more carefully its sources, sink, and variability.

2. Monitoring of space shuttle reentry tests beginning in 1979/1980 for effects on the lower ionosphere.

---

*tg = teragrams = 10^{12} grams

3. Measurements of natural impulsive NO perturbations, such as aurorae, large solar flares, and winter anomalies, to investigate the consequences and fate of NO injected into the mesosphere.

4. Execution of a nitric oxide chemical release in the D- and E-regions.

The experimental techniques that might be used to carry out these experiments include:

1. Nitric oxide detection based on γ-band resonant fluorescence of sunlight, from rockets or satellites (in place or planned).

2. Observation of nitric oxide infrared and chemiluminescent emissions using ground- or rocket-based photometry.

3. Electron concentration measurements from rockets (using probes of radio propagation) or from the ground (using radar backscatter on partial reflection).

4. Ion concentration measurements by mass spectrometry.

5. Radiowave propagation changes at HF and VLF using ground-to-ground or ground-to-air communication links.

There are serious technical problems associated with all of the suggested experiments. An example is the problem of tracking a rocket reentry plume, as already mentioned. With regard to the study of NO produced by auroral events, as a simulation of SPS rocket-reentry, one would need to reconcile several fundamental differences between mesospheric conditions at middle and high latitudes, such as the sunlight intensity, temperature, and background composition and ionization levels. Similarly, winter anomalies are, at best, only poorly understood (on a physical basis) at this time.

To our knowledge, only one NO chemical release has been made in the upper atmosphere (18.5 pounds of NO at 106 km over New Mexico; Pressman et al., 1956). On that occasion, the airglow emissions were observed from the ground for about 10 minutes. In some ways, an NO release is simpler than an H_2O release: NO will not condense upon release as may H_2O, background mesospheric NO concentrations are much lower than H_2O concentrations, and NO may produce more distinct emissions by which to trace its dispersion. Nevertheless, it is not clear that rocket reentry effects can be properly studied through NO releases.

2.11.8 Conductivity Experiments (Vondrak)

The most useful requirement for the evaluation of SPS effects on conductivity is improved modeling and theoretical understanding of the present global distribution of ionization in the middle atmosphere and lower ionosphere. Such modeling is needed in order to make a sensible evaluation of the significance of perturbations to the natural distribution of ionization. A three-dimensional specification of electron concentration can be used to compute the two-dimensional distribution of height-integrated conductivity. Although derived from and compared with experimental data, such a model is

most effective when based on an understanding of the underlying physical processes. In addition, the variability and dynamics of the natural ionosphere need to be included in such a model or, at least, be better understood than at present.

Active experiments that alter the ionospheric conductivity by the enhancement or depletion of ionization are possible, particularly in the F-region. However, they are generally localized and are effective over regions with horizontal scale-size smaller than 100 km. Because the more significant effects involve an alteration of conductivity over much larger or even global dimensions, it is not expected that small-scale active experiments would be useful for SPS assessment. In addition, charge polarization may occur in small-scale modifications making the results difficult to interpret or to extrapolate correctly to global scale.

Natural perturbations of the normal global conductivity are probably the most useful experimental simulation of SPS effects. Examples of such perturbations include particle precipitation and the formation of detached plasma regions during magnetic storms, auroral zone conductivity changes, and relativistic electron precipitation (REP) events. Measuring and understanding the effects of these phenomena would provide data needed for model calibration and development for SPS assessment.

3 EFFECTS OF HYDROGEN AND WATER INJECTIONS ON THE IONOSPHERE

3.1 PHENOMENOLOGY OF HYDROGEN IN THE UPPER ATMOSPHERE

3.1.1 The Overall Problem

The atmosphere of the earth as a whole loses hydrogen atoms by diffusion at a rate on the order of 10^{34} atoms/year (see Donahue, 1977). Presumably most of this hydrogen comes from water or methane transported from the ground into the stratosphere and then dissociated by chemical and photochemical reactions. The loss rate of hydrogen is not uniform -- for exospheric temperatures below 800 K, there may be little loss, and indeed there is a discrepancy by a factor of 4-5 between the water burden in the stratosphere and the escape flux -- but the general flow of hydrogen does appear to be upward, out of the atmosphere.

The SPS annual injection rate of hydrogen in the atmosphere above 75 km is of the order of 10^{35} atoms/year (see Table 3), and if a significant fraction of it leaves the atmosphere, a non-negligible perturbation to the atmospheric loss of hydrogen may be produced. What is the fate of the injected hydrogen? and what effects may be anticipated from this enhanced loss rate? This problem is addressed in Section 3.1.2, following.

Most of the hydrogen injected is deposited below 120 km (97% of the total, see Table 3). Of this hydrogen, three quarters comes out as water, that mixes with ambient mesospheric water, as reviewed in Section 2, but one quarter is emitted as H_2, and much of this diffuses upward and can give rise to permanent ionospheric depletion. The depletion problem is reviewed in Section 3.2, where the possibility of a major ionospheric depletion arising from upward transport of H_2 (and possibly also H_2O) from the HLLV second stage is discussed.

The rest of the water, which is emitted at LEO, in the passage to, or at, GEO, is considered in detail in Section 3.1.3. After ejection, roughly half of it, or about 1.5% of the total water emitted, falls under gravity to altitudes of 120-150 km, where it presumably mixes with the bulk of upper atmospheric water. Of the total amount of water emitted at GEO, about 0.9% is trapped in long-lasting orbits; about 0.7% may either escape or fall, depending on the rate that the ice crystals formed in expansion from the rocket nozzle evaporate (to permit the resulting molecules to equilibrate by collisions with the ambient atmosphere); and about 0.1% will escape from the earth's atmosphere.

Note that the specific problems of H_2O/H_2 emission in the magnetosphere are discussed in Section 4.2.

3.1.2 Fate of H_2O/H_2 Injected in the Thermosphere (Zinn)

The ultimate fate of the exhaust molecules is to form hydrogen atoms that escape from the atmosphere. SPS activities will increase this rate of escape, possibly by as much as a factor of 2. This in itself is not serious, since as far as we know hydrogen atoms have always been escaping from the

earth's atmosphere. It is a more serious matter that the increased hydrogen loss due to SPS activities would be at the expense of fossil hydrocarbon fuels rather than water alone.

If the rate of escape of hydrogen atoms were not to increase, the concentration of hydrogen atoms in the upper atmosphere would tend to build up, possibly with a factor of 2 as an upper bound. A factor of 2 buildup would probably be serious as it could lead to changes in thermospheric wind patterns, changed in the stability of the radiation belts, changes in nighttime ionization by scattered Lyman-α and Lyman-β radiation from the expanded geocorona (see Section 3.1.4), along with the possibility of significant increases in satellite drag. Possible effects on F-region ionization are discussed in Section 3.2.

3.1.3 Some Details of the Distribution of Propulsion Effluents (Park)

A. Mass Budget. In Table 8 some assumptions are made about the distribution of propulsion effluents of different elements of the SPS transportation system. Here we present the logic underlying that partition. It is clear that the HLLV circularization and deorbit burns occur at or very close to LEO. Regarding the POTV, which uses chemical propulsion to go from LEO to GEO and return, evidently much of the burn will occur at or close to LEO, with the remainder (30%, see below) taking place at or very near GEO. In any case, the POTV emissions near LEO should be combined with the HLLV circularization and deorbit burns to provide a source of H_2O/H_2 at or near LEO. There is a certain ambiguity in the relative source strengths of HLLV and POTV, with the latter providing perhaps 80% or 30% of HLLV, depending on whether one uses the figures in Table 2 (from RSR, 1978, silicon reference system listed in the text) or in Table 4, which comes from the Boeing study (RSR, 1978, p. B-100). (While not critical, this should be resolved.) We shall take a figure of 1.5 times the HLLV circularization and deorbit burns as the hypothesized injection near LEO, and shall assume that 30% of POTV injections of 10^5 kg hydrogen, or 6×10^{31} H-atoms are emitted near GEO.

For the electric propulsion COTV, things are somewhat different, as chemical rockets are used only for attitude control. Thus we shall assume that the use of the chemical rockets is proportional to the main propulsion, so that the emission of H_2O/H_2 as a function of altitude or time is proportional to the corresponding emission of argon.

An additional problem that has been raised deals with ambient heating due to exothermal chemical reactions involving propulsion effluents. If we hypothesize a net exothermicity of 3 eV per H-atom, then the total COTV and POTV emission of 1.3×10^{33} H-atoms per year corresponds to an energy dissipation rate of 6.3×10^{14} J/yr of 1% of the kinetic energy of the argon ions.

B. Condensation of Water Vapor in Rocket Exhausts Expanding in Vacuum. The exhaust effluents from an H_2-O_2 rocket engine leave the exit plane of the rocket motor at about 4.0 km/sec, while those of a CH_4-O_2 engine move at around 3.0 km/sec. The effluents accelerate outside the rocket motor in the first ten meters or so to attain the "limiting velocity," which can be taken to be approximately 4.5 km/sec for the H_2-O_2 system and about 3.5 km/sec

for the CH_4-O_2 system. Most exhaust effluent matter is confined in a cone of full-apex angle of roughly 10 degrees. The effluents continually cool as they expand. Temperature falls roughly as inverse square-root of the distance from the engine exit, while density falls roughly as inverse-square. At a point where the cross section of the exhaust plume is about 3000 times that of the throat of the rocket engine, the local pressure and temperature are typically 1 torr and 250 K, respectively. This condition is the saturation point condition for the H_2O molecules. For the first stage engines of the POTV, the saturation point occurs at about 140 meters behind the exit plane of the rocket engines, at which point the plume diameter is about 25 meters, number density about 4×10^{16} cm^{-3}, mean-free-path about 0.004 cm, and collision frequency is of the order of 10^6 sec^{-1}. For the second stage POTV engines, the same thermodynamic conditions occur at approximately 100 meters behind the engine where the plume diameter is about 18 meters.

Beyond the saturation point, supersaturation conditions exist wherein condensation of H_2O molecules is expected to occur. In all cases of interest, the condensation should lead directly to the solid state rather than the liquid state. Condensation could occur in both homogeneous and heterogeneous modes. Homogeneous condensation of water vapor is known to occur in the absence of high energy nucleation centers whenever the saturation ratio (the ratio of the local vapor pressure to the equilibrium vapor pressure) exceeds 6 (see Hill, 1966). Heterogeneous condensation occurs around the high energy nucleation centers, which in the case under consideration would consist of (1) atomic and molecular ions, (2) electronically or vibrationally excited atoms and molecules, and (3) metallic contaminants originating from the walls of rocket motors. When such nucleation centers are present, the heterogeneous nucleation can occur before the saturation ration reaches 6. As condensation progresses, heat is generated, which may lead to a pressure overshoot (Hill, 1966). Eventually, however, the heat released during condensation will be carried away by the effluent gas molecules that surround the particles that are undergoing cooling. Even when H_2O molecules are completely removed by condensation, there will be the "inert" molecules such as H_2 (in the H_2-O_2 system) or CO_2 (in the CH_4-O_2 system) that could cool the particulates. There are two questions that need to be answered. They are: (1) What is the extent of condensation? i.e., What fraction of H_2O molecules convert to the condensed phase? and (2) What are the average sizes and size distributions of the particulates formed?

Regardless of the actual mechanism of nucleation, the extent of condensation can be estimated by use of the homogeneous condensation theory, which is well developed. One can use the theory because the extent of condensation is independent of the nucleation mechanism. In the thermodynamic environments of concern, the speed of cooling and density change are sufficiently slow to cause almost complete condensation. Within about 50 meters behind the saturation point, most (i.e., at least 90%) of the H_2O molecules should be in the condensed phase.

The question of particle size is more difficult to answer. If nucleation is homogeneous, one can calculate the final sizes, using the existing homogeneous condensation theory. A cursory examination indicates that the final particle sizes should be at most about 10^{-5} cm. If the nucleation process is heterogeneous, then it becomes virtually impossible to calculate the size distribution because the concentration and characteristics

of the high energy nucleation centers are unknown. One knows, however, that the average number of H_2O molecules in a particulate should be close to the reciprocal of the fractional concentration of the nucleation center population present prior to nucleation. Since the fraction of nucleation center population could be as high as 10^{-4} in the non-equilibrium expansion process on hand, the average number of H_2O molecules in an ice particle could be as low as 10^4. The diameter of the particles could then be as small as 8×10^{-7} cm. The above reasoning leads one to estimate that the typical sizes of the ice crystals formed should be between 10^{-6} and 10^{-5} cm.

Due to electrostatic interaction among the ice crystals, however, the particulates may coagulate into larger particles. Coagulation phenomenon is observed commonly in a laboratory experiment with solid suspensions, but there is no theory to describe the phenomenon. Hence, the final sizes of the ice crystals deposited into the ambient vacuum are presently unknown.

C. Orbital Mechanics of Effluents from POTV (see Figure 5). A POTV mission required five engine burns. They are named here for convenience Burns 1 through 5: Burn 1, the acceleration burn at LEO using the first stage engines to deorbit from the LEO; Burn 2, the acceleration burn at LEO using the second stage engines to circularize at the GEO; Burn 3, the deceleration burn at the GEO using the second stage engines to deorbit from the GEO; Burn 4, the deceleration burn at the LEO using the second stage engines to circularize at the LEO; and Burn 5, the deceleration burn at the LEO of the first stage vehicle using the first stage engines for circularization at the LEO. In time sequence, the Burn 5 occurs prior to Burn 3. The masses of the fuel burned, the absolute velocities of effluents, and the eventual fates of the effluents are listed in Table 8 (see also Fig. 5). In the table, the negative sign denotes the direction opposite to the earth's rotation. The finite range in the velocities given are due to the fact that the vehicles change velocity during burns. The fates of the effluents are judged simply by comparing the absolute velocities with the escape velocities, which are 10.76 km/sec at the LEO and 4.34 km/sec at the GEO.

As indicated in the table, the effluents of Burn 2 are trapped in an earthbound orbit. The center of gravity of the effluent mass has a perigee of 14,400 km above sea level, an apogee of 35,800 km above sea level (GEO), and a period of 18 hours. But the effluents are spread over a wide range: some particles have a perigee as high as 30,000 km while others have one of only 3000 km.

The effluents from Burns 4 and 5 will escape provided the effluents are in the condensed phase. If they are in a gaseous state, molecular collisions will slow them down and prevent escape. In the case of their being slowed down, their fate will be dictated by the velocity of the ambient molecules. One cannot assume that the ambient molecules are at rest: the construction of the SPS will inject a large momentum in the direction of the earth's rotation, so it is likely that the ambient mass will be moving in the same direction. In the imaginary donut-shaped ring around the earth, 1000-km wide and 100-km thick at around 500-km altitude wherein a large amount of rocket effluents will be deposited, the total mass of the ambient atmosphere is only of the order of 10,000 tons. The amount of matter the space activity will inject in a year far exceeds this value. However, the average velocity of the matter (including HLLV) injected into the LEO is slightly under the circular orbital

TABLE 8

POTV EFFLUENTS

IDENTIFICATION	FUEL (TON)	VELOCITY (km/s)	FATE
BURN 1	246	4.294 ± 1.185	FALL
BURN 2	80	-2.153 ± 0.723	TRAPPED
BURN 3	56	6.847 ± 0.723	ESCAPE
BURN 4	58	13.29 ± 1.185	ESCAPE
BURN 5	20	13.20 ± 1.185	ESCAPE

velocity of 7.6 km/sec. One expects, therefore, that the ambient atmosphere will be moving at a velocity slightly smaller than 7.6 km/sec., which means that the effluents from Burns 4 and 5 will eventually fall if they are in the gaseous state.

For the same reason, if the effluents from Burn 1 are in the gaseous state, they will be accelerated by the ambient gas molecules. Their speed of falling will be considerably slower than otherwise.

3.1.4 Effect of H_2O/H_2 Injections on Geocoronally Scattered Lyman-α and Lyman-β Radiation (Prasad and Forbes)

The massive injection of hydrogen atoms due to propulsion effluents in the upper thermosphere might increase the amount of hydrogen escaping from the earth's atmosphere, because it may enhance the slow diffusion of hydrogen-containing compounds up from the lower atmosphere. This effect may cause an increase in the amount of Lyman-α and Lyman-β radiation that is geocoronally scattered into the nighttime ionosphere. The ionization of NO below 100 km and of O_2 above 100 km by geocoronally scattered Lyman-α and Lyman-β radiation, respectively, are important mechanisms for maintaining the nighttime D- and E-region ionization. Changing the lower ionosphere at night will change the ionospheric conductivity and perturb VLF communication links.

3.2. MORPHOLOGY OF PERTURBED IONOSPHERIC REGIONS (Fedder)

3.2.1 Ionospheric Depletion due to a Single Burn

At altitudes above about 160-180 km most ambient atmospheric ions are atomic, mainly O^+, and recombine very slowly with free electrons. However, in the presence of additional H_2O or H_2 molecules, the positive ion changes by

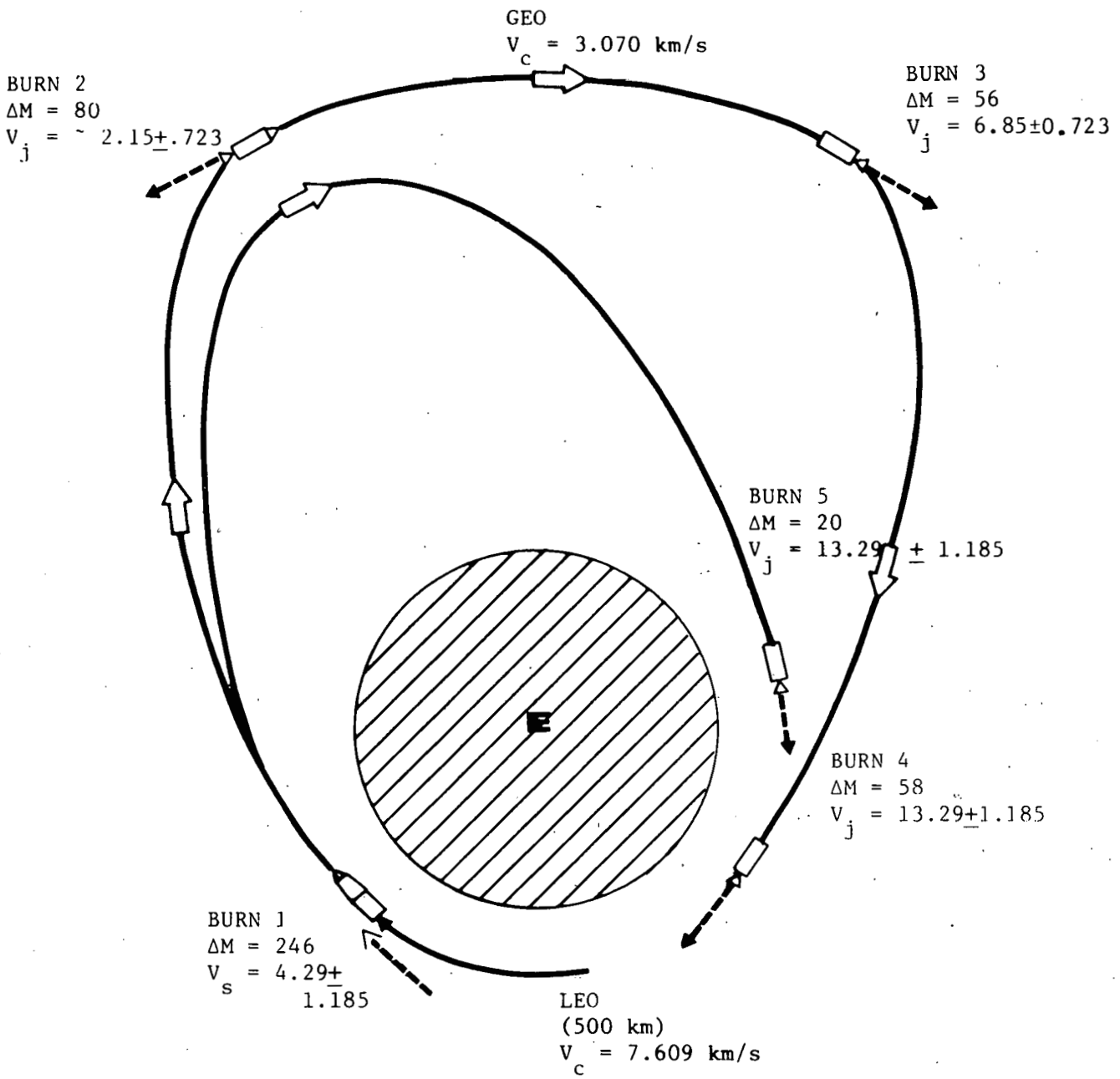

ΔM = Mass of Fuel Used, Metric Tons
V_s = ABS VEL of Effluent, km/s
(Escape VEL: LEO = 10.76 km/s
GEO = 4.34 km/s)

Figure 5. POTV Effluent Deposition

charge transfer or ion-molecule reaction to H_2O^+ or OH^+, which recombine very rapidly with free electrons by dissociative recombination; 10^4-10^5 times faster than do atomic O^+ ions. In this way an "ionospheric hole" is created and has been observed previously, in particular after the launch of Skylab-I (Mendillo et al., 1975a, b).

Preliminary calculations for a single HLLV second stage burn indicate a 40-50% electron density depletion in the F-region at night, with negligible depletion by day, and a 3-4 day recovery time. These effects are limited to altitudes above which the air ions are atomic, roughly 160-180 km; at lower altitudes the water/hydrogen injections will have a far smaller and more subtle effect (see Zinn et al., 1978, 1979; Mendillo et al., 1979).

Zinn et al. (1979) have made a fairly detailed comparison with the Skylab observations, and find reasonable agreement with the Sagamore Hill-ATS3 observations for appropriate values of the various parameters, in particular ionospheric winds, since their calculations indicate that the ionized hole disappears because it is blown out of the line of sight rather than because of re-ionization.

Clearly these single injection calculations do not tell us all that we need to know about the multiple launches associated with SPS construction, and this problem is discussed next.

3.2.2 Ionospheric Depletion due to the Multiple Launches during SPS Construction

As a result of the frequent (almost daily) launches associated with SPS construction operations one would expect to find a large region of constantly depleted ionization located near the launch site, which presumably would be Kennedy Space Center (Lat. 28.5°N, Long. 80.5°W). The largest effect will be due to the low altitude (70-120 km) burn of the HLLV second stage, and in particular due to H_2 rather than to H_2O emissions. At the altitudes of injection the H_2 is not photodissociated rapidly, but is oxidized slowly to water. However, it mostly diffuses upward into regions where there are large concentrations of O-atoms and a higher temperature, so that the oxidation to H_2O becomes rapid. In this way the HLLV gives rise to a relatively large concentration of H_2O in the atmosphere above 120-150 km where there is normally very little water. (By contrast, the injection of H_2O due to the HLLV second stage is probably not as important: it is not photodissociated but goes into a region in which there are significant quantities of water already, and it tends to freeze out and fall down. It cannot diffuse upward as rapidly as H_2 can, and thus is unlikely to affect the ionospheric F-region to the same extent.)

The effective de-ionization chemistry is somewhat complex; see Zinn et al. (1979) for an overall discussion, and Section 3.2.3 for details of the dissociative recombination of H_2O^+ and OH^+.

Overall, one may expect a region of reduced ionization at altitudes above 160-180 km (at lower altitudes most ions in the normal ionosphere are molecular NO^+ and O_2^+, which recombine quite fast with electrons, so that the addition of H_2O is unlikely to produce a very large effect), and up to several

hundred km above the F2-peak. The horizontal extent of the region of reduced ionization is hard to estimate. North-south dispersion will spread the cloud for a distance of perhaps 1000-3000 km about the latitude of injection (cf Section 2.6, in particular Table 7 and Figure 3). As a result of zonal (east-west) winds, it is likely that the depleted region extends completely around the globe at the latitude of injection, but some non-zonal behavior may occur.

The magnitude of the reduction in ionization may range from 40% to a factor of 2 in electron density at night, and significantly less in the daytime, perhaps as low as 10-20%. Note that these estimates are not based on detailed calculations or observation, and must be verified. Section 3.2.4 outlines how one would undertake the difficult task of verifying this prediction.

3.2.3 Dissociative recombination of H_2O^+ and OH^+ (Bernhardt -- prepared after the Workshop)

If we believe that condensation of water vapor in rocket exhaust is on the order of 10% or less, then water plays an important role in F-layer modification. The charge exchange reaction with O^+ is

$$H_2O + O^+ \rightarrow H_2O^+ + O \ , \qquad \text{rate: } 2.3 \times 10^{-9} \text{ cm}^3/\text{sec} \ .$$

The charge exchange reaction rate is known within ± 10% (Howard, Dundle and Kaufman, 1970).

The dissociative recombination process for the H_2O^+ is less well known. The ($H_2O^+ + e^-$) dissociative recombination (D-R) rate is estimated to be 3×10^{-9} cm^3/sec, based on D-R rates of similar ions (Biondi, 1973). The dissociative channels for H_2O^+ are: (See Wadt, Hay and Cartwright, 1977.)

$$H_2O^+(1^2B_1) + e^- \rightarrow O(^3P) + H_2(^1\Sigma_g^+) + 7.5 \text{ eV} \qquad (1)$$

$$\rightarrow OH(^2\Pi) + H(^2S) + 7.4 \text{ eV} \qquad (2)$$

$$\rightarrow O(^1D) + H_2(^1\Sigma_g^+) + 5.5 \text{ eV} \qquad (3)$$

$$\rightarrow OH(^2\Sigma^+) + H(^2S) + 3.4 \text{ eV} \qquad (4)$$

$$\rightarrow O(^1S)\ H_2(^1\Sigma_g^+) + 3.3 \text{ eV} \qquad (5)$$

$$\rightarrow O(^3P) + H(^2S) + H(^2S) + 2.9 \text{ eV} \qquad (6)$$

$$\rightarrow O(^1D) + H(^2S) + H(^2S) + .9 \text{ eV} \qquad (7)$$

The last two channels (6 and 7) involve O+2H formation. They arise from predissociation of the $OH(^2\Sigma^+)$ that is produced by channel (4). $OH(^2\Sigma^+)$ may also be lost by radiative transition to the ground electronic state. Three channels for $OH(^2\Sigma^+)$ loss are:

$$OH(^2\Sigma^+) \rightarrow OH(^2\Pi_i) + h\nu_{3050} \quad \Big\} \text{ radiative} \qquad (6')$$

$$\left.\begin{array}{l} \rightarrow O(^3P) + H(^2S) \\ \\ \rightarrow O(^1D) + H(^2S) \end{array}\right\} \text{ predissociation} \qquad (7')$$

The radiative and predissociation lifetime depends on the vibrational state of the excited hydroxyl. $\nu' = 0$, 1 and 2 indicate the first three vibrational states of the OH. The lifetimes given below are from Smith (1970):

ν'	Radiative Lifetime (nsec)	Predissociation Lifetime (nsec)
0	850	∞
1	750	6700
2	550	1560

The wavelength of emission from $OH(^2\Sigma^+)$ also depends on the vibrational state. The table below gives the most probable transition for radiation from the first four vibrational levels (Crosley and Lengel, 1975):

$OH(^2\Sigma^+)\nu' \rightarrow OH(^2\Pi_i)\nu$		Wavelength (Å)
ν'	ν	
0	0	3064
1	1	3122
2	1	3875
3	2	2945

These wavelengths can be observed during laboratory or space experiments involving H_2O^+ recombination. The $O(^1D)$ and the associated 6300 Å emission, produced by H_2O^+ dissociative recombination, may come by way of channel (3) or channel (7'). Care should be taken not to confuse the two.

A similar set of reactions results from the H_2 component in rocket exhaust.

$$H_2O + O^+ \rightarrow OH^+ + H \qquad \text{rate: } 2.0 \times 10^{-9} \text{ cm}^3/\text{sec} \pm 30\%$$

(Fehsenfeld, Schmeltekopf and Ferguson, 1967)

followed by

$$OH^+ (1^3\Sigma) + e^- \rightarrow O(^3P) + H(^2S) + 8.8 \text{ eV} \quad \text{(a)}$$

$$\rightarrow O(^1D) + H(^2S) + 6.8 \text{ eV} \quad \text{(b)}$$

$$\rightarrow O(^1S) + H(^2S) + 4.6 \text{ eV} \quad \text{(c)}$$

Again the excited atomic oxygen will fluoresce. H_2O^+ is produced in the molecular hydrogen atmosphere by the reaction

$$OH^+ + H_2 \rightarrow H_2O^+ + H$$ (Fehsenfeld, Schmeltekopf and Ferguson, 1967)

Consequently, the H_2O^+ ion is formed from both H_2 and H_2O releases into the ionosphere.

3.2.4 Verification of the Extent of the Depleted F-Region of Section 3.2.2

Because of the large scale of F-region depletion envisioned, simulation experiments involving actual releases of combustion products are not feasible, but instead we must rely on physically-based, numerical computations to predict the morphology. Two-dimensional and small-scale, three-dimensional calculations can close a large part of the gap. Such calculations can be made quite accurate and can be verified by comparison with small-scale release experiments.

However, in the final analysis we must rely on large-scale numerical simulation of the large-scale morphology. The model must include a good representation of the neutral atmosphere, including winds, tides, and possibly also waves. It must include self-consistent electric fields, plasmaspheric depletion, and plasma photochemistry and dynamics, including the effects of temperature variation.

This type of model development is a major problem involving a relatively long lead-time (3-5 years) on account of the requirements for verification, which include:

1. "bench-marking" against smaller 2-D and 3-D calculations;

2. testing the model against ambient diurnal and seasonal ionospheric variations; and

3. inter-comparison of different models.

3.2.5 Possible Experimental Verification: Some Relevant Natural Phenomena (Carlson -- prepared after the workshop)

In assessing the impact of SPS injections on the thermosphere/ionosphere, one should consider the normal morphology of the region, both as a frame of reference and as a potential source of answers to some of the questions raised. Two examples are given:

1. A regular natural perturbation feature of the nighttime ionosphere at lower altitudes and mid-latitude leads to a factor of three to ten decrease in F-region electron concentration over a time scale of about one hour, corresponding to a displacement of about 1500 km in longitude. In the case of this natural event, the perturbation is due to an interruption or sometimes reversal of the component of neutral wind upward along the direction of the geomagnetic field lines. The interruption of this transport term, which initially maintains the ionospheric plasma in a region of very low recombination rate, allows the plasma to descend in altitude by one to two neutral scale heights so that it recombines rapidly. In the case of SPS operations it is a perturbation of the plasma recombination rate at a given altitude, rather than a transport perturbation bringing the plasma to an altitude of much higher recombination coefficient (see Hanson & Carlson, 1977, p. 94).

2. What is the impact of a major ionospheric F-region depletion on the ion concentration in the conjugate hemisphere? Under typical nighttime solstice conditions, the trans-equatorial, F-region, interhemispheric winds tend to push the ionospheric plasma upward along geomagnetic field lines to regions of low recombination in the summer hemisphere, and downward to regions of rapid recombination in the winter hemisphere. This leads to strong asymmetries of plasma concentration for a given F-region and topside altitude at conjugate ends of the field lines. At latitudes within about 20° of the magnetic equator this pressure asymmetry is believed to cause strong ion temperature, T_i, asymmetries (cold T_i near and above say 1000 km altitude on the summer side and hot T_i in the conjugate region). The argument is in terms of interhemispheric plasma transport upward along the field lines on the summer high plasma pressure end, involving cooling by non-adiabatic expansion conductive heating while the plasma is at high altitudes, and compressional heating while the plasma is descending along the winter end of the field line. An absence of observation of this effect at greater latitudes, and the interpretation of such a cutoff, would directly relate to the parallel conjugate plasma pressure asymmetry problem for the SPS case (Hanson & Carlson, 1977, p. 93).

3.2.6 Effects of the Reduced Ionization of HF Propagation (Bauer)

The potential effect of reduced ionization in the F-region on global skywave HF communication is very significant. A reduction in F-region electron density by a factor of two reduces the maximum usable frequency (MUF) by a factor $\sqrt{2}$, so that in the relevant geographic region the available frequency band is reduced from 3-30 MHz to (say) 3-21 MHz. However, for long-range communication the upper portion of the band, say 15-30 MHz, is optimal, so that a reduction of MUF from 30 to 21 MHz reduces the available band from 15 to 6 MHz. This is a very serious effect because:

1. the HF band is very heavily used, internationally;
2. lesser developed countries (LDCs) in particular depend heavily on this cheap and simple communication medium;
3. a reduction in F-region ionization near latitude 30°N or even closer to the equator would be particularly significant for many LDCs, that are located at these low latitudes;

4. frequency allocations are subject to international negotiation, and the USA is under considerable pressure to reduce its use of this frequency band, thus the suggestion that SPS would reduce the available band might well be received rather unfavorably; and

5. the medium for negotiations is the CCIR, and negotiations for the current revision of frequency allocations are at present under way in Switzerland.

Three additional comments may be made:

(1) Skywave HF Communication is inherently a variable medium because of normal ionospheric variations. However, while a 40% variation in MUF on a day-by-day basis over a given path is possible, and is accepted as being due to natural ionospheric changes, yet a permanent reduction in the total band by 40% would probably not be considered generally acceptable, although it is unlikely that a single event such as the launch of Skylab-I or of HEAO-C would lead to international repercussions.

(2) The various higher altitude burns of circularization, de-orbit, POTV, etc., involve small, highly localized, high-altitude depletions in ionization, that generally will not affect HF skywave propagation in a surface-to-surface mode. Thus it seems quite unlikely that their effects would be significant in the present context.

(3) Effects on the mesosphere ("Domain A"), i.e., on the ionospheric D- and E-regions, may be significant for LF, VLF, ELF (i.e., less than 100 kHz), which have some military and navigation (LORAN) uses, but these effects are unlikely to be important for HF signals that transit these low-lying ionized regions without significant attenuation. For the AM Broadcast band (MF) skywave propagation is not an important mode, so that the additional attenuation is unlikely to be critical.

3.2.7 Ionospheric Irregularities Associated with the Depleted Regions

At the edges of depleted regions there presumably will be a variety of irregularities, such as bubbles of depleted ionization, which will give rise to Spread F types of ionospheric irregularities and also to traveling ionospheric disturbances (TIDs). The overall scale, morphology and hence impact of this major perturbation is being calculated. It is important but difficult to be sure that nothing has been omitted, and yet an adequate atmospheric simulation is hard to achieve because of the different types of phenomena that may be anticipated on different scales for the depleted region.

The morphology of the depleted ionospheric regions will be a strong function of the source characteristics of the H_2O and H_2 resulting from combustion. These sources are twofold, namely, the upward diffusion of H_2 molecules from the HLLV second stage main burn, and the injection of combustion products at F-region altitudes due to HLLV circularization and deorbit and due to POTV main engine burns.

In conclusion, we make a few remarks about ionospheric irregularities. We now know of two distinct types of plasma instabilities that actually lead to irregularity growth in the ionosphere. They are the $\vec{E}x\vec{B}$ Gradient Drift instability, which is responsible for striations in barium clouds, and the Gravitational Rayleigh-Taylor instability, which is responsible for the growth of Equatorial Spread F. Both of these instabilities have been well studied and are reasonably well understood and both may be associated with the ionospheric morphology produced by SPS operations. However, it cannot now be asserted whether that morphology will lead to growth or damping of irregularities. The Current Convective instability has recently been proposed as also occurring in the natural ionosphere. It could also be associated with SPS ionospheric morphology but has not yet been well studied. In summary, there are a number of plasma instabilities that might cause irregularities, but the morphology associated with the SPS scenario is insufficiently well known to state with some confidence which, if any, might actually apply.

3.3 EFFECTS ON SATELLITE DRAG (Curtis)

The drag force on a satellite is given by

$$F_{drag} = 1/2\ \bar{\rho}\ v^2\ S\ C_D \tag{3.1}$$

where $\vec{v}$ is the satellite velocity, S is its projected surface area normal to $\vec{v}$, C_D is the drag coefficient (dimensionless number of order one) and $\bar{\rho}$ is the mean atmospheric mass density

$$\rho = (1/n_T)\ \Sigma_i\ m_i\ (n_i/n_T)\ . \tag{3.2}$$

Here n_T is the total number density of the thermosphere and m_i and n_i are the mass and number density of the i-th constituent.

The change in effective satellite altitude, z, is related to the density through the relation (Cook, et al., 1960; King-Hele, 1962; Cook and King-Hele, 1963)

$$dz/dt\ \alpha\ \bar{\rho}\ . \tag{3.3}$$

Thus one obtains a given change in altitude Δz for a circular orbit of period T which lies within a density enhancement $\Delta\rho$ for a time ΔT:

$$\Delta\ z \propto \bar{\rho}\ (T-\Delta T) + (\bar{\rho} + \Delta\bar{\rho})\ \Delta T\ . \tag{3.4}$$

The enhanced change in z is then

$$\sigma(\Delta z) \propto \Delta\bar{\rho}\ \Delta T \ . \qquad (3.5)$$

For a given source strength, with a fraction ΔC of the circumference C of the orbit lying within the region of enhanced density, we have $\Delta\rho \propto (\Delta C)^{-2}$, $\Delta T \propto \Delta C$, and hence $\delta(\Delta z) \propto (\Delta C)^{-1}$. Thus, the more extended the density enhancement the less is the drag enhancement, given that the satellite passes through the region of enhancement. Of course, the smaller ΔC is, the easier can the enhanced region be avoided.

Determination of the significance of drag effects is thus equivalent to determining the change in mean density.

Possible mechanisms for enhancement in $\bar{\rho}$ are:

1. Deposition of O and O_2 from the HLLV.

2. Heating of the thermosphere by direct HLLV exhaust heating, or from the exothermicity of the dissociative recombination reactions of the ionized HLLV exhaust, such as $H_2O^+ + e^-$.

3. Heating of the polar regions caused by argon deposition in the plasmasphere. The deposition moves the plasmapause outward and thus moves the precipitation to higher latitudes. If the precipitation remains constant, the resulting concentration of precipitation towards the pole could increase the heating of polar regions. The increase in polar heating would increase $\Delta\rho$ and hence the drag, which may adversely affect the orbital lifetime of polar orbiting satellites.

In summary, what needs to be done is:

1. to determine the steady state magnitude of $\Delta\bar{\rho}$, given the SPS transportation requirements; and

2. to determine the horizontal spatial extent of the region of enhanced density, in which $\Delta\rho \neq 0$.

3.4 AIRGLOW (Turco)

The release of H_2O and H_2 in the mesosphere and thermosphere will lead to changes in the hydrogen and oxygen balances of these regions. As a result, alterations in airglow emissions are anticipated. The most obvious candidate for change is the OH infrared band system (~ 0.6-3.0 μm). Other emissions that might be affected include the $O(^1D)$ and $O(^1S)$ red (630 nm) and green (557.7 nm) lines, and the singlet molecular oxygen atmospheric band of $O_2(^1\Delta_g)$ at 1.27 μm and of $O_2(^1\Sigma_g^+)$ at 0.76 μm. The atomic oxygen singlets are expected to be influenced by ion chemistry (e.g., $OH^+ + e^- \rightarrow H + O^*$), while the molecular oxygen singlets may be affected by changes in odd-oxygen chemistry (e.g., $O + OH$, $O + O + M$, and $O_3 + h\nu$ reactions). Finally, enhanced UV and IR radiation from NO, NO^+ and $N(^2D)$ may occur in reentry plumes in which air is heated to several thousand degrees Kelvin and N and NO are produced in large amounts (see Park and Menees, 1978).

A. OH. The near-infrared band emissions of OH have been studied extensively since their discovery by Meinel in 1950. They are a prominent feature of both the nightglow and the dayglow. The OH airglow is found everywhere over the globe, and its morphology has been described by Jones (1973), among others. The principal mesospheric excitation mechanism is the reaction (Meinel, 1950)

$$H + O_3 \rightarrow OH(v) + O_2$$

where vibrational states up to v = 9 are populated. Through detailed calculations, it is found that following the $H + O_3$ reaction, the number of photon emitted in the vibrational sequences $\Delta v = 1, 2, 3, 4$ are roughly 2, 3, 0.04, 0.005, respectively. Although there is some controversy over the degree of rotational equilibrium of the nightglow OH emission, Krassovsky et al. (1977) have presented evidence showing that the rotational temperatures of different vibrational bands are roughly equal when viewed simultaneously to within an experimental precision of 10-20 K, and correspond to ambient temperatures within this same precision. Thus, high resolution OH emission spectra may be utilized to determine (crudely) air temperatures in the upper mesosphere, but (with current instrumentation) only at night when background light levels are low.

When water is released in the thermosphere, charge exchange with O^+ produces H_2O^+, which, upon recombination with electrons, generates hydroxyl radicals. The degree of vibrational and electronic excitation of the OH formed in this way is unknown, but should be determined. In this regard, M. Pongratz (private communication) notes that very little OH vibrational emission in the (9,4) and (5,1) bands was observed following the LAGOPEDO F-region water release. This implies little excitation of the v = 9 and v = 5 OH vibrational levels.

The concentration of hydrogen atoms in the atmosphere is directly related to the total amount of hydrogen in all forms residing there. Above 80 km, injected water vapor will be decomposed by sunlight and ion-molecule reactions; the resultant hydrogen is partitioned between H and H_2, with some of the H-atoms being continuously recycled betwen H and OH. Thus, the spatial and temporal changes in airglow intensity caused by the passage of a rocket will depend on the amount of water vapor released, on its rate of dispersal and removal as against decomposition, and its photochemical partitioning into H, OH, and H_2. (In addition, it must be noted that in typical H_2-O_2 rocket motors, perhaps 25% of the hydrogen is emitted at H_2 rather than as H_2O.)

The major impact of enhanced OH emission rates may be their influence on the mesopause temperature and, consequently, their possible connection with noctilucent cloud formation (Chenurnoy and Charina, 1977). Interestingly, Moreels and Herse (1977) have observed wave-like structures in OH emision patters that match some noctilucent cloud patterns.

B. Singlet oxygen. The $O(^1D)$ 630 nm red line and the $O(^1S)$ 557.7 nm green line are well-studied emissions whose morphology is fairly well established. The lines can be excited photochemically ($O_2 + h\nu$, $O + O + O$) and through ion neutralization reactions, and normally originate about 90 km.

The emissions often color auroral displays, and they are a prominent feature of some high-altitude nuclear explosions. More to the present issue, enhanced $O(^1D)$ emissions have been observed during a large F-region explosive release that emitted large quantities of H_2O and CO_2 (Pongratz et al., 1978). However, it is thought that much of this emission comes from CO_2^+ recombination rather than OH^+ recombination (Pongratz, private communication), but J.M. Forbes (private communication) suggests that the predominant source is O_2^+ recombination since the reaction

$$CO_2 + O^+ \rightarrow O_2^+ + CO$$

is the dominant path for removal of CO_2 molecules in the F-region. Thus, it is not yet clear what changes in the intensity of $O(^1D)$ and $O(^1S)$ emissions are to be expected as a result of SPS rocket activity.

The molecular oxygen singlets, $O_2(^1\Delta)$ and $O_2(^1\Sigma)$, are responsible for some of the strongest atmospheric emissions in the near IR, which are easily monitored. With regard to SPS rocket activity, these emissions could be affected by changes in the photochemical reaction cycle of oxygen constituents caused by water vapor.

C. NO emissions. The long wavelength atmospheric emissions due to NO reactions are discussed by Ogawa (1976). In the wake of a reentering spacecraft, one should observe the strong NO + O chemiluminescence in the visible and near IR regions. After some dispersion, NO and NO^+ IR emissions at 5.3 and 2.8 μm, respectively, might be detectable from rockets or satellites, as might resonant scattering of solar UV by the NO γ-bands. In addition, the weak emission from $N(^2D)$ at 520 nm, mainly from above 120 km, might be affected by large water vapor releases.

D. NaD emission. Emissions at 589 nm are well correlated with OH emissions (Takahashi et al., 1979, and other references cited therein). Hence, changes in OH emission (see subsection A) should lead to changes in NaD emissions.

3.5 POTENTIALLY IMPORTANT PHENOMENA (Vondrak)

The following issues are most relevant to the terrestrial environment and to users of operational systems:

1. Ionospheric Depletions. These include large but localized depletions associated with HLLV circularization burns, more widespread but smaller effects of insertion burns and POTV burns, and other depletion such as draining of plasmaspheric flux tubes and depletions in the conjugate region by interhemispheric transport. The major user impact affects communication in the following two ways.

   (a) HF skywave communication may be degraded by altering the ionospheric morphology (H, H). (See in particular Section 3.2.6.)

(b) Transionospheric communication may be adversely affected by the formation of irregularities at the large density gradients associated with the edges of ionospheric holes. (U/H, H). (See Section 3.2.7.)

2. Increase in Airglow, Reflectivity (due to Ice Crystals), and IR Emissivity of the thermosphere reduce the effectiveness of satellite-borne systems for surveillance and remote sensing. (H, U)

3. An increased thermospheric density (by heating or increase in H-atom density) alters the satellite drag. (H, U/L)

3.6 ATMOSPHERIC EXPERIMENTS

3.6.1 Rocket Experiments (Pongratz)

The questions at issue are: What can be learned from planned rocket launches, such as Atlas-Centaur? and, Can any dedicated launches or experiments be justified?

Among outstanding questions vis-a-vis B-Domain depletions are the H_2O^+ dissociative recombination branching ratios, ice crystal sublimation and chemistry, and the generation of ionospheric irregularities.

Many experimenters (L. Duncan, LASL; M. Mendillo, B.U.; among others) plan to measure electron density and neutral winds with the Arecibo radar, airglow, and amateur (HAM) radio signals during the upcoming HEAO-C/Atlas-Centaur launch. A prime result of these observations is likely to be code verification. The TEM experiments (McIntyre, 1978) could be used to study ice crystal sublimation. The Space Shuttle and deorbit burns beginning in 1980 should shed light on whether or not ionospheric irregularities are produced following depletion; sounding rocket launches from India may be able to diagnose the phenomenology resulting from these burns.

Dedicated launches may involve diagnostic sounding rockets following larger target of opportunity rocket launches, non-operational Space Shuttle burns, and dedicated depletion experiments. The most likely significant impacts of depletions would be the generation of irregularities and that the models of depletion should be tested against these sources. Planned depletion experiments conducted from Kwajalein seem to provide a feasible method to test the models. Kwajalein has three key features regarding the issue of irregularities resulting from ionization depletion:

1. incoherent scatter radar: to diagnose plasma irregularities.

2. sounding rocket launch capabilitites: according to Anderson and Bernhardt, (1978), small sounding rockets may be capable of carrying payloads that could produce depletion in ionization and in turn cause irregularities; and

3. correct magnetic field geometry for the gravitational Rayleigh-Taylor instability.

Dedicated experiments could involve the monitoring of airglow from high altitude satellites. Such monitoring could detect the depletions resulting from target-of-opportunity launches, and perhaps determine the branching ratios from the $H_2O^+ + e^-$ dissociative recombination reaction.

3.6.2 LAGOPEDO- Type Releases (Fedder)

This type of release is important for the following reasons:

1. The data provides a checkpoint for theoretical and morphological code work.

2. The data can provide one bound on the chemistry calculations and thus a check on their prediction.

3. The data may demonstrate the growth or damping of irregularities and therefore of scintillation phenomena.

4. The data can provide some estimate of ice-vapor fractionation. However, because of the difference in specific enthalpies, this estimate is not directly applicable to the question of condensation in rocket exhausts.

Undoubtedly new experiments are necessary and valuable, but complete analysis of the LAGOPEDO data is of primary importance, should have the highest priority, and should be completed at an early date.

3.6.3 Ionospheric Irregularities (Bernhardt)

Three types of studies are proposed:

1. Active experiments in the thermosphere.

2. Laboratory studies.

3. Theoretical studies.

The object of these studies is to reduce uncertainties in chemistry, transport, and/or temperature change.

The chemistry of the ionosphere has been studied for many years. Ion-molecule reaction rates are readily available from laboratory measurements, as are many electron-ion recombination rates, but not the ones of greatest interest here:

$$H_2O^+ + e^- \rightarrow \begin{cases} OH + H \\ H_2 + O \\ H + H + O \end{cases}$$

$$OH^{+} + e^{-} \longrightarrow O + H$$

for which we need the branching ratios and states of excitation of the products as well as the rate constants.

Regarding transport processes in the thermosphere, diffusion coefficients are well known, but the data base on neutral winds is not very adequate.

Thermal changes due to ionopsheric depletion have been estimated by Bernhardt (1976). The electron temperature can increase by factors of 2-4, and this will change the chemical reaction rates in the ionospheric plasma to second order. To first order the plasma transport will be affected by plasma temperature increases. Questions related to the actual situation of a hot, tenuous plasma imbedded in a cold, dense plasma should be considered.

Irregularity formation due to plasma instabilities should be considered. At middle or high latitudes a gradient drift instability can be driven by a neutral wind perpendicular to the geomagnetic field lines. At equatorial latitudes, a gravitationally driven instability can produce Spread F irregularities, and Traveling Ionospheric Disturbances (TIDs), which are gravity waves propagating upward from disturbances in the lower atmoshere, can also give rise to equatorial Spread F.

A significant question to ask is the following:

- What effects produced by injections of exhaust are not seen in nature?
- ANSWER: New species and energy injected in to the F-region and the subsequent strong, localized depletion and, possibly, irregularities.

We need experiments to study phenomena that do not occur naturally.

3.6.4 Other Experiments (Aikin)

Conjugate point release experiments should receive a high priority; the Space Shuttle chemical release facility would be useful to accomplish such experiments.

Chemical reactions can be studied in the space environment by use of the Shuttle release and diagnostic facility.

Laboratory Experiments

1. Study of the electron-ion dissociative recombination coefficient for H_2O^{+}. Determine the rate, identification, and energy of the products.

2. Surface neutral chemistry on ice crystals.*

3. Attachment of electrons to ice crystals.*

4. Cross section of O-H collision for excitation of fine structure transitions in atomic oxygen because collisional excitation of these transitions in O-H collisions might cool atomic hydrogen below the ambient thermospheric temperature, and thereby reduce its escape (Fahr and Nass, 1979).

*First of all do a simple model calculation to see whether the effects could be significant.

4 MAGNETOSPHERIC EFFECTS

4.1 INTRODUCTION

As one goes to outer regions of the earth's atmosphere where plasma effects become important, the character of the problem changes. In this very low density regime the relative injections of both mass and energy are large, and on account of the infrequency of collisions and of the predominance of long-range interactions associated with the geomagnetic field, the possible distance scale of phenomena becomes very large, and so do the unknowns and major uncertainties.

Chemical rockets produce large injections of hydrogen atoms both from the personnel vehicle, POTV, which is chemically propelled and makes some 12-17 flights per year between LEO and GEO, each with a duration of a few hours, and also from the cargo vehicle, COTV. The COTV uses electrical propulsion as its primary mode, and thus one round trip from LEO to GEO takes 160-180 days because of the very low thrust of its argon ion engines. Nevertheless, while it uses chemical (H_2-O_2) engines only for attitude control and other auxiliary power, yet the total number of hydrogen versus argon atoms emitted is comparable (see Table 3).

The main propulsion for COTV is provided by a series of 1-5 keV Ar ion engines, which also put out a neutralizing beam of electrons. The energy distribution of the argon ions is approximately thermal, so that the ion beam is less efficient at exciting plasma instabilities than is a monoenergetic ion beam. The quantities of injectants per flight and per year are listed in Tables 1 and 3, respectively. The reason why so many hydrogen atoms are emitted is that each argon ion provides perhaps 5000 times as much energy and 400 times as much thrust (i.e., momentum) as does a hydrogen atom.

The phonomenology of H_2O/H_2 injections is sketched in Section 4.2, while that of Ar^+ ion injections is outlined in Section 4.3. Some possible effects are mentioned in Section 4.4. The need for a synthesis of H and Ar^+ injections, and some possibly important phenomena, are discussed in Section 4.5, and some possibly relevant atmospheric experiments are reviewed in Section 4.6.

4.2 PHONOMENOLOGY OF H_2O/H_2 INJECTION IN THE PLASMASPHERE AND MAGNETOSPHERE (Zinn)

The fate of H_2O and H_2 molecules injected in the F-region and the changes that they produce in electron and ion concentrations have been discussed in great detail (see Mendillo (1978, 1979), Zinn et al. (1978, 1979), and Section 3 of this report). For injections at higher altitudes, the same phenomena will occur, provided that the molecules are not injected with velocity vectors such that they become trapped in stable orbits or escape from the earth. That is, if they can fall, they will fall to 270 km, or so, where they produce the now familiar F-layer effects.

There are several situations among the proposed SPS rocket scenarios where the exhaust molecules can escape or become trapped. Some of those

situations, for the POTV, are discussed in Section 3.1.3. Another situation is the deorbit burn of the HLLV, where most of the molecules are ejected with velocities sufficient for escape.

If the molecules escape, we believe they can be forgotten, since they do not represent a significant H or O loss compared to that which occurs normally in nature. On the other hand, if they are trapped in orbits, they can react with H^+ or O^+ ions, provided that they do not photodissociate first. At LEO altitudes the $O^+ + H_2O$ charge exchange reaction is considerably faster than the H_2O photodestruction. Therefore, trapped exhaust molecules in LEO or in orbits passing through the 300-600-km altitude range will lead to destruction of ions, with consequent depletion of the F-layer and protonosphere. Such depletions will be very widespread spatially, but probably small in terms of percentages of ions removed because the absolute numbers of exhaust molecules injected in trapped orbits are comparatively small.

4.3 INJECTION OF keV PLASMA (Palmadesso)

4.3.1 Potential Consequences

A. Alter radiation belt populations. Chiu et al. (1979) have argued that in the worst case (complete capture of the argon beam in the near magnetosphere, and long lifetime for the trapped argon) the hydrogen ion cyclotron instability that normally leads to scattering and precipitation of energetic electrons will be suppressed, thus allowing the electrons to increase in number until their population approaches an asymptotic upper limit. In this worst case scenario, the energetic electron density is increased by a factor of the order of 2. (See discussion by Davidson in Appendix F, item F.5.)

B. Production of energetic argon ions via convection (HZE problem). By a process which is only partially understood at present, some oxygen and other ions injected into the magnetosphere are accelerated to very high energies. Adiabatic earthward convection energizes particles, but in order to be accelerated to extremely high energies the particles must move away from the earth without much energy loss and repeat this process several times. Other mechanisms that are thought to accelerate ions are interactions with ion cyclotron waves, electric fields along the magnetic field lines, and magnetospheric circulation forward to the magnetopause, to the magnetotail, and again forward to the inner magnetosphere. Presumably the number of particles accelerated to a given energy decreases rapidly as the energy increases. Thus the number of high Z argon ions that might be energized in this way is not now known.

C. Gross change in plasmasphere composition and temperature. If the argon ion and energy injections in the magnetosphere are long-lasting, the temperature, density, and chemical composition of large portions of the inner magnetosphere may be altered substantially by the stopping of the Ar^+ exhaust beam in these regions. The practical consequences of this, if any, are not known at present. Generally, however, an increase in plasma density stabilizes the radiation belts.

D. Enhanced generation of geomagnetic storms. This is a somewhat more speculative possibility, based on the assumption that the ion beam will not be contained in the inner magnetosphere but will instead penetrate great distances. If the beam is directed into the earth's magnetotail, it may alter the local resistivity in the merging region and thus change the merging rate.

4.3.2 Phenomenology Issues to be Resolved

A. Beam stopping distance. There is a certain question about how rapidly the ion beam is stopped in the magnetosphere. Chiu et al. (1979), using the observations of Haerendel and Lust (1970) on a barium cloud in the magnetosphere, suggest that the ions are stopped even in the very tenuous outer magnetosphere; Curtis and Grebowski (1979) have questioned this. In view of our limited understanding of ion motions in the magnetosphere, this issue calls for further work.

B. Argon lifetime in the magnetosphere. This is a critical question. The loading of argon in the magnetosphere will be determined by balancing injection rates with the loss rates associated with diffusion and pitch angle scattering processes. If the loss rates are high, the argon loading will be relatively small (short argon lifetime). In the opposite case, argon accumulates for a long time and the loading is large. The lifetime of Ar^+ in the magnetosphere is a parameter that must be determined or estimated in order to make quantitative assessments of the possible consequences of argon injection.

C. Energy lifetime in the magnetosphere. This is similar to B above. The argon energy may be shared with ambient ions, and we must estimate an energy lifetime in order to assess the magnetospheric energy loading.

D. Relativistic Electron Precipitation (REP) events. The proton cyclotron instability discussed in Item A of Section 4.3.1 above may not be the only mechanism for precipitating energetic electrons; indeed, some REP events cannot be explained on this basis. If another process does exist and can be identified, the likelihood of occurrence of the proton cyclotron instability and/or the severity of its effect may be reduced.

4.4 SOME POSSIBLE EFFECTS

4.4.1 Enhancement of Trapped Radiation (Chiu)

Modification of the plasmaspheric composition, from a natural H^+ plasmasphere to one consisting mainly of the heavier O^+ and Ar^+ ions, may lead to the suppression of ion cyclotron wave generation. This activity in turn means a possible enhancement of trapped relativistic electron dosage level to about 2-3 times the present level, although it must be noted that pitch angle scattering by ion cyclotron waves is not the only mechanism by which relativistic electrons are precipitated into the atmosphere.

Argon ions may possibly be recycled and energized by radial diffusion, ion cyclotron turbulence, electronic fields, and magnetospheric circulation to

high energies (hundreds of MeV), thus enhancing the population of HZE particles.

The dosage level of HZE particles is very important for the question of radiation dosage for space workers and for the degradation of surfaces by sputtering, while the dosage level of relativistic electrons is significant for the rate of degradation of spacecraft instrumentation as well as for health problems of space workers.

Suggestions for experimentation and for the utilization of targets of opportunity in this area are integrated into Sections 4.6.2 and 4.6.3.

4.4.2 Dumping of the Radiation Belts (Aikin, Cladis)

A. Inner Belt Protons. Inner radiation belt protons may be precipitated into the stratosphere and mesosphere as a result of plasma turbulence caused by Ar^+ ions from the ion thruster engine. Proton interaction with the atmosphere creates ionization at altitudes between 30 and 100 km, leading to a possible disruption of VLF communications and a modification of the ozone distribution. The magnitude of the effect is limited by the rate of repopulation of the inner belt protons. Since the mechanism for repopulation is the decay of albedo neutrons resulting from cosmic radiation, a long time, perhaps as much as 100 years, is required for repopulation. It is expected that following the initial dumping of the belt, subsequent precipitation will be limited by the low belt population. The amount of ozone destroyed initially needs to be calculated, but is less than that of the August 1972 Solar Proton Event.

The high energy, inner-belt proton fluxes are very stable, and it is very unlikely that their distribution would be appreciably altered by the presence of the Ar^+ beam or by an enhanced trapped Ar^+ population. In fact, the enhanced plasma density would make the proton distribution more stable. If it is assumed, however, that the distribution were destabilized by some unknown mechanism, such that the protons were precipitated at the "strong" pitch-angle diffusion rate, the flux of precipitating protons of energy greater than 50 MeV (penetrating to 30 km) would be less than about 3×10^3 cm^{-2} sec^{-1}. This flux is about the highest that can be expected; and, at this rate, the proton reservoir would be depleted in about an hour. During the solar proton events of 3-11 August 1972, the flux of protons of energy 29-100 MeV incident on the atmosphere at high latitudes exceeded 2×10^5 cm^{-2} sec^{-1}, and it remained high for several days. Hence, it appears that the effects of the precipitation of the trapped energetic protons will be small in comparison to the effects produced by large solar proton events.

B. Outer Belt Electrons. The precipitation of electrons from the outer radiation belt will cause atmospheric ionization at geomagnetic latitudes outside the equatorial zone. The magnitude and frequency of occurrence of the effect needs to be determined. Communications will be affected and some ozone will be destroyed. In fact, this is a relativistic electron precipitation (=REP) event, and it can be shown -- see Bauer (1978), Figure 2-1 and Appendix E -- that the effect of an REP on ozone is small compared to that of a solar proton event or to galactic cosmic rays.

Questions:

1. What is the frequency of occurrence and magnitude of electron precipitation as a function of geomagnetic latitude?

2. What is the influence on the D-region?

3. What is the influence of ionization caused by electrons and accompanying bremsstrahlung on atmospheric ozone?

4.4.3 Depletion versus Enhancement of the Radiation Belts (Curtis)

The question of whether the radiation belt fluxes are depleted or enhanced depends strongly on the deposition mechanism for the Ar^+ beam in the plasmasphere. Three mechanisms of beam stopping have been suggested, namely, stopping of the ion cloud, loss of the beam sheath, and plasma instabilities.

If the beam is stopped by an ion-cloudlike mechanism (Chiu, et al. 1979) the deposited Ar^+ will have energies much lower than the beam energy. Thus the deposited Ar^+ will be essentially cold, i.e., it will have energies of the order of plasma energies in the plasmasphere. The cold Ar^+ can suppress the ion cyclotron instability and hence enhance the flux of radiation belt electrons.

If, however, the ion beam sheath loss mechanism of Curtis and Grebowsky (1979) is the dominant effect, the Ar^+ deposited in the magnetosphere has energies of the order of the beam energy, and hence the deposited Ar^+ is hot and anisotropic. The hot Ar^+ will give rise to plasma wave turbulence and hence pitch angle scattering of both the hot Ar^+ and radiation belt protons will occur. In this case the radiation belt protons could perhaps be depleted if the resonance relations have the appropriate numerical values.

Plasma instabilities could give rise to either hot or cold Ar^+, depending on whether pitch angle scattering or energy degradation is the dominant result of the plasma instability.

Although the hot Ar^+ cools off during its residence in the plasmasphere via electron Coulomb scattering and driving plasma instability turbulence, it is not clear that the hot Ar^+ has sufficient time to become cold Ar^+ before it is removed from the plasmasphere via precipitation and charge exhange.

Thus, it may well be the case that the initial beam dissipation mechanisms outlined here will strongly determine the character of the modifications to the radiation belt.

Since the greatest radiation belt fluxes occur near the magnetic equator, plasmasphere heating which can increase O^+ in the plasmasphere and hence suppress ion cyclotron turbulence will be limited to the lower levels of the plasmasphere, and most likely would not be as important as cold Ar^+ in ion cyclotron suppression.

4.4.4 Phenomenology Associated with Large Space Structures (Vondrak)

In addition to the transportation system used between LEO and GEO and any possible effects due to microwaves (which are not considered here), another potential source of magnetospheric modification is provided by the SPS satellite structure itself. The satellite interacts with the magnetosphere in the following ways:

1. The structure will be a sink that absorbs particles striking it. This flux tube blockage is analogous to the sweeping of the Jovian radiation belts by the Galilean satellites. (See also Kesler and Cour-Palais, 1978).

2. The satellite will charge, probably to a negative potential, and the ambient ion population will be accelerated to it.

3. The structure wll be a localized source of IR and reflected visible light. This has been reviewed in a workshop held recently, whose report (Stokes, 1979) has not yet been published. See also Item F.4 of Appendix F.

4. The satellite will emit photoelectrons. These relatively cool electrons may interact with the ambient plasma.

5. The structure will be a source of contaminant gases that may form a ring of neutral gases at GEO. Neutral gases are also emitted at GEO by ACS thrusters. The interaction of such neutral gas molecules with the ambient plasma at GEO is not well understood.

6. Meteoritic impact and energetic particle sputtering of spacecraft sufaces may be a substantial source of particulate material at GEO.

4.4.5 A Ring of Neutral Gases Associated with the Satellite (Garrett)

Vondrak (1977, 1979) has suggested that the possibility exists for the formation of a permanent ring of neutral gas around the earth. In Garrett and Forbes (1979), the likelihood of the formation of such a ring forming in geosynchronous orbit has been considered. The problem readily reduces to that of determining the ionization rate of the neutral cloud formed in the immediate vicinity of the emitter (the SPS satellite in this case). Over the long-term SPS mission, the major continuing contaminant would be neutral gas from the control thrusters. For Ar thrusters, given the current configuration, Garrett and Forbes find that the neutral cloud created would have a characteristic ionization time of 15 days. The Ar^+ cloud created would have a maximum density of only 0.01 cm^{-3} under normal conditions at the edge of a cloud 40 km in radius. Hence, the impact of the ions would be insignificant. The long ionization period, however, would allow a neutral ring with density of about 2 cm^{-3} to form. The impact of this cloud is not clear. Likewise, the H_2 and H_2O emitted by the POTV may also contribute to such a ring. As existing analytic techniques are capable of estimating the distribution of such a cloud, it is recommended that this analysis be carried out.

4.5 SYNTHESIS OF MAGNETOSPHERIC EFFECTS AND POSSIBLY IMPORTANT PHENOMENA (Chiu)

The two major elements of propellant release effects leading to environmental modification in the magnetosphere are:

(a) deposition of COTV Ar^+ beam energy in the magnetosphere giving rise to composition and density modifications of the magnetosphere; and

(b) deposition of H_2O and H_2 neutrals from POTV and COTV at high concentrations in the equatorial regions representing an artificial charge-exchange medium that may reduce the trapped radiation belt particles.

The resulting modification of the magnetosphere also alters the magnetospheric response to geomagnetic storms. These major elements are mutually interacting, and thus it is necessary to take a synergistic approach to the problem of magnetospheric modifications due to SPS.

The key questions to be addressed in such a synthesis are the following:

1. What is the time scale for Ar^+ energy deposition in the presence of H_2O/H_2 neutral diffusion and chemistry?

2. What are the charge exchange, ionization, and dissociation time scales of H_2O/H_2? and How do they compare with the time scale for falling in the earth's gravitational field, taking particular account of the condensation and evaporation of H_2O (see Section 2.5)?

3. How are the magnetospheric-ionospheric-thermospheric coupling processes changed in this modified scenario?

The answers (or partial answers) to this sequence of questions may help formulate a synergistic approach to address the total effects of modifications to the radiation belts and of changes to the communication environment and to estimate increases in satellite drag due to thermospheric heating.

A partial list of important phenomena can be made:

1. Plasma depletions (as distinguished from holes in the ionospheric F-region due to charge exchange of ambient ions with H_2O/H_2 neutrals). (U, H)

2. Modification in Geomagnetic Activity. Changes in magnetospheric convection patterns and in the radial position of the plasmapause will change the location and intensity of geomagnetic activity, and could give rise to powerline surges and changes in the satellite drag environment. (U, H)

3. Radiation belt modifications, including short-term reductions due to charge exchange, intermediate-term enhancement of relativistic electrons due to changes in the composition of the plasmasphere, and long-term recycling and energization of some argon ions into HZE particles. (U, H)

4. Can stratospheric ozone be reduced by the enhanced precipitation of high energy particles? (Probably not, see Section 4.4.2.) (U/L, H)

5. The physical size of SPS and its characteristics create a number of problems such as flux tube blockage, IR sources, photoelectrons, and spacecraft charging that give rise to local rather than global consequences. (H, U)

6. Enhancement of airglow, especially the nitrogen (N_2, N_2^+) airglow due to enhanced precipitation of energetic Ar^+ ions into the atmosphere. (Note that this enhancement appears to be much larger than the effects discussed in Sections 2 and 3 above.) (H, U)

4.6 CONCEIVABLE ATMOSPHERIC EXPERIMENTS

4.6.1 High-Altitude Injection of Gases, Plasmas, and Electron/Ion Beams (Pongratz)

Here we examine experiments that could explore the phenomenology of the Ar^+ engine burns. Two target-of-opportunity experiments may be relevant:

1. A Japanese Space Shuttle/Spacelab ion beam experiment (Dr. Obayashi), to be conducted in 1984-85.

2. GREYHOUND, which is proposed by N. J. Stevens of NASA-Lewis as a test of ion engines (see also Section 4.6.3, Item 3).

The ideal experiment would involve a full-scale Ar^+ engine and should be conducted on long- and short-field lines. Long-term studies of possible ion acceleration should be possible. The energy and pitch angle distributions of energetic ions should be measured as a function of distance (parallel and perpendicular to the magnetic field lines) from the engine burn. Electrostatic and possibly electromagnetic waves generated by the ion engine pulses should be monitored. Wave frequencies between the lower hybrid resonance and ion cyclotron frequencies, and below, would be the relevant ambient plasma parameters, which should be monitored before, during, and after the ion engine pulses. Most likely a mother/daughter satellite configuration would be required. The planning and construction of this experiment could take more than six years and several hundred million dollars.

Long-term ion energization studies may require optical techniques, and here the use of Ca^+ ions would provide a tracer of mass close to that of argon but which could be traced optically. However, we know of no technology for producing large quantities of Ca^+ in space.

4.6.2 Relevance of SCATHA (P78-2) to SPS (Chiu)

SCATHA (Spacecraft Charging At High Altitudes) is an integrated satellite to study spacecraft-environmental interactions at geosynchronous orbit, sponsored jointly by the USAF and NASA. It has relevance for SPS assessment in the following areas:

(a) Spacecraft charging by energetic plasma and photoelectric effects is expected to be an important problem for the design and development of SPS which has 50 km^2 of surface area.

(b) Potentials established on the spacecraft can accelerate and decelerate plasma components to tens of keV, as demonstrated by SCATHA experiments. This would impact the geosynchronous plasma environment.

(c) The plasma environment has direct impact on klystron operations by forming electron sheaths in resonant cavities ("multipacting"). This has been demonstrated by SCATHA and other satellites.

(d) SCATHA, ISEE, ATS, and GEOS are elements in the coordinated IMS (International Magnetospheric Study)project to define the physics of the geosynchronous plasma. The basis physical understanding gained would be very important in resolving the question of the long-term recycling and energization of argon ions in the magnetosphere.

(e) Effects of contaminant from satellite operations such as water, outgassing, and neutrals are studied by the ML-12 experiment on SCATHA.

As a result of considering the relevance of SCATHA to the SPS assessment, we recommend that:

1. Coordination should be maintained with SCATHA experiments.

2. Consideration should be given to SCATHA-like instrumentation in conjunction with possible FIREWHEEL-like diagnostic configuration and a high-powered ion engine operation experiment similar to GREYHOUND. (More details of these experiments are given in Section 4.6.3)

3. Consideration of results from joint SCATHA/GEOS II Xe^+ beam propagation studies should be included in planning any Ar^+ experiments.

4.6.3 CAMEO, FIREWHEEL and Other Experiments (Chiu)

1. CAMEO. This involved a release of barium from a satellite at L ~ 7-9 at approximately 1000-km altitude. The results indicate that

(a) ions are accelerated by natural electric field which may influence the formation of HZE particles from Ar^+, and

(b) plasma irregularities were observed at very high altitudes (~ 1 R_E).

Such releases at high altitudes at the equator would be most relevant for SPS. Other targets of opportunity in this area are a NASA/Max Planck Institute barium release at 6.6 R_E and the BUARO barium jet release by LASL (Koons & Pongratz, 1979, Simons et al. 1979).

2. FIREWHEEL. This experiment consists of barium and lithium releases in the night-side magnetosphere at 7 and 95 R_E by the Max Planck Institute group in March 1980. The unique feature of this experiment, which constitutes

a target of opportunity for SPS assessment, is that a mother satellite releasing Ba and Li will also release instrumented daughter satellites as diagnostic tools. Studies on momentum exchange of the injected plasma with the ambient plasma and tracing the redistribution and acceleration of the injected plasma in the magnetosphere, among others, will throw some light on the fate of Ar^+ in the magnetosphere. Less certain longer term targets of opportunity may be the NASA OPEN (Origin of Plasmas in the Earth's Neighborhood, see NASA, 1979) program.

3. GREYHOUND and other ion beam/ion engine operations in space. GREYHOUND is a proposed test of ion engine space transportation in the 1985 time frame. In the same time frame, a Japanese/US experiment on Spacelab I will also test plasma beams, but the power will probably not be high enough for resolution of the Ar^+ ion beam problem.

We suggest that an experiment, perhaps a slight modification of the GREYHOUND operation, with diagnostic configuration of the FIREWHEEL type (mother-daughter satellites) and instrumentation of the SCATHA-type on the mother satellite, would be needed to study the short-term fate of the Ar^+ beam. The question of how to observe Ar^+ ions optically must also be addressed. Calcium (Ca^+) has the potential of being easily observable, and of having a mass very close to that of argon. GREYHOUND seems to be a target of opportunity in the 1985 time frame.

4.6.4 Starfish and Other Past Nuclear Explosions (Palmadesso)

The question asked is: Should Starfish and other past nuclear explosions be considered as part of the experimental data base for SPS assessment?

The conclusion is generally negative for the following reasons:

1. Nuclear phenomenology is substantially different from SPS phenomenology.

2. The nuclear data base is incomplete. With some exceptions, data taking was confined to low altitudes and short times after the burst. Late time and high altitude physical effects, which offer the greatest promise of similarity to the SPS phenomenology, were not well diagnosed.

3. Examples of physical effects apparently similar to SPS phenomena, which on closer examination are not worth pursuing, are the following:

(a) Starfish produced enhancements in the number of very energetic radiation belt electrons that persisted for several years. These are thought to be due to fission beta particles rather than to any reduction in precipitation as discussed in Section 4.4.1.

(b) Jetting of plasma across magnetic field lines was observed visually after Starfish. The phenomena could not be diagnosed quantitatively at that time; the distance traveled by the jetted material and the temperature, density, etc., of the material are not known.

Thus, we recommend that a low priority should be assigned to the study of nuclear tests for SPS evaluation purposes.

5 CONCLUSIONS AND RECOMMENDATIONS

5.1 INTRODUCTION

During the workshop it quickly became apparent that many of the technical problems associated with the environmental effects of SPS propulsion effluents in the upper atmosphere are very broad and poorly defined. Hence, before one plans to do any dedicated field experiments, which are inevitably costly in both time and money, it is appropriate first to undertake a variety of preliminary theoretical and laboratory studies and, where possible, also to use targets of opportunity for initial studies.

One problem, the effect on HF skywave propagation due to permanent F-region depletion associated with HLLV launches, surfaced right after the workshop at a briefing given at the Naval Ocean Systems Center (see Appendix F, item F.3). This problem is of such clear importance that it is discussed next, in Section 5.2. Other problems involving H_2O/H_2 and NO injections, are discussed in Section 5.3 and those involving Ar^+ injections, in Section 5.4. During the workshop we were unable to agree on a unique order of priorities for the various items, so they simply are presented in a logical sequence, with appropriate comments on their importance to SPS.

It should be noted that the present considerations are not limited to SPS propulsion, but would apply to any very large space transportation project using H_2/O_2 chemical propulsion and ion propulsion as appropriate.

5.2 PERMANENT DEPLETION OF F-REGION IONIZATION

As a result of hydrogen emission from the HLLV second stage rocket and the upward diffusion of the hydrogen, and to some extent also of the water vapor emitted, it is anticipated that there will be a belt of reduced ionization at the latitude of launch. The extent of this region would be several thousand kilometers in the north-south direction, extending around the globe at constant latitude, and beginning at 160-180 km altitude and going to the F2-region peak and above. The mean reduction in ionization may be as much as 50% at night; in the daytime it will be much less, perhaps 10-20%.

The critical consequence of such a reduction in ionization is that it drastically reduces the available HF frequency band that can be used for long-range skywave communication at a time when this band is already heavily overcommitted internationally (see Section 3.2.6 and item F.3 in Appendix F). Thus it is clearly of the highest priority to verify the predictions, including atmospheric variability and the overall uncertainty bounds. The specific items that require study are the following:

1. Upward transport of H_2 and H_2O injected in the 70-120 km altitude range into the F-region and the associated photochemistry. This includes the dissociation and ionization/deionization, and a resolution of the relative importance of H_2O and H_2.

2. Experimental (laboratory) study of the dissociative recombination of H_2O^+ and OH^+, including the state of excitation of the products (see Section 3.2.3).

3. Experimental (field) study of the dispersion of tracers in the mesosphere at relatively long times after release (see Section 2.6, especially Fig. 3).

4. An overall 3-D/2-D model calculation of the steady-state F-region depletion to quantify the estimates quoted here (which are not based on any very detailed calculations) and also to identify any further critical unknowns. This is not a simple task (see Section 3.2.4 for an indication of the work called for).

5. To verify the adequacy of the model predictions, it is appropriate to analyze previous results (e.g., the Skylab-I and LAGOPEDO observations), to study and observe targets of opportunity such as the Atlas-Centaur launch of HEAO-C in September 1979, and to study any relevant natural phenomena (see the discussion of Section 3.2.5).

5.3 PROBLEMS INVOLVING H_2O, H_2, AND NO (MAINLY, BUT NOT ENTIRELY, IN THE MESOSPHERE AND THERMOSPHERE)

1. Water vapor concentration in the mesosphere. This is very poorly known at present, but various ongoing and planned satellite measurements should produce a great improvement over the next 10 years or so. If the SPS project goes into detailed engineering development, it will be vital for project management to initiate a long-term water vapor monitoring program over at least a 20-25 year period, so that it can later be established whether SPS rocket activity does indeed enhance the level of water vapor in the mesosphere as anticipated. On a short-term basis two action items are: (See Section 2.11.1).

1.1 The development of ground-based microwave techniques.

1.2 The intercomparison of different potentially useful techniques for water vapor measurement.

2. High altitude clouds and contrails. While the expected climatic effects of both high altitude artificial clouds and rocket contrails are small, they are not clearly negligible. Moreover, there are possible effects on remote sensors. Thus, as in the case of water vapor, a long-term data base on noctilucent and nacreous clouds must be developed once SPS engineering development is under way. However, there is another class of problems relating to the physical mechanisms for condensation and evaporation of water for both natural clouds (which may be enhanced by SPS) as well as for any long-lived contrails. These problems are important at the present stage of analysis because the ultimate impact of water injections by rockets depends on its rate of removal from the upper atmosphere, which is much faster for aerosols than for vapor.

3. Fate of injected H_2O/H_2. Theoretical studies are needed to understand all aspects of the water/hydrogen budget of both low-altitude

(mesosphere) and high-altitude rocket injections. Problems needing particular emphasis are the details of injection mechanics (see Section 3.1.3, which was prepared by C. Park after the workshop), condensation and evaporation processes (see Section 2.5), estimates of dynamical transport in the mesosphere and thermosphere (see Section 2.6 and 3), and, of course, any problems related to F-region depletion (see Section 5.2 above). One output of these studies will be the design of experiments to increase our understanding in critical areas.

4. Environmental effects of H_2O/H_2 injections. In addition to the F-region depletion, there are other potential problems that should be examined to see whether detailed investigation beyond what has been done thus far is necessary. Specific problems that have to be resolved and documented are:

4.1 Effects of hydrogen injections on the magnetosphere.

4.2 Changes in airglow.

4.3 Effects on satellite drag.

Items 1-4 have the highest priority in this group, although the long-term monitoring aspects of items 1 and 2 will only become time-urgent once SPS goes into advanced engineering development. Some other problems, of somewhat lesser priority, are the following:

5. Heterogeneous chemistry on ice crystals. This is a very difficult and obscure subject. As part of item 3 above, a calculation should be done to see whether the effects would be significant; if so, an experimental program should be considered.

6. NO production on reentry, and its fate. Experimental verification is needed of theoretical predictions of NO generation by reentry vehicles, which have been based mainly on small-scale shock tube and comparable observations. This can readily be achieved from observations of Space Shuttle reentry. Also, the fate of NO produced or injected in the mesosphere is not well understood.

7. Effects of water, hydrogen, and NO injections on the lower inosphere. It should be established to what extent the SPS injections will affect VLF/ELF propagation; if the effects are significant, they should be considered as part of the communications aspect of the SPS Environmental Assessment.

5.4 PROBLEMS INVOLVING ARGON ION INJECTIONS IN THE PLASMASPHERE AND MAGNETOSPHERE (Carlson and Vondrak)

The principal issues are:

1. Fate of Ar^+. The problems of beam stopping and the lifetime of the ions need to be resolved. (See Section 4.3.)

2. Ion energization and HZE particles. (HZE = high atomic number of high energy). The overall question of ion energization and the production of

HZE particles in the magnetosphere is not understood, but a hazard to people and electronics would arise if a sufficiently large intensity of HZE particles were to be produced. This point needs to be clarified.

3. If the fate of Ar^+ is understood, including the energization aspects, one can predict the *alteration of the trapped radiation,* including the plasmasphere and ring current. The alterations may lead to various effects on the atmosphere, of which probably the most important is the increased radiation hazard to spacecraft. Other effects that need investigation are possible communication interference, power line transients, and changes in airglow and in stratospheric ozone.

In the short term, these action items are largely paper studies, but they may include the observation of targets of opportunity.

THIS PAGE

WAS INTENTIONALLY

LEFT BLANK

APPENDIX A

LIST OF WORKSHOP PARTICIPANTS (*)

AND

INITIAL DISTRIBUTION OF REVIEW DRAFT

NAME AND ADDRESS	TELEPHONE COMMERCIAL	F.T.S.
*Dr. Arthur C. Aikin Code 964 NASA Goddard Space Flight Center Greenbelt, MD 20771	(301)344-8913	344-8913
Dr. David Almgren Arthur D. Little, Inc. Cambridge, MA 02140		
Dr. Nathaniel Barr SPS Project Office Dept. of Energy/OER Rm. 509, 400 First St., NW Washington, DC 20545	(202)376-9362	376-9362
*Dr. Ernest Bauer (La Jolla Institute) 8109 Fenway Road Bethesda, MD 20034	(301)469-6726	(202)558-1611 Arlington Office
*Dr. Paul A. Bernhardt Radioscience Laboratory Dept. of Electrical Engineering Stanford University Stanford, CA 94305	(415)497-3522	
Mr. Warren W. Berning (New Mexico State University) 11007 Candlelight Lane Potomac, MD 20854	(301)299-8970	
*Dr. Kenneth L. Brubaker Code EES-12 Argonne National Laboratory 9700 South Cass Avenue Argonne, IL 60439	(312)972-7630	972-7630
*Dr. Herbert C. Carlson Code ATM National Science Foundation Washington, DC 20550	(202)632-4185	632-4185

APPENDIX A - Continued

NAME AND ADDRESS	TELEPHONE COMMERCIAL	F.T.S.
Dr. A. W. Castleman, Jr. Department of Chemistry Campus Box 215 University of Colorado Boulder, CO 80309	(303) 492-8028	
Dr. Joseph W. Chamberlain SRI-JASON Box 1892 Rice University Houston, Texas 77001	(713) 528-4141	
Dr. Barbara Ching The Aerospace Corporation Post Office Box 92957 Los Angeles, CA 90009		
*Dr. Yam T. Chiu Space Science Laboratory The Aerospace Corporation Post Office Box 92957 Los Angeles, CA 90009	(213)648-5328	
*Dr. John B. Cladis Lockheed Palo Alto Research Laboratory 2440 Sharon Oaks Drive Menlo Park, CA 94025	(415) 493-4411 Ext. 45755	
*Dr. Steven A. Curtis Code 621 NASA Goddard Space Flight Center Greenbelt, MD 20771	(301)344-8409	344-8409
Dr. G. T. Davidson Lockheed Palo Alto Research Laboratory 3251 Hanover Street Palo Alto, CA 94304	(415)493-4411	
*Dr. Hugh W. Ellsaesser L-262 Lawrence Livermore Laboratory Post Office Box 808 Livermore, CA 94550	(415)422-1809	532-1809
*Dr. Joel A. Fedder Code 6780 U.S. Naval Research Laboratory 4555 Overlook Avenue, SE Washington, DC 20375	(202)767-2875	

APPENDIX A - Continued

NAME AND ADDRESS	TELEPHONE COMMERCIAL	F.T.S.
*Dr. Jeffrey M. Forbes Space Data Laboratory Boston College Chestnut Hill, MA 02167	(617)969-0100 Ext. 4328	
*Capt. Henry B. Garrett, USAF Code PHG U.S. Air Force Geophysics Laboratory Hanscom Field, MA 01731	(617)861-3103	
Dr. Peter Hammerling La Jolla Institute Post Office Box 1434 La Jolla, CA 92038	(714)454-3581	
Dr. James Heppner Code 625 NASA Goddard Space Flight Center Greenbelt, MD 20771	(301)344-8797	344-8797
*Dr. Adolf R. Hochstim La Jolla Institute Post Office Box 1434 La Jolla, CA 92038	(714)454-3581	
Dr. Frank P. Hudson Code OHER, Mail Stop E-201 U.S. Department of Energy Washington, DC 20545	(301)353-4066	233-4066
Dr. Donald Hunt Code RD-1 NOAA Headquarters 6010 Executive Boulevard Rockville, MD 20852	(301)443-8971	
Dr. M. Kelley Radioscience Laboratory Department of Electrical Engineering Cornell University Ithaca, NY 14853		
Dr. Louis J. Lanzerotti Bell Telephone Laboratories Murray Hill, NJ 07974	(201)582-2279	

APPENDIX A - Continued

NAME AND ADDRESS	TELEPHONE COMMERCIAL	F.T.S.
Dr. C. A. Lundquist NASA Marshall Space Flight Center Huntsville, AL 35812	(205)453-3105	
*Dr. P. Mahadevan M.S. 130/121 The Aerospace Corporation Post Office Box 92957 Los Angeles, CA 90009	(213)648-7615	
*Dr. Billy M. McCormac Dept. 52-10, Bldg. 202 Lockheed Palo Alto Research Laboratory 3251 Hanover Street Palo Alto, CA 94304	(415)493-4411 Ext. 5554	
Dr. R. J. McNeal Code ATM National Science Foundation Washington, DC 20550	(202)632-1976	632-1976
*Dr. Michael J. Mendillo Graduate School Boston University 725 Commonwealth Avenue Boston, MA 02215	(617)353-2690	
Professor M. Nicolet (University of Brussels) 30 Avenue Den Doorn B-1180 Brussels, Belgium		
Professor J. J. Olivero Department of Meteorology Pennsylvania State University State College, PA 16801		
Mr. W. A. Page Code-SSG Mail Stop 245-5 NASA Ames Research Center Moffett Field, CA 94035	(415)965-5404	
*Dr. Peter J. Palmadesso Code 6780 U.S. Naval Research Laboratory 4555 Overlook Avenue, SW Washington, DC 20375	(202)767-3630	

APPENDIX A - Continued

NAME AND ADDRESS	TELEPHONE COMMERCIAL	F.T.S
*Dr. Chul Park Mail Stop 229-4 NASA Ames Research Center Moffett Field, CA 94035	(415)965-6086	448-6086
*Dr. Morris E. Pongratz Mail Stop 664 Los Alamos Scientific Laboratory Los Alamos, NM 87545	(505)667-4740	
*Dr. Sheo S. Prasad Jet Propulsion Laboratory CalTech 4800 Oak Grove Drive Pasadena, CA 91103	(213)354-6423/2140	792-6423
Dr. George C. Reid Aeronomy Laboratory, NOAA Boulder, CO 80303	(303)499-1000 Ext. 3304/3219	323-3304 Ext. 3219
*Dr. Arthur D. Richmond NOAA/SEL Boulder, CO 80302	(303)499-1000 Ext. 4479	323-4479
Dr. J. H. Richter Code 532, Naval Ocean Systems Center San Diego, CA 92152	(714)225-7919	
*Dr. Donald M. Rote Code EES-12 Argonne National Laboratory 9700 South Cass Avenue Argonne, IL 60439	(312)972-3786	972-3784 or 3786
Dr. R. D. Rundel Code SD-5, NASA Johnson Space Center Houston, TX 77058		
Dr. Charles M. Rush NTIA/ITS, Boulder, CO 80302	(303)499-1000 Ext. 3460	323-3460
Dr. F. Carl Schwenk Code RES-1, NASA Headquarters Washington, DC 20546	(202)755-2450	755-2450
Dr. Erwin R. Schmerling Code ST, NASA Headquarters Washington, DC 20546	(202)755-3685	755-3685

APPENDIX A - Continued

NAME AND ADDRESS	TELEPHONE COMMERCIAL	F.T.S.
Dr. Robert Seals Code NASA Headquarters Washington, DC 20546		
Dr. Fred S. Simmons Advanced Programs Division The Aerospace Corporation Post Office Box 92957 Los Angeles, CA 90009	(213)648-6874	
Dr. Robert A. Stokes Battelle Observatory Battelle Pacific Northwest Laboratories Richland, WA 99352	(509)942-7301	444-7301
*Dr. N. Sundararaman High Altitude Pollution Program Federal Aviation Administration AEE-300 800 Independence Avenue, SW Room 836-G Washington, DC 20591	(202)755-8933	755-8933
*Dr. Charles Sve Aerophysics Laboratory The Aerospace Corporation Post Office Box 92957 Los Angeles, CA 90009		
Dr. Shelby G. Tilford Code EBT-8 NASA Headquarters Washington, DC 20546	(202)755-8596	755-8596
*Dr. Richard P. Turco R&D Associates Post Office Box 9695 Marina Del Rey, CA 90291	(213)822-1715 Ext. 508	
*Dr. Anthony R. Valentino Code EES-12 Argonne National Laboratory 9700 South Cass Avenue Argonne, IL 60439	(312)972-8060	972-8060

APPENDIX A - Continued

NAME AND ADDRESS	TELEPHONE COMMERCIAL	F.T.S
Dr. William V. Vaughan Code S-81 NASA Marshall Space Flight Center Huntsville, AL 35812		
*Dr. Richard Vondrak SRI International 333 Ravenswood Avenue Menlo Park, CA 94025	(415)326-6200 Ext. 4732	
*Dr. Robert C. Whitten Mail Stop 245-3 NASA Ames Research Center Moffett Field, CA 94035	(415)965-5498	448-5498
*Dr. John Zinn Mail Stop 664 Los Alamos Scientific Laboratory Los Alamos, NM 87545	(505)667-6403	

THIS PAGE

WAS INTENTIONALLY

LEFT BLANK

APPENDIX B

SCENARIO FOR SPS CONSTRUCTION (SEE RSR, 1978)

The SPS construction rate is assumed to be two 5-GW systems per year, proceeding over a 30-year time period. (Each satellite is designed to have a 30-year operating life.) One 5-GW system consists of an array of photovoltaic cells in geosynchronous orbit, including the microwave transmission link (at 2.45 GHz, i.e., λ = 12.2 cm) to send the received power down to a rectifying antenna (rectenna) on the ground. A satellite has a size of order 5 km x 10 km, using either Si cells (more reliable) or GaAlAs (lighter in weight). In geostationary orbit the array receives continuous power input from the sun except for periods of up to 40 minutes during several nights at the spring and fall equinox when the array is in the earth's shadow. Thus the scheme provides baseload, i.e., continuous, electric power from the sun, and it is claimed that the effective power per unit area is ten times as large as for an equivalent array on the ground (AIAA, 1979). The rectenna for a 5-GW system has an area of 10 x 13 km at latitude 35°; the power density of microwaves is designed to be 23 mw/cm^2 at the center of the rectenna and 1 mw/cm^2 at the edge.

Construction will be carried out in geostationary orbit (GEO) using a crew of approximately 550 (see Fig. B.1). The principal structural material will be graphite composite. People and freight will be transported first to Low Earth Orbit (LEO, 500 km, nominal), using a "Hohmann transfer elliptical trajectory." That is, rather than burn the main engine all the way from ground to low earth orbit, the second stage main burn goes up to 120 km, and then the vehicle gains speed while losing a little altitude (see Fig. 1). Now the HLLV moves in an elliptical path up to LEO, and there a short circularization burn puts it into a circular orbit. This procedure is more efficient from the standpoint of payload into orbit per unit mass of propellant than is a direct injection such as was used on Skylab I that produced its large "ionospheric hole." Five hundred km is rather high for a parking orbit; presumably it is used because the elements for the construction of the solar power satellite are so large that the drag at a lower altitude, say 200 km, would be significant.

Once the HLLV deposits its payload in LEO there is another relatively short deorbit burn as the vehicle starts on its descent and reentry into the atmosphere, and goes down to the surface for another round trip.

The SPS concept involves using two types of vehicles for transportation from the ground to LEO, and another two for transportation from LEO to GEO. The various space vehicles are described briefly in Table B.1. For transportation from the ground to LEO both vehicles use H_2-O_2 second stage engines, and the larger of the two vehicles, the HLLV, has a very much greater impact on the atmosphere so that no explicit reference is made to the smaller vehicle, the PLV.

For transportation from LEO to GEO most of the weight is carried by the electrically powered COTV, which uses argon ion engines as principal propulsion, with solar energy collected in the panels of solar cells being transported into GEO as power source for the ion rockets. However, note that the COTV uses H_2-O_2 engines for attitude control and auxiliary power. From

	SILICON	GALLIUM
SPS MASS	50,984 MT	34,159 MT
PAYLOADS		
HLLV	424 MT	424 MT
PLV	75 PEOPLE	75 PEOPLE
POTV	160 PEOPLE 400 MT	160 PEOPLE 400 MT
COTV	4,000 MT	3,500 MT
PACKING FACTORS		
HARDWARE	85%	95%
PROPELLANTS	95%	95%

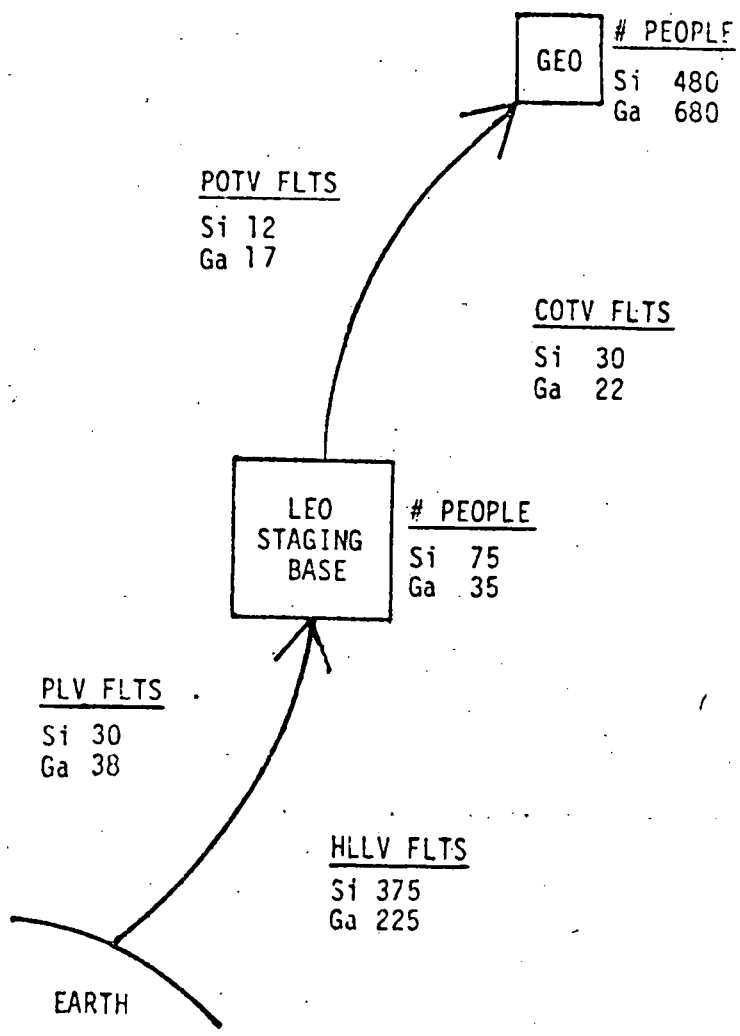

Figure B. 1. Scenario for Construction of Two 5-GW Satellite/year

Source: (RSR, 1978, p. 74)

TABLE B.1

SPACE TRANSPORTATION VEHICLES FOR SPS PROJECT

1. Heavy Lift Launch Vehicle (HLLV).

   * Surface to LEO with 400 ton payload, approximately 5 times as large as Space Shuttle.

   * First stage: LO_2-hydrocarbon. Burns out at 75 km, not considered here.

   * Second stage: LO_2-LH_2, main burn 76-120 km, circularization and deorbit burns near LEO -- see Fig. 1.

2. Personnel Launch Vehicle (PLV).

   * Surface to LEO with passenger payload, a modified Space Shuttle orbiter.

   * Not considered here, as it only provides a small addition to HLLV effects.

3. (Electric) Cargo Orbit Transfer Vehicle (COTV).

   * LEO to GEO using Argon Ion engines with supplemental chemical (LO_2-LH_2) propulsion.

   * Very large: uses arrays of solar cells in transit to provide power.

   * Ion engines have very low thrust, thus travel time from LEO-GEO is 130-160 days, 30 days back down.

   * Adequate for cargo, but not for taking people through the radiation belts because of long travel time.

4. Personnel Orbit Transfer Vehicle (POTV).

   * LEO to GEO, two stage vehicle with LO_2-LH_2 chemical rockets, for transporting people and priority cargo rapidly (several hours) through the radiation belts.

Note:

   * all vehicles are fully reusable.

   * see Fig. B.1 for the numbers of flights per year of each vehicle, for the Si and Ga options.

   * source: RSR, 1978, p. 47ff.

the nature of ion engines, which have very low thrust but very high specific impulse, or thrust per unit mass of propellant, this is a very slow vehicle, which takes 130-160 days to go from LEO to GEO, and perhaps 30 days for the return trip. Thus the COTV cannot be used for transporting people because the radiation dose during this very slow passage through the earth's radiation belts would just be too great. Accordingly, there is a POTV for people and priority cargo, which uses H_2-O_2 chemical rockets and takes only several hours for the trip.

The scale of the operation is very large: Figure B.1 gives the construction scenario for both the more conservative (Si) and the more advanced (Ga) options, which are described in more detail in RSR, 1978. The two options have been developed, respectively, by Boeing using Si solar cells and greater total mass (50,000 metric tons per unit) and more conservative technology (I_{sp} = 7000 sec for the ion engines, etc.), while the more advanced technology developed by Rockwell uses GaAlAs photocoltaic cells, lighter weight (37,000 metric tons per unit) and even higher impulse ion engines (I_{sp} = 13,000 sec). The injection model used here, in Table 3, comes from the Boeing scenario (see RSR, 1978, p. B-100).

Table B.2 supplements the data of Fig. 1 in presenting the emission of the main burn of the HLLV.

TABLE B.2

EMISSION OF THE MAIN BURN OF THE HLLV SECOND STAGE

HEAVY LIFT LAUNCH VEHICLE

STEP	TIME (SEC)	ALTITUDE (KM)	DELTAZ (KM)	VELOCITY (M/SEC)	ROCKET MASS (KG)	KE (J)	PE (J)	DELTAE (J)
1	3.0800 01	1.71200D 00	1.71200 00	5.5600D 01	9.65689D 06	1.49265D 10	1.62129D 11	1.77056D 11
2	6.0000 01	7.71200D 00	6.00000 00	2.1500D 02	8.34564D 06	1.92859D 11	6.31170D 11	6.47003D 11
3	9.0000 01	1.90000D 01	1.12830 01	5.2300D 02	6.99846D 06	9.75530D 11	1.30399D 12	1.45546D 12
4	1.2000 02	3.47340D 01	1.57340 01	9.5870D 02	5.65095D 06	2.59691D 12	1.92483D 12	2.24222D 12
5	1.5520 02	5.67940D 01	2.20600 01	1.6982D 03	4.20736D 06	6.06677D 12	2.34329D 12	3.88832D 12
6	1.8920 02	7.74310D 01	2.06370 01	2.3143D 03	3.97945D 06	1.06569D 13	3.02167D 12	5.26854D 12
7	2.2920 02	9.65840D 01	1.91530 01	2.5001D 03	3.71717D 06	1.16171D 13	3.52067D 12	1.45914D 12
8	2.6920 02	1.10779D 02	1.41950 01	2.8924D 03	3.45489D 06	1.44518D 13	3.75316D 12	3.06717D 12
9	3.0920 02	1.20026D 02	9.24700 00	3.2954D 03	3.19261D 06	1.73353D 13	3.75773D 12	2.88813D 12
10	3.4920 02	1.24355D 02	4.32900 00	3.7981D 03	2.93033D 06	2.11358D 13	3.57341D 12	3.61619D 12
11	3.8920 02	1.24033D 02	-3.22000-01	4.3985D 03	2.66805D 06	2.58091D 13	3.24515D 12	4.34503D 12
12	4.2920 02	1.20012D 02	-4.02100 00	5.0940D 03	2.40577D 06	3.12135D 13	2.83128D 12	4.99048D 12
13	4.6920 02	1.14110D 02	-5.90200 00	5.9282D 03	2.14349D 06	3.76649D 13	2.39856D 12	6.01875D 12
14	5.0470 02	1.10958D 02	-3.15200 00	6.8868D 03	1.91856D 06	4.54967D 13	2.08756D 12	7.52075D 12

MASS EMISSIONS (KG)

STEP	CO2	H2O	H2	CO	OH	SO2
1	7.61320D 05	6.21480D 05	0.0	0.0	0.0	3.10740D 02
2	7.21770D 05	5.89180D 05	0.0	0.0	0.0	2.95000D 02
3	7.41550D 05	6.05330D 05	0.0	0.0	0.0	3.02670D 02
4	7.31110D 05	6.03700D 05	2.69440D 02	7.40960D 03	4.71520D 03	3.02670D 02
5	7.83190D 05	6.46700D 05	2.88490D 02	7.93710D 03	5.15110D 03	3.24240D 02
6	0.0	2.19940D 05	7.97700D 03	0.0	0.0	0.0
7	0.0	2.53100D 05	9.17950D 03	0.0	0.0	0.0
8	0.0	2.53100D 05	9.17950D 03	0.0	0.0	0.0
9	0.0	2.53100D 05	9.17950D 03	0.0	0.0	0.0
10	0.0	2.53100D 05	9.17950D 03	0.0	0.0	0.0
11	0.0	2.53100D 05	9.17950D 03	0.0	0.0	0.0
12	0.0	2.53100D 05	9.17950D 03	0.0	0.0	0.0
13	0.0	2.53100D 05	9.17950D 03	0.0	0.0	0.0
14	0.0	2.17060D 05	7.87270D 03	0.0	0.0	0.0

MOLE EMISSIONS (MOLES)

STEP	CO2	H2O	H2	CO	OH	SO2
1	1.72639D 07	3.44973D 07	0.0	0.0	0.0	4.85054D 03
2	1.63670D 07	3.27044D 07	0.0	0.0	0.0	4.60484D 03
3	1.68155D 07	3.36009D 07	0.0	0.0	0.0	4.72457D 03
4	1.65788D 07	3.35104D 07	1.33655D 05	2.64529D 05	2.77244D 05	4.72457D 03
5	1.77598D 07	3.53973D 07	1.43104D 05	2.83362D 05	3.02874D 05	5.06127D 03
6	0.0	1.22035D 07	3.95696D 06	0.0	0.0	0.0
7	0.0	1.40492D 07	4.55346D 06	0.0	0.0	0.0
8	0.0	1.40492D 07	4.55346D 06	0.0	0.0	0.0
9	0.0	1.40492D 07	4.55346D 06	0.0	0.0	0.0
10	0.0	1.40492D 07	4.55346D 06	0.0	0.0	0.0
11	0.0	1.40492D 07	4.55346D 06	0.0	0.0	0.0
12	0.0	1.40492D 07	4.55346D 06	0.0	0.0	0.0
13	0.0	1.40492D 07	4.55346D 06	0.0	0.0	0.0
14	0.0	1.20486D 07	3.90523D 06	0.0	0.0	0.0

TABLE B.2 - Continued

ALTITUDE RANGE (KM)	MASS AND NUMBER INJECTION RATES (KG, MOLECULES) CO2	H2O	H2	CO	OH	SO2
0.0 TO 5.000D 00	1.15685D 06	9.44351D 05	0.0	0.0	0.0	4.72400D 02
	1.57976D 31	3.15572D 31	0.0	0.0	0.0	4.44065D 27
5.000D 00 TO 1.000D 01	4.76547D 05	3.89006D 05	0.0	0.0	0.0	1.94639D 02
	6.50760D 30	1.30034D 31	0.0	0.0	0.0	1.83012D 27
1.000D 01 TO 1.500D 01	3.28468D 05	2.68130D 05	0.0	0.0	0.0	1.34067D 02
	4.48548D 30	8.96208D 30	0.0	0.0	0.0	1.26026D 27
1.500D 01 TO 2.000D 01	3.09242D 05	2.52873D 05	1.71247D 01	4.70929D 02	2.99682D 02	1.26490D 02
	4.22292D 30	8.45289D 30	5.11551D 27	1.01246D 28	1.06113D 28	1.18903D 27
2.000D 01 TO 2.500D 01	2.32334D 05	1.91846D 05	8.56235D 01	2.35465D 03	1.49841D 03	9.61834D 01
	3.17270D 30	6.41290D 30	2.55776D 28	5.06231D 28	5.30563D 28	9.04143D 26
2.500D 01 TO 3.000D 01	2.32334D 05	1.91846D 05	8.56235D 01	2.35465D 03	1.49841D 03	9.61834D 01
	3.17270D 30	6.41290D 30	2.55776D 28	5.06231D 28	5.30563D 28	9.04143D 26
3.000D 01 TO 3.500D 01	2.29418D 05	1.89437D 05	8.45469D 01	2.32503D 03	1.48081D 03	9.49762D 01
	3.13287D 30	6.33240D 30	2.52560D 28	4.99376D 28	5.24330D 28	8.92794D 26
3.500D 01 TO 4.000D 01	1.77514D 05	1.46578D 05	6.53876D 01	1.79893D 03	1.16752D 03	7.34905D 01
	2.42408D 30	4.89970D 30	1.95327D 28	3.86767D 28	4.13400D 28	6.90825D 26
4.000D 01 TO 4.500D 01	1.77514D 05	1.46578D 05	6.53876D 01	1.79898D 03	1.16752D 03	7.34905D 01
	2.42408D 30	4.89970D 30	1.95327D 28	3.86767D 28	4.13400D 28	6.90825D 26
4.500D 01 TO 5.000D 01	1.77514D 05	1.46578D 05	6.53876D 01	1.79898D 03	1.16752D 03	7.34905D 01
	2.42408D 30	4.89970D 30	1.95327D 28	3.86767D 28	4.13400D 28	6.90825D 26
5.000D 01 TO 5.500D 01	1.77514D 05	1.46578D 05	6.53876D 01	1.79893D 03	1.16752D 03	7.34905D 01
	2.42408D 30	4.89970D 30	1.95327D 28	3.86767D 28	4.13400D 28	6.90825D 26
5.500D 01 TO 6.000D 01	6.36919D 04	8.67601D 04	1.26270D 03	6.45474D 02	4.18906D 02	2.63684D 01
	8.69760D 29	2.90017D 30	3.77197D 29	1.38772D 28	1.48328D 28	2.47868D 26
6.000D 01 TO 6.500D 01	0.0	5.32878D 04	1.93269D 03	0.0	0.0	0.0
	0.0	1.78127D 30	5.77337D 29	0.0	0.0	0.0
6.500D 01 TO 7.000D 01	0.0	5.32878D 04	1.93269D 03	0.0	0.0	0.0
	0.0	1.78127D 30	5.77337D 29	0.0	0.0	0.0
7.000D 01 TO 7.500D 01	0.0	5.32878D 04	1.93269D 03	0.0	0.0	0.0
	0.0	1.78127D 30	5.77337D 29	0.0	0.0	0.0
7.500D 01 TO 8.000D 01	0.0	5.98569D 04	2.17093D 03	0.0	0.0	0.0
	0.0	2.00086D 30	6.48502D 29	0.0	0.0	0.0
8.000D 01 TO 8.500D 01	0.0	6.60732D 04	2.39636D 03	0.0	0.0	0.0
	0.0	2.20865D 30	7.15844D 29	0.0	0.0	0.0
8.500D 01 TO 9.000D 01	0.0	6.60732D 04	2.39636D 03	0.0	0.0	0.0
	0.0	2.20865D 30	7.15844D 29	0.0	0.0	0.0
9.000D 01 TO 9.500D 01	0.0	6.60732D 04	2.39636D 03	0.0	0.0	0.0
	0.0	2.20365D 30	7.15844D 29	0.0	0.0	0.0
9.500D 01 TO 1.000D 02	0.0	8.18400D 04	2.96820D 03	0.0	0.0	0.0
	0.0	2.73570D 30	8.86664D 29	0.0	0.0	0.0
1.000D 02 TO 1.050D 02	0.0	8.91511D 04	3.23336D 03	0.0	0.0	0.0
	0.0	2.98009D 30	9.65873D 29	0.0	0.0	0.0
1.050D 02 TO 1.100D 02	0.0	8.91511D 04	3.23336D 03	0.0	0.0	0.0
	0.0	2.98009D 30	9.65873D 29	0.0	0.0	0.0
1.100D 02 TO 1.150D 02	0.0	3.84649D 05	1.39509D 04	0.0	0.0	0.0
	0.0	1.28578D 31	4.16743D 30	0.0	0.0	0.0
1.150D 02 TO 1.200D 02	0.0	3.51274D 05	1.27401D 04	0.0	0.0	0.0
	0.0	1.17422D 31	3.80574D 30	0.0	0.0	0.0
1.200D 02 TO 1.250D 02	0.0	7.60526D 05	2.75830D 04	0.0	0.0	0.0
	0.0	2.54224D 31	8.23963D 30	0.0	0.0	0.0

APPENDIX C

ABBREVIATIONS AND ACRONYMS

ACS	Attitude Control System
ATS	Satellite, referenced in Section 4.6.2, not explained
Barium Release	Atomic barium has a metastable state which is "pumped" by sunlight so that its effective ionization potential is very low ($\sim$ 5 eV). Thus a barium release enhances the ionization. In this sense it is the opposite of a water or hydrogen release which reduces the ambient ionization.
Birkeland Currents	These are strong and variable currents observed in the auroral zone. They run along the geomagnetic field lines and connect the cold ionospheric plasma with the hot plasma in the magnetosphere. These currents increase during magnetic storms when auroral activity increases.
CAMEO	Satellite experiment, see Section 4.6.3, Item 1
COTV	Cargo Orbital Transfer Vehicle, see Appendix B
Domain A	70-120 km }
B	450-500 km, } See Table 2
C	500-35,000 km }
EA	Environmental Assessment
FIREWHEEL	Satellite experiment, see Section 4.6.3, Item 3
GEO	Geostationary Earth Orbit (36,000 km approximately)
GEOS	Satellite, referenced in Section 4.6.2, not explained
GREYHOUND	Satellite experiment, see Section 4.6.1, Item 2
GW	Gigawatt (10^9 watt)
HEAO-C	Third High-Energy Astrophysical Observatory, satellite launched in September 1979
HF	High Frequency (3-30 MHz), refers to radiowaves which are reflected from the ionospheric F-region and are thus useful for long-range telecommunications. The technology is simple and inexpensive and the frequency band is very heavily used, both domestically and internationally.

APPENDIX C - Continued

Highwater	Release of water ballast at 100-200 km during two initial Saturn flights. See Debus et al, 1964
HLLV	Heavy Lift Launch Vehicle, see Appendix B
HZE	(Particles), High Atomic Number (Z) and Energy particles in magnetosphere, present major radiation hazard to people and electronics
IMS	International Magnetospheric Study
ISEE	Satellite, referenced in Section 4.6.2, not explained
Ionosphere	Region in upper atmosphere in which ionization is important. One distinguishes between the D-region (<90 km), the E-region (90-150 km), and the F-region (>150 km; maximum in ionization near 300 km), which have successively higher electron densities and thus scatter successively high frequency electromagnetic waves.
keV	kilo-electron volt (1.6×10^{-9} erg)
LAGOPEDO	Water injection in F-region, through burn of approximately 100 kg high explosive which puts HO, CO_2 and N_2, etc., in the atmosphere, and thus reduces ionization locally. Launched by rocket.
LEO	Low Earth Orbit (500 km nominal)
L-values	Geomagnetic coordinate, distance from center of earth as a fraction of earth radius
MT	Metric Ton (10^3 kg). Term used in RSR, 1978 and PEA, 1978
MT-HE	Megaton of High Explosive (4.18×10^{15} joule)
Mesosphere	Region in the atmosphere from the temperature maximum near 50 km, the "stratopause" to the temperature minimum near 85 km, the "mesopause". Includes much of the ionospheric D-region. The temperature maximum at the stratopause is due to the absorption of solar UV by ozone.
Nacreous Clouds	See Section 2.4.2
NLC	Noctilucent Cloud, see Section 2.4.1
OMS	Orbital Maneuvering System (on Space Shuttle)
OPEN	See Section 4.6.3, Item 2
PEA	Preliminary Environmental Assessment, reference PEA, 1978.

APPENDIX C - Continued

PF	Perturbation Factor, see Equation (1), Section 1.2
PLV	Personnel Launch Vehicle, see Appendix B
POTV	Personnel Orbital Transfer Vehicle, see Appendix B
REP	Relativistic Electron Precipitation (from Radiation Belts)
RSR	Reference System Report, reference, RSR, 1978
SCATHA	Satellite, see Section 4.6.2
SPE	Solar Proton Event
SPS	Satellite Power System
Spread F	Ionospheric Irregularity in F-region, due to plasma turbulence, etc. So called because of its signal on an ionosonde. A region of enhanced or depleted F-region ionization tends to give rise to this effect.
TID	Traveling Ionospheric Disturbance
Thermosphere	Region of the upper atmosphere from the mesopause (85 km) on outward, perhaps to 500-1000 km. So called because the temperature increases mainly because solar radiation (UV and X-rays) is absorbed by the atmosphere. Includes much of the ionosphere. The terms mesosphere and thermosphere are used to emphasize the temperature structure and the neutral composition, and the term ionosphere stresses the changing electron density with its impact on charged particles and on electromagnetic wave propagation
WATERHOLE	See Section 2.5.3, analogous to LAGOPEDO
1-D, 2-D, 3-D	Used in the context of computer modeling of the structure and dynamics of the atmosphere. "1-D", a one-dimensional model considers only the variation of parameters (density, temperature, composition, etc.) with height, while a "2-D" model also shows variation with latitude but still involves averaging over longtitude ("zonal average"). A "3-D" (three-dimensional) model presents a proper representation for all geometric/geographic factors. Conceptually, both 1-D and 2-D models should involve an averaging over day-night conditions, although often 1-D and 2-D day-time and night-time calculations are made to illustrate diurnally varying effects.

APPENDIX D

AMBIENT ATMOSPHERIC LOADINGS FOR DIFFERENT SPECIES

For orientation, the ambient atmospheric loadings of relevant species in the appropriate domains are listed here. Some of the numbers are written with three digits to minimize internal roundoff errors: this does not imply significance. In integration over height z, the symbol (A) means that 70 km $\leq$ z $\leq$ 120 km, i.e., the integration goes over Domain A, (B) means that 450 km $\leq$ z $\leq$ 500 km (Domain B), and 500 km $\leq$ z $\leq$ 1000 km (Domain C-1). The surface area of the earth is written as $A_e = 5.11 \times 10^{14}$ m^2.

D.1 WATER IN DOMAIN A.

(a) From the recent compilation of A. Aikin shown in Fig. D.1, we have

$$A_e \int_{(A)} n(H_2O)\, dz = 3.94 \times 10^{34} . \qquad (D.1a)$$

(b) If one uses the suggestion of a mixing ration of 5 ppmv (see, e.g., Section 2.3) and the number density data from USSA, 1976, pp. 91-92, one finds

$$A_e(5 \times 10^{-6}) \int_{(A)} n_{(tot)}\, dz = 2.84 \times 10^{34} . \qquad (D.1b)$$

The agreement between these two estimates must be considered satisfactory in view of the poor knowledge we have of water in the mesophere. Note that 98% of all this water vapor lies below 90 km altitude.

For comparison, from Fig. D.1 we find

$$A_e \int_{(A)} n(H_2)\, dz = 7.32 \times 10^{33} \qquad (D.1c)$$

$$A_e \int_{(A)} n(H)\, dz = 1.66 \times 10^{33} \qquad (D.1d)$$

so that, using Aikin's results, in Domain A approximately 83% of all hydrogen atoms are found as H_2O, 15% as H_2 and 2% as H.

D.2 NITRIC OXIDE IN DOMAIN A

From Fig. D.1 we find

$$A_e \int_{(A)} n(NO)\, dz = 3.47 \times 10^{32} . \qquad (D.2)$$

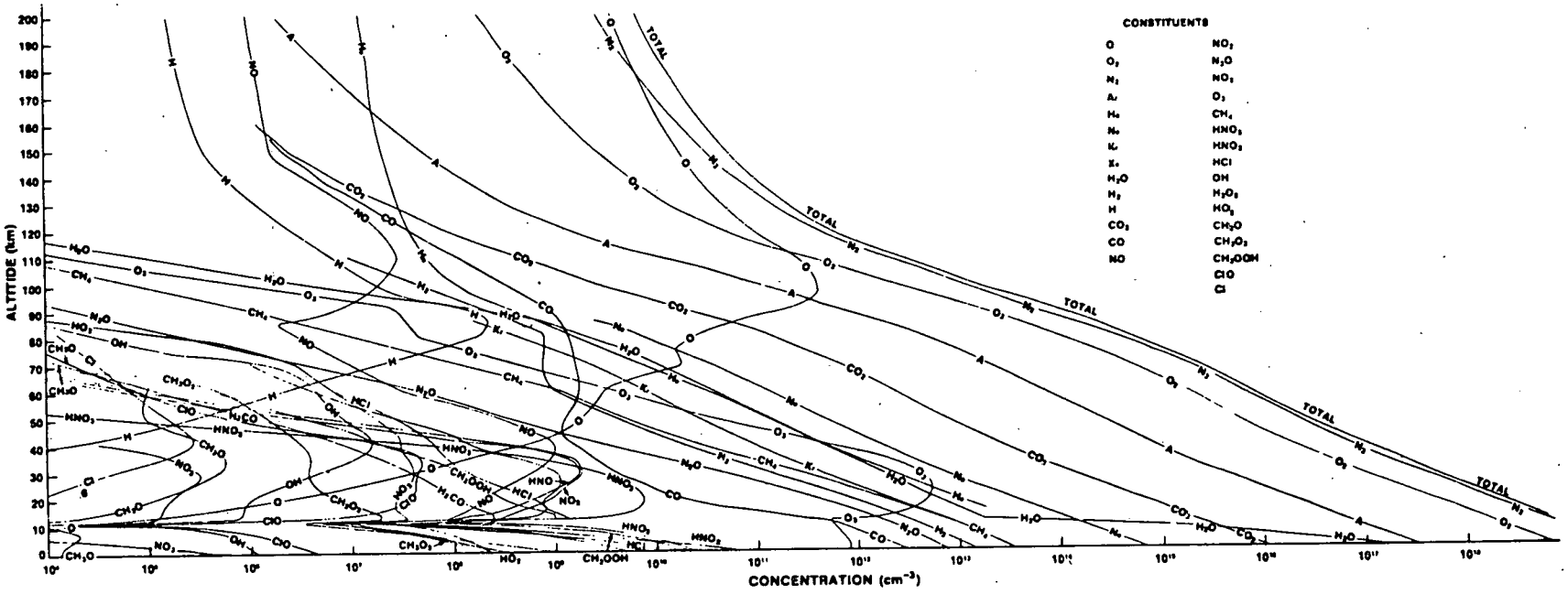

Figure D.1. Atmospheric Species Concentrations

(Source: A.C. Aikin, NASA/GSFC, 1978)

By contrast, using measurements by Meira and Tisone (see, Sechrist, 1977, Fig. 6.3, p. 105) gives total burdens of 1.43×10^{32} and 8.99×10^{32}, respectively.

D.3 DOMAIN B

From USSA, 1976, pp. 96, 213-214, we find

$$A_e \int_{(B)} n(H)\, dz = 1.05 \times 10^{30} , \tag{D.3}$$

$$A_e \int_{(B)} n(O)\, dz = 3.64 \times 10^{32} , \tag{D.4}$$

$$A_e \int_{(B)} n_{tot}\, dz = 4.74 \times 10^{32} . \tag{D.5}$$

D.4 DOMAIN C

Here this is divided into three different regions, namely the upper thermosphere, C-1, 500-1000 km where there are data from USSA, 1976, the plasmasphere, which is treated essentially as ionized atomic hydrogen corotating with the earth, and the outer magnetosphere, which consists of a very dilute plasma, mainly of ionized hydrogen.

C.1 Upper Thermosphere

From USAA, 1976, pp. 214-215, we have

$$A_e \int_{(C-1)} n(N_2)\, dz = 4.71 \times 10^{30} , \tag{D.6}$$

$$A_e \int_{(C-1)} n(O_2)\, dz = 7.33 \times 10^{28} , \tag{D.7}$$

$$A_e \int_{(C-1)} n(O)\, dz = 5.88 \times 10^{32} , \tag{D.8}$$

$$A_e \int_{(C-1)} n(H)\, dz = 1.62 \times 10^{32} , \tag{D.9}$$

$$A_e \int_{(C-1)} n(Ar)\, dz = 4.38 \times 10^{25} , \tag{D.10}$$

$$A_e \int_{(C-1)} n(He)\, dz = 3.62 \times 10^{32} , \tag{D.11}$$

$$A_e \int_{(C-1)} n_{tot}\, dz = 9.70 \times 10^{32} . \tag{D.12}$$

C-2 Plasmasphere

The domain is torus, of major radius approximatley 3 R_e (R_e = radius of earth, = 6380 km) and minor radius 2 R_e. From Cladis et al. (1973), p. 2-15, we find that if $L_{max} = 4$, the volume is 3×10^{28} cm^3, which if $L_{max} = 4.5$, the volume is 4.5×10^{28} cm^3. The number density of particles is 10^3-$10^4 cm^{-3}$, so that on a mean basis we have

$$\int_{(C-2)} n_{tot}\, dz = 1.2 \times 10^{32} \text{ (H-atoms, mainly).} \qquad (D.13)$$

C-3 Outer Magnetosphere

This may be treated as a sphere of radius 6.6 R_e, the radius of a geosynchronous orbit. Its volume is 3.1×10^{29} cm^3, so that if there is one particle per cm^3, the region contains 3×10^{29} particles.

D.5 ENERGY IN DOMAIN C

At altitudes above 150 km, the geomagnetic field energy $B^2/8\pi \sim 10^{-2}$ erg/cm^3 is larger than the thermal energy density ankT (a = 1.5 for monatomic and 2.5 for diatomic gases). Thus in the magentosphere whose volume is 3×10^{29} cm^3 the total geomagnetic field energy is 3×10^{20} joules.

Annual energy dissipation due to dynamical processes is much smaller than this. Thus, Burch, 1977, p. 51, quotes magnetic to substorm power dissipation levels as 10^{11}-10^{12} watts, with a mean duration of perhaps 20 minutes, occurring several times per day on the average. This rate of power dissipation occurring 1/10 of the time corresponds to an energy dissipation per year of 3×10^{17}-3×10^{18} joules, which is very much larger than the energy in the exhaust of the COTV argon ion engines.

Y.T. Chiu (private communication) points out that this energy estimate applies to the total dynamo, most of which is used in driving the tail current system, so that an estimate of 10% or 3×10^{16} - 3×10^{17} J/yr is suggested as appropriate for the field energy in the ring current. See also Akasofu (1977), especially pp. 54, 274, 348, 356, 561, and Table D.1 for representative values of the total energy flux in "geospace," the near-earth interplanetary medium of which the ionosphere and magnetosphere are important parts.

TABLE D.1

REPRESENTATIVE VALUES OF THE GLOBAL ENERGY FLOW IN GEOSPACE

ENTRY

Solar wind energy incident on the magnetosphere . . 10^{20} - 10^{21} erg/s*

Solar wind energy flow into the magnetosphere . . . 10^{18} - 10^{19}

STORAGE

Energy stored in the magnetotail. . . . . 3×10^{22} - 3×10^{23} erg

Energy stored in the ring current . . . . . 2×10^{22} - 10^{23}

TRANSPORT AND LOSS

Auroral particle precipitation. . . . . 2×10^{17} - 10^{18} erg/s

Joule heating by ionospheric currents . . . . . 2×10^{17} - 10^{18}

Ring current injection. . . . . 10^{18} - 10^{19}

Auroral luminosity. . . . . 10^{16} - 10^{17}

Auroral kilometric radiation. . . . . 10^{14} - 10^{16}

Total energy flow-magnetospheric substorm . . . . . $\sim 3 \cdot 10^{18}$ erg/s

-intense geomagnetic storm . . . . $\sim 10^{19}$

* 10^{20} erg/s = 10^{13} W = 3.16×10^{20} joule/year

Note: 1) COTV energy input of 6.1×10^{16} joule/year (see Table 3) is equivalent to 2×10^{16} erg/sec.

2) the variability with time and location is much larger than the ranges indicated.

(Source: NASA, 1979, Table 1)

APPENDIX E

REFERENCES

AIAA (1979), "Solar Power Satellites: An AIAA Position Paper," Astronautics & Aeronautics, 17, 14.

S.I. Akasofu (1977),"Physics of Magnetosphere Substorms," D. Reidel, Dordrecht, Holland.

D.N. Anderson and P.A. Bernhardt (1978), "Modeling the Effects of an H_2 Gas Release on the Equatorial Ionosphere," J. Geophys. Res. 83, 4777.

P.R. Arendt (1971), "Ionospheric Undulations following Apollo 14 Launching," Nature, 231, 438.

P.R. Arendt (1972), "Ionospheric Shock Front from Apollo 15 Launching," Nature, 236, 8.

F. Arnold and D. Krankowsky (1977), "Water Vapor Concentrations at the Mesosphere," Nature, 268, 218.

AWS (1974) "Defense Meteorological Satellite Program (DMSP) Users Guide," Report AWS-TR-74-250, Air Weather Service, U.S.A.F.

K.D. Baker, A.F. Nagy, R.O. Olsen, E.S. Oran, J. Randhawa, D.F. Strobel and T. Tohmatsu (1977, "Measurement of the Nitric Oxide Altitude Distribution in the Mid-latitude Mesosphere," J. Geophys. Res. 82, 3281.

C.A. Barth (1966), "Nitric Oxide in the Upper Atmosphere," Ann. Geophys. 22, 198.

E. Bauer (1974), "Dispersion of Tracers in the Atmosphere and Ocean: Survey and Comparison of Experimental Data," J. Geophys. Res. 79, 789.

E. Bauer (1978),"A Catalog of Perturbing Influences of Stratospheric Ozone, 1955-1975," Report FAA-EQ-78-20, Federal Aviation Administration, September 1978.

E. Bauer (1979), "Workshop on the Possibilities of Upper Atmospheric Experiments in Support of the Satellite Power System - Environmental Assessment - Strawman Draft," La Jolla Institute LJI-TN-79-023.

B. Benech and J. Dessens (1974), "Mid-Latitude Artificial Noctilucent Clouds Initiated by High-Altitude Rockets," J. Geophys. Res. 79, 1299.

P.A. Bernhardt (1976), "The Response of the Ionosphere to the Injection of Chemically Reactive Vapors," Stanford Electronics Labs., Technical Report #17.

M.A. Biondi (1973), "The Effects of Ion Complexity on Electron-ion Recombination," Comments At. Mol. Phys. 4, 85.

N. Brice (1970), "Artificial Enhancement of Energetic Particle Precipitation through Cold Plasma Injection: A Technique for Seeding Substorms?" J. Geophys. Res. 75, 4890.

K.L. Brubaker (1979), "Proceedings of Workshop on Stratospheric and Mesospheric Impacts of Satellite Power System," held in Chicago in September 1978, DOE Report, CONF-7809197.

C. Buffalano (1971), "A Physical Model of the Apollo Oxygen Releases," J. Geophys. Res. 76, 27.

J.L. Burch (1977), "The Magnetosphere," Chapter 2 in The Upper Atmosphere and Magnetosphere, National Academy of Sciences.

A.W. Castleman, Jr. (1979), "Nucleation and Molecular Clustering about Ions," Advances in Colloid & Interface Science 10, 73.

V.N. Chenurnoy and G.A. Charina (1977), "Semi-annual Temperature Variations in the Thermosphere and Their Relation with Atmospheric Circulation and Mesospheric Clouds," Geomag. Aeronomy 17, 58.

Y.T. Chiu, J.G. Luhman, B.K. Ching, M. Schultz, and D.J. Boucher, Jr. (1978), "Magnetospheric and Ionospheric Impact of Large-Scale Space Transportation with Ion Engines," Report SSL-78 (3960-04)-3, The Aerospace Corporation, September. Astronautics and Aeronautics, February 1980, p. 46.

Y.T. Chiu, J.M. Cornwall, J.G. Luhman and M. Schultz (1979), "Argon-ion Contamination of the Plasmasphere," Report No. SSL-79 (7824)-1, The Aerospace Corporation, accepted for publication in Progress in Astronautics and Aeronautics, AIAA.

J.B. Cladis, G.T. Davidson, and L.L. Newkirk, Editors (1973), "The Trapped Radiation Handbook," DNA 2524H, Defense Nuclear Agency, Revised, November.

G.E. Cook, D.G. King-Hele, and D.M.C. Walker (1960), "The Contraction of Satellite Orbits under the Influence of Air Drag. I. Spherically Symmetrical Atmosphere," Proc. Roy. Soc. A257, 224.

G.E. Cook and D.G. King-Hele (1961), "The Contraction of Satellite Orbits under the Influence of Air Drag. II. Oblate Atmosphere," Proc. Roy. Soc., A264, 88.

G.E. Cook and D.G. King-Hele (1963), "The Contraction of Satellite Orbits under the Influence of Air Drag. IV. Scale Height Dependent on Altitude," Proc. Roy. Soc., A275, 357.

T.E. Cravens and A.I. Stewart (1978), "Global Morphology of Nitric Oxide in the Lower E Region," J. Geophy. Res. 83, 2446.

D.E. Crosley and R.K. Lengel (1975), "Radiative Transition Probabilities and the Electronic Transition Moment in the A-X System of OH," J. Quant. Spectrosc. Radiat. Transfer 15, 579.

P.J. Crutzen, I.S.A. Isaksen, and G.C. Reid (1975), "Solar Proton Events: Stratospheric Sources of Nitric Oxide," Science 189, 457.

S.A. Curtis and J.M. Grebowsky (1979), "Changes in the Terrestrial Atmospheric-Ionospheric Magnetospheric System due to Ion Propulsion for Solar Power Satellite Placement," TM-79719, NASA/CSFC, February, submitted to Space Solar Power Review.

S.A. Curtis and J.M. Grebowsky (1979), "Energetic Ion Beam-Magnetosphere Injection and SPS Transportation," submitted to J. Geophys. Res.

N. D'Angelo and E. Ungstrup (1976), "On the Occurrence of Widely Observed Noctilucent Clouds," J. Geophys. Res. 81, 1777.

K.H. Debus, W.G. Johnson, R.V. Hembree, and C.A. Lundquist (1964), "A Preliminary Review of the Upper Atmosphere Observations made During the Saturn High Water Experiment," Proc. XIIIth Int. Astronaut. Cong., Varna, 1962, Springer-Verlag.

T.M. Donahue (1977), "Hydrogen," Chapter 4 in The Upper Atmosphere and Magnetosphere, National Academy of Sciences.

T.M. Donahue, B. Guenther, and J.E. Blamont (1972), "Noctilucent Clouds in Daytime; Circumpolar Particulate Layers Near the Summer Mesophere," J. Atmos. Sci. 29, 1205.

B.T. Draine and E.E. Salpeter (1975), "Time-Dependent Nucleation Theory," J. Chem. Phys., 67, 2230.

H.D. Edwards (1962), "Optical Observations of a High Altitude Release of Water over Wallops Island, VA, on March 2, 1962," Technical Report No. 1, Proj. A-597, Georgia Inst. Tech., Atlanta.

H.J. Fahr and H.U. Nass (1979), "Concerning the Structure of the Transition Layer Between the Terrestrial Thermosphere and Exosphere," Ann. Geophys. 34, 219.

F.C. Fehsenfeld, A.L. Schmeltekopf and E.E. Ferguson (1967), "Thermal-Energy Ion-Neutral Reaction Rates, VII, Some Hydrogen-Atom Abstraction Reactions," J. Chem. Phys., 46, 2802.

B. Fogle and B. Haurwitz (1966), "Noctilucent Clouds," Space Sci. Rev., 6, 279.

B. Fogle, S. Chapman, and C. Echols (1965), Geophys. Inst. Rpt. UAG R-162, Univ. of Alaska.

J.H. Gardner and P.H. Rogers (1979), "Thermospheric Propagation of Sonic Booms from the Concorde Supersonic Transport," Memorandum Report 3904, Naval Research Laboratory, February.

H.B. Garrett and J.W. Forbes (1979), "Time Evolution of Ion Contaminant Clouds at Geosynchronous Orbit," manuscript submitted to Geophys. Res. Letters.

R.A. Goldberg and G. Witt (1977), "Ion Composition in a Noctilucent Cloud," J. Geophys. Res., 82, 2619.

G. Haerendel and R. Lust (1970), "Electric Fields in the Ionosphere and Magnetosphere," in Particles and Fields in the Magnetosphere (B.M. McCormac, Ed.) p. 212, D. Reidel, Dordrecht, Holland.

K.D. Hage (1964), "Particle Fallout and Dispersion below 30 km in the Atmosphere," Travelers Research Center Report SC-DC-64-1463 prepared for Sandia Corporation (available from N.T.I.S.).

W.B. Hanson and H.C. Carlson (1977), "The Ionosphere," Ch. 5 in National Academy of Sciences, ("The Upper Atmosphere and Magnetosphere").

J.E. Harries (1976), "The Distribution of Water Vapor in the Stratosphere," Revs. Geophys. and Space Phys., 14, 565-575.

C.L. Hemenway, R.K. Soberman, and G. Witt (1964), "Sampling of Noctilucent Clouds," Tellus, 16, 84 ibid 96.

H. Henderson and D. Hilton, "Sonic Boom Ground Pressure Measurements from the Launch and Reentry of Apollo 16," NASA-TN-D7606, August 1974, and "Sonic Boom Measurements in the Focus Region during Ascent of Apollo 17," NASA-TN-D-7806, December 1974; both NASA Langley Research Center.

J.R. Herman and A.R. Goldberg (1978), "Sun, Weather and Climate," NASA SP-429.

P.G. Hill (1966), "Condensation of Water Vapor During Supersonic Expansion in Nozzles," J. Fluid Mech., 25, 593.

D. Hilton, H. Henderson, and R. McKinney (1972), "Sonic Boom Ground Pressure Measurements from Apollo 15," NASA-TN-D-6950, NASA Langley Research Center, September.

C.O. Hines (1974), "A Possible Mechanism for the Production of Sun-Weather Correlations," J. Atmos. Sci. 31, 589.

H. Hoerlin (1976), "U.S. High-Altitude Test Experience: A Review Emphasizing the Impact on the Environment," Monograph LA-6405, Los Alamos Scientific Laboratory, October.

H.G. Horak, D.J. Simons, and J.H. Wolcott (1978), "Photometry of Lagopedo Uno and Dos," AM Geophys. Union Spring Meeting, Paper SA 23.

J.J. Horvath and C.J. Mason (1978), "Nitric Oxide Mixing Ratios Near the Stratopause Measured by a Rocket Borne Chemiluminescent Detector," Geophys. Res. Lett. 5, 1023.

C.J. Howard, H.W. Dundle, and F. Kaufman (1970, "Gas-Phase Rates of Some Positive Ions with Water at 296 K," J. Chem. Phys., 53, 3745.

J.R. Hummel and J. Olivero (1976), "Satellite Observations of the Mesospheric Scattering Layer and Implied Climatic Consequences," J. Geophys. Res., 81, 3177.

A.V. Jones (1973), "The Infrared Spectrum of the Airglow," Space Sci. Res., 15, 355.

W.W. Kellogg (1964), "Pollution of the Upper Atmosphere by Rockets," Space Sci. Revs., 3, 275.

JANAF (Joint Army-Navy-Air Force) (1971), Thermochemical Tables, Report NSRDS-NBS 37, 2d Ed., discussion on H_2O.

D.J. Kessler and B.G. Cour-Palais (1978), "Collision Frequency of Artificial Satellites: the Creation of a Debris Belt," J. Geophys. Res., 83, 2637.

D.G. King-Hele (1962), "The Contraction of Satellite Orbits under the Influence of Air Drag. II. High-Eccentricity Orbits ($0.2 < e < 1$)," Proc. Roy. Soc., A267, 541.

H.C. Koons and M.G. Pongratz (1979), "Ion Cyclotron Waves Generated by an Ionospheric Barium Injection," J. Geophys. Res., 84, 533.

V.I. Krasovsky, B.P. Potapov, A.I. Semenov, V.G. Sobolev, M.V. Shagaev, and N.N. Shefov (1977), "On the Equilibrium Nature of the Rotational Temperature of Hydroxyl Airglow," Planet. Space Sci., 25, 596.

R.T.V. Kung, L. Cianciolo, and J.A. Myer, (1975), "Solar Scattering from Condensation in Apollo Translunar Injection Plane," AIAA J., 13, 432.

C.A. Lundquist (1962), "A Preliminary Review of the Upper Atmosphere Observations Made During the Saturn Highwater Experiment," Proc. XIII International Astronomical Congress, Varna, Bulgaria, p. 182.

C.A. Lundquist (1970), "Photometry from Apollo-Tracking," Space Research X, 25.

T.D. McCay, and H.M. Powell (1978), "Direct Mass Spectrometer Measurements on a Highly Expanded Rocket Exhaust Plume," J. Spacecraft & Rockets, 15, 133.

W.K. McGregor (1978), "On the Radiation from Small Particles," J. Quant. Spectry. Rad. Transfer 19, 659.

A.L. McIntyre (1978), "Multispectral Measurements Program (MSMP) Results and Status," Proc. Society of Photo-Optical Instrumentation Engineers (Redondo Beach, CA) 156, 116 (August).

H.J. Mastenbrook (1968), "Water Vapor Distribution in the Stratosphere and High Troposphere," J. Atmo, Sci., 25, 299-311.

H.J. Mastenbrook (1971), "The Variability of Water Vapor in the Stratosphere," J. Atmo Sci., 28, 1495-1501.

H.J. Mastenbrook (1974), "Stratospheric Water Vapor Distribution and Variability," in Vol. I, Proc. International Conference on Structure, Composition, and General Circulation of the Upper and Lower Atmosphere and Possible Anthropogenic Perturbations," Jan. 14-25, 1974, Melbourne, Australia, pp. 233-248, Dr. W.L. Godson, ed., Atmospheric Environment Service: Downsview, Ontario, Canada.

A.B. Meinel (1950), "Hydroxide Emission Bands in the Spectrum of the Night Sky," Astrophys. J. 111, 207; ibid. 112, 120.

A.B. Meinel, B. Middlehurst and E. Whitaker (1963), "Low-Latitude Noctilucent Cloud of 15 June 1963," Science, 141, 1176.

L.G. Meira, Jr. (1971), "Rocket Measurements of Upper Atmospheric NO and Their Consequences to the Lower Ionosphere," J. Geophys. Res., 76, 202.

M. Mendillo, G.S. Hawkins, and J.A. Klobuchar (1975a), "A Large-Scale Hole in the Ionosphere Caused by the Launch of Skylab," Science, 187, 343.

M. Mendillo, G.S. Hawkins, and J.A. Klobuchar (1975b), "A Sudden Vanishing of the Ionospheric F-Region Due to the Launch of Skylab," J. Geophys. Res., 80, 2217.

M. Mendillo, B. Herniter, and D. Rote (1979), "Modification of the Aerospace Environment by Large Space Vehicles," AIAA Paper 79-0391, January.

R.C. Molander and H.G. Wolfhard (1969), "Explanation of Large Apollo 8 (J-2) Rocket Plume Observed during Trans-Lunar Injection," Note N-610, Institute for Defense Analyses, February.

G. Moreels and M. Herse (1977), "Photographic Evidence of Waves Around the 85-km Level," Planet. Space Sci., 25, 265.

NASA, Science Def. Working Group (1979), "Origin of Plasma in the Earth's Neighborhood (=OPEN)," NASA/GSFC.

R.E. Newell, J.W. Kidson, D.G. Vincent, G.J. Boer (1974), "The General Circulation of the Tropical Atmosphere, and Interaction with Extratropical Latitudes," especially Ch. 10 in Vol. 2, M.I.T. Press.

N.T. Novozhilov (1979), "Characteristics of the Structure of the Upper Stratosphere and the Mesosphere in the Presence of Noctilucent Clouds," Solar Syst. Res., 12, 157.

T. Ogawa (1976), "Excitation Processes of Infrared Atmospheric Emissions," Planet. Space Sci., 24, 749.

C. Park (1976), "Estimate of NO Production by Lifting Spacecraft on Reentry," Atmos. Environment, 10, 309-313.

C. Park (1979), "Equivalent-cone Calculation of Nitric Oxide Production Rate During Space Shuttle Entry" (to be published).

C. Park and G.P. Menees (1978), "Odd Nitrogen Produced by Meteroids," J. Geophys. Res., 83, 4029.

PEA (1978),"Preliminary Environmental Assessment for the Satellite Power System (SPS)," DOE/ER-0021, U.S. Department of Energy.

R. Penndorf (1978), "Analysis of Ozone and Water Vapor Field Measurement Data," Report No. FAA-EE-78-29, available from NTIS, Springfield, Va.

J. Pressman, L.M. Aschenbrand, F.F. Marmo, A. Jursa, and M. Zelikoff (1956), "Synthetic Atmospheric Chemiluminescence Caused by the Release of NO at 106 km," J. Chem. Phys., 25, 187.

H.E. Radford, M.M. Litvak, G.A. Gottlieb, E.W. Gottlieb, S.K. Rosenthal, and A.E. Lilley (1977), "Mesospheric Water Vapor Observed from Ground-Based Microwave Absorption," J. Geophys. Res., 82, 472.

J.V. Rakich, H.E. Bailey and C. Park (1975), "Computation of Nonequilibrium Three-Dimensional Inviscid Flow Over Blunt-nosed Bodies at Supersonic Speeds," AIAA Paper No. 75-835.

G.C. Reid (1975), "Ice Clouds at the Summer Polar Mesospause," J. Atmos. Sci., 32, 523.

R.G. Roble and P.B. Hays (Dec. 1979), "A Quasi-Static Model of Global Atmospheric Electricity: Vol. 2, Electrical Coupling Between the Upper and Lower Atmosphere," J. Geophys. Res., 84, 7247-7256.

J.W. Rogers, A.T. Stair, Jr., T.C. Degges, C.L. Wyatt, and D.J. Baker (1977), "Rocketborne Measurement of Mesospheric Water in the Auroral Zone," Geophys. Res. Letters, 4, 366.

D.M. Rote (1978), "Proceedings of Workshop on Ionospheric and Magnetospheric Impacts of Satellite Power System," held in Chicago in August 1978, DOE Report, CONF-7808115.

RSR (1978), "SPS Reference System Report," DOE/ER-0023, U.S. Department of Energy.

D.W. Rusch and G.A. Barth (1975), "Satellite Measurements of Nitric Oxide in the Polar Region," J. Geophys. Res., 80, 3719.

D.W. Rusch (1973), "Satellite Ultraviolet Measurements of Nitric Oxide Fluorescence with a Diffusive Transport Model," J. Geophys. Res., 78, 5676.

T.G. Scholz, D.H. Ehhalt, L.E. Heidt and E.A. Martell (1970), "Water Vapor, Molecular Hydrogen, Methane, and Tritium Concentrations Near the Stratopause," J. Geophys. Res., 75, 3049.

A.F.D Scott (1974), "Association Between the Mid-winter Stratospheric Circulation and the First Observation in the Following Summer of Noctilucent Clouds," Nature, 247, 269.

C.F. Sechrist, Jr. (1977), "The Ionspheric D-Region," Chapter 6 in The Upper Atmosphere and Magnetosphere, National Academy of Sciences.

R.D. Sharma and C. Buffalano (1971), "Temperature and Size Histories of Liquid H_2, O_2 and H_2O Particles Released in Space," J. Geophys. Res., 76, 232.

D.J. Simons, M.B. Pongratz and S.P. Cary (1979), "Prompt Striations in Ionospheric Barium Clouds due to a Velocity Space Instability," submitted to J. Geophys. Res.

W.H. Smith (1970), "Radiative and Predissociation Probabilities for the OH $A^2\Sigma^+$ State," J. Chem. Phys., 53, 792.

J.L. Stanford and J.S. Davis (1974), "A Century of Stratospheric Cloud Reports: 1887-1972," Bull. Amer. Met. Soc. 55, 213.

D.P. Stern (1978), "Solar-Terrestrial Programs, A Five Year Plan," Office of Space Sciences, NASA.

A.I. Stewart and T.E. Cravens (1978), "Diurnal and Seasonal Effects in E-Region Low-Altitude Nitric Oxide," J. Geophys. Res., 83. 2453.

R.A. Stokes (1979), "Report of a Workshop of Effects of SPS on Ground-Based Astronomy," held in Richland, WA, in May. Report in preparation.

D.F. Strobel (1971), "Odd Nitrogen in the Mesosphere," J. Geophys. Res., 76, 8384.

H. Takahashi, P.P. Batista, B.R. Clemesha, D.H. Simonich, and Y. Sahai (1979), "Correlation Between OH, NaD and OI-5577A Emissions in the Airglow," Planet. Space Sci., 27, 801.

J.S. Theon, W. Nordberg, and W.S. Smith (1967), "Temperature Measurements in Noctilucent Clouds," Science, 157, 419.

G.C. Tisone (1973), "Measurements of NO Densities During Sunrise at Kauai," J. Geophy. Res., 78, 746.

T. Tohmatsu and N. Iwagami (1975), "Measurements of Nitric Oxide Distribution in the Upper Atmosphere," Space Res. XV, 241.

W.F. Tozer and D.E. Beeson (1974), "Optical Model of Noctilucent Clouds Based on Polarimetric Measurements from Two Sounding Rocket Campaigns?" J. Geophys. Res., 79, 5607.

W.A. Traub and M.T. Steir (1976), "Theoretical Atmospheric Transmission in the Mid- and Far-Infrared at Four Altitudes," Appl. Opt. 15, 364.

B. Vonnegut (1979), "Middle Atmosphere Electrodynamics," Report of the Workshop on the Role of the Electrodynamics of the Middle Atmosphere on Solar Terrestrial Coupling, Reston, Va., Jan. 17-19, 1978, NASA-CP 2090.

W.R. Wadt, P.J. Hay, and D.C. Cartwright, "Dissociative Recombination," LASL internal memorandum (February 18, 1977) and AM Geophys. Union Spring Meeting, Paper SA18 (April 1978).

G. Witt (1969), "The Nature of Noctilucent Clouds," Space Res. IX, 157.

B.J.C. Wu (1975), "Possible Water Vapor Condensation in Rocket Exhaust Plume," AIAA J., 13, 727.

J. Zinn, C.D. Sutherland, M.P. Pongratz (1979), "Effects of Rocket Exhaust Products in the Thermosphere and Ionosphere," Los Alamos Scientific Laboratory report LA-7926-MS, previous informal distribution as LA-UR-79-1512.

J. Zinn, C.D. Sutherland, M.B. Pongratz (1978), "Update on Predicted Ionospheric Effects for Launches of Heavy Lift Rocket Vehicles for Construction of SPS," LA-UR-1590, Los Alamos Scientific Laboratory.

USSA (1976), "United States Standard Atmosphere, 1976," NOAA-NASA-USAF.

THIS PAGE

WAS INTENTIONALLY

LEFT BLANK

APPENDIX F

SUPPLEMENTARY MATERIAL

This appendix consists of various items that were contributed at the workshop which do not fit exactly into the report but which should be drawn to the attention of the reader. Each item is accompanied by an editorial comment explaining why the item is included here rather than in the text.

F.1 Abstracts of Selected Current Papers

UPPER ATMOSPHERE MODIFICATIONS DUE TO CHRONIC DISCHARGES OF WATER VAPOR FROM SPACE LAUNCH VEHICLE EXHAUSTS

Jeffrey M. Forbes*

Dept. of Astronomy, Boston University, Boston, MA 02215

(Preliminary Draft)

Prepared for:

"Space Systems and Their Interactions with the Earth's Space Environment"

(H.B. Garrett and C.B. Pike, Editors)

June, 1979

in Revised form

July, 1979

*Permanent Affiliation: Space Data Analysis Laboratory, Boston College, Chestnut Hill, MA 02167

ABSTRACT

A simple time-dependent analytic formalism is developed and utilized to predict the influences of transport, photodissociation, and frequency of injection on the global redistribution of water deposited in the earth's upper atmosphere by repeated launches of large rockets. As an example, possible future Satellite Power System (SPS) activities are simulated by injections of 7.0×10^{31} molecules of H_2O between 70 and 120 km by second stages of heavy lift launch vehicles (HLLVs), with launch frequencies ranging between 8 day^{-1} and 2 $week^{-1}$. Generally, measurable environmental effects are found to occur when the mesospheric water vapor mixing ration (χ) exceeds 100 ppmv, which can occur over areas of the order of 20,000 km^2 for the SPS scenarios adopted here. Possible environmental effects quantitatively evaluated for χ>100 ppmv include: (a) a 50% reduction in D-region ionization due to screening of L_α radiation by water (and a smaller contribution, by thermospheric hydrogen produced by photolysis of the injected H_2O below 120 km); (b) an additional 50% reduction of D-region ionization resulting from conversion of ambient NO^+ and O_2^+ ions to heavy water cluster ions that possess more rapid recombination rates; and (c) at least a doubling of OH concentrations below 100 km. Radiative cooling produced by the injected H_2O is found to have a negligible effect on the general circulation of the mesosphere and lower thermosphere, and at mid-latitudes mixing ratios of order 10^3 ppmv would be required to reach the frost-point temperatures necessary for the maintenance of clouds at the mesopause. Qualitatively, atomic hydrogen released by photolysis of H_2O is expected to increase the loss rate of ozone between 75 and 95 km, to significantly increase OH concentrations and accompanying airglow emissions, and also act to increase nighttime E-region ionization by geocornonally scattering L_α and L_β radiations after diffusing into the upper thermosphere. These effects of hydrogen released by H_2O photolysis may indeed encompass the most important upper atmosphere environmental impacts to be researched.

Unclassified

SECURITY CLASSIFICATION OF THIS PAGE (When Data Entered)

REPORT DOCUMENTATION PAGE		READ INSTRUCTIONS BEFORE COMPLETING FORM
1. REPORT NUMBER AFGL-TR-77-0288	2. GOVT ACCESSION NO.	3. RECIPIENT'S CATALOG NUMBER
4. TITLE (and Subtitle) MODELING OF THE GEOSYNCHRONOUS ORBIT PLASMA ENVIRONMENT – PART I		5. TYPE OF REPORT & PERIOD COVERED Scientific. Interim. 6. PERFORMING ORG. REPORT NUMBER AFSG No. 380
7. AUTHOR(s) Henry B. Garrett, Capt, USAF		8. CONTRACT OR GRANT NUMBER(s)
9. PERFORMING ORGANIZATION NAME AND ADDRESS Air Force Geophysics Laboratory (PHG) Hanscom AFB Massachusetts 01731		10. PROGRAM ELEMENT, PROJECT, TASK AREA & WORK UNIT NUMBERS 76610801 62101F
11. CONTROLLING OFFICE NAME AND ADDRESS Air Force Geophysics Laboratory (PHG) Hanscom AFB Massachusetts 01731		12. REPORT DATE 14 December 1977 13. NUMBER OF PAGES 46
14. MONITORING AGENCY NAME & ADDRESS(if different from Controlling Office)		15. SECURITY CLASS. (of this report) Unclassified 15a. DECLASSIFICATION/DOWNGRADING SCHEDULE
16. DISTRIBUTION STATEMENT (of this Report) Approved for public release; distribution unlimited.		
17. DISTRIBUTION STATEMENT (of the abstract entered in Block 20, if different from Report)		
18. SUPPLEMENTARY NOTES		
19. KEY WORDS (Continue on reverse side if necessary and identify by block number) Spacecraft charging Environmental modeling Plasma interactions		

20. ABSTRACT (Continue on reverse side if necessary and identify by block number)

Although the role of the environment in generating spacecraft potential variations at geosynchronous orbit is well documented, variations in the ambient environment itself have not been well-defined. Similarly, no studies of the environment have attempted an analytic formulation of the various parameters needed to model the spacecraft charging phenomenon. This paper describes the parameters needed to formulate such a model and outlines a systematic procedure for constructing a simple analytic model that includes

DD FORM 1 JAN 73 1473 EDITION OF 1 NOV 65 IS OBSOLETE

Unclassified

SECURITY CLASSIFICATION OF THIS PAGE (When Data Entered)

Unclassified

SECURITY CLASSIFICATION OF THIS PAGE(When Data Entered)

20. Abstract (Continued)

the effects of local time and geomagnetic activity. Observational data from the ATS-5 satellite are analyzed using this procedure to give a preliminary analytic description of the geosynchronous environment in the form of a FORTRAN program.

Unclassified

SECURITY CLASSIFICATION OF THIS PAGE(When Data Entered)

SPACE SYSTEMS AND THEIR INTERACTIONS WITH THE EARTH'S SPACE ENVIRONMENT

H. B. Garrett and C. P. Pike, Editors

CONTENTS (31 March 1979)

D. Surface Discharge Effects
K. G. Balmain

E. Active Charge Control Effects on Space Vehicles
C. K. Purvis

F. Computer Modeling of Spacecraft Charging Interactions
A. G. Rubin, G. Schnuelle

IV. RADIATION EFFECTS ON SPACE SYSTEMS

A. Radiation Effects on Space Systems and Their Modeling (Review)
A. Vampola

B. Radiation Effects on Electronic Devices
W. Shedd and P. Vail

C. Cosmic Ray Effects on VLSI
J. N. Bradford

D. Radiation Effects on Solar Cells
P. Rahilly

E. Radiation Induced Electric Fields in Dielectrics
A. R. Frederickson

F. Soft Errors in Space Electronic Systems
P. J. McNulty, G. F. Farrell, R. Wyatt, R. C. Filz and P. L. Rothwell

V. LARGE SPACE SYSTEMS INTERACTIONS

A. Space Environmental Interactions with Biased Spacecraft Surfaces
N. J. Stevens

B. Plasma Sheath Theory for Large High-Voltage Space Structures
L. W. Parker

C. Current Leakage for Low Altitude Satellites
J. McCoy, A. Konradi, and O. K. Garriott

F.2 Bauer "Specific Enthalpy for Different Water Releases"

This is an elementary thermodynamic analysis to compare the specific enthalpy and effective temperature for Highwater (Lundquist, 1962), LAGOPEDO, and various HLLV and POTV burns of hydrogen-oxygen engines. The conclusion is that these water injections correspond to a very wide range of effective enthalpies or temperatures.

Highwater. One may assume that the material was injected as liquid water at approximately 15°C, at apogee of the carrier rocket so that no kinetic energy was contributed due to the motion of the rocket. Relative to ice at 0 K the enthalpy of injected material was 0.12 Kcal/gm (see JANAF Thermochemical Tables, Report NSRDS-NBS 37, 2nd Ed., 1971, discussion on H_2O).

LAGOPEDO. The water is produced by combustion of high explosives near the apogee of a sounding rocket. The combustion temperature may be taken as 2500 K so that the enthalpy (relative to ice at 0 K) is 2.13 Kcal/gm.

H_2-O_2 Rocket Engine Burns. We assume that the exhaust is 70% H_2O, 30% H_2, so that the effective molecular weight is 13.2. The limiting exhaust velocity in vacuum is taken to be 4.5 km/sec (see Section 3.1.3,B) corresponding to an enthalpy of 31.9 Kcal/mol relative to ice at 0 K, or to a combustion temperature of 2950 K. However, because of the motion of the vehicle the enthalpy of the actual burns is quite different. Thus for the HLLV second stage burn shown in Fig. 1, in intervals 11 to 13 the vehicle speed ranges from 4.4 to 6.9 km/sec, so that the actual enthalpy of exhaust gas ranges from 0 up to 9.1 Kcal/mol, or the temperature may be as high as 1050 K. For the HLLV circularization and deorbit burns the effective velocity of 7.6 km/sec (circular orbit velocity) less 4.5 km/sec, giving a net velocity of 3.1 km/sec, an enthalpy of 15.2 Kcal/mol, corresponding to 1600 K. For the POTV burns (see Table 8) the absolute exhaust velocity ranges from 2.15 to 13.3 km/sec, enthalpies lie in the range 7.3 to 280 Kcal/mol, corresponding to temperatures from 850 K to above 10,000 K.

F.3 Bauer "Memo to Rote, SPS Ionospheric Impact"
This outline a priority impact.

LaJolla INSTITUTE
P.O. BOX 1434 • LA JOLLA • CALIFORNIA 92038 • PHONE (714) 454-3581
Ernest Bauer, 8109 Fenway Rd., Bethesda, MD 20034. (301)469-6726

Memorandum for Dr. Don Rote, Argonne National Laboratory

Subject SPS Ionospheric Impact

Date 12 July 1979

Following our workshop on "Upper Atmospheric Research in Support of the SPS Environmental Assessment" at La Jolla, CA I briefed a U.S.Navy Communications group at Naval Ocean Systems Center, San Diego (J.H.Richter, D.Sailors, W.Moler, Messrs. Argo and Ferguson) on the project and on our study on 3 July.

One prediction which concerned these Navy communications experts very much came from a morphology subgroup chaired by J.Fedder of NRL, and calls for a region in which the ionization is depleted by roughly a factor of two, extending globally at the latitude of injection, several thousand kilometers in width and extending upward from approximately 160 km.

The ionization is depleted because H_2O and H_2 molecules from the rocket exhaust (HLLV second stage, circularization and deorbit burns, POTV and COTV) react with the ambient atomic (O^+) ions to form molecular ions, OH^+ and H_2O^+, which recombine very much faster with electrons than do the atomic ions, thus reducing the effective ionization.

The effect of this on global HF long-haul (sky wave) communications is extremely serious as the band (3-30 MHz) is extremely crowded, and indeed at an International Conference of CCIR next year the USA expects to lose some frequency allocations to developing nations which depend on (cheap and simple) HF Com rather than use higher frequency satellite communications.

Dr. Sailors (714-225-7400) explained that reducing the electron density by a factor 2 reduces the maximum usable frequency (which is reflected from the ionosphere) by $\sqrt{2}$, thus reducing the band limit of 30 MHz to 21 MHz. For long-range communications the upper portion of the band, say 15-30 MHz is optimal. This would be cut to the range 15-21 MHz, or to 6 MHz from 15 MHz, which is indeed a drastic reduction in a crowded band. (The numbers are all illustrative only).

I discussed the matter later with Dr. Gabriel Frenkel at IDA (another CCIR participant) and he confirmed Dr. Sailors' statements, the pressure on the band, and the problems of the International negotiations.

This problem is one of which Dr. Charles Rush should take cognisance, as he is in the CCIR community. I got the impression that this effect is so serious that it might prove to be a "program stopper" for SPS because of the international implications.

Let me stress that the estimate of the depleted ionospheric region is not based on detailed calculations but just on educated guesses. Computing the morphology of the disturbed ionospheric region presents a significant and high priority aspect of the SPS Upper Atmospheric Environmental Assessment. Explicitly the "factor 2" represents just an initial estimate which must be improved upon.

Ernie Bauer

Ernest Bauer.

F.4 Cladis & McCormac "Emission of IR Radiation from the SPS."

A workshop was held at Battelle Pacific Northwest Laboratory on 23-24 May 1979 on the effect of SPS on optical, IR and radio astronomy (Dr. R.A. Stokes, Chairman). The conclusion was that IR radiation from SPS, while large in absolute power, is unimportant from an overall standpoint. This note should be considered in the context of the workshop, the report of which is in preparation (Stokes, 1979).

EMISSION OF INFRARED RADIATION FROM THE SOLAR POWER SATELLITE

John B. Cladis and Billy McCormac

Lockheed Palo Alto Research Laboratory

An estimate is made of the black-body temperature and radiance of the SPS in the infrared. This estimate indicates that the SPS will appear as a bright IR star, but that the effect of the IR radiation on the earth's atmosphere will be negligible.

The black-body temperature is given approximately by the equation,

$$(1) \qquad 0.9\, S_p\, A + \frac{S_p\, r_a\, \pi R_e^{\,2} A}{4\pi (6.6\, R_e)^2} = 2A\varepsilon\delta T^4$$

where

S_p = Solar Radiation Power Intensity ($\sim$ 1400 W/m^2)

A = Area of solar-cells

r_a = Albedo of Earth ($\approx$ .38)

R_e = Radius of Earth

ε = Emissivity of SPS in IR

δ = Stephen-Boltzman constant (5.67×10^{-8} W/m^2/°K)$^{1/4}$

and

T = Radiation temperature of SPS .

Here it is assumed that the surface A absorbs 100% of the solar energy and that 10% is radiated to earth by microwaves. Taking $\varepsilon = 0.95$, the solution of (1) gives $T = 329$ K.

The radiance, p, at this temperature is 5×10^{-3} watts/cm^2/2π rad at the peak of the black-body radiation ($\lambda \approx 9\ \mu$). At the surface of the earth the IR intensity, I, is

(2) $$I_{SPS} = \frac{pA}{2H^2}$$

where H is the altitude of the SPS. Assuming $A = 50 \times 10^{10}$ cm^2, we obtain $I = 1.02 \times 10^{-10}$ watts/ cm^2 or 1.02×10^{-3} erg/cm^2/sec.

The radiance of the sun, assumed to be black-body radiator with a temperature of 6000 K, at $\lambda = 9$ μ, is about 1 watt/cm^2/2π rad. For this source, the intensity at the earth's surface is

(3) $$I_\Theta = \frac{P_\Theta}{8} \left(\frac{\pi\delta_\Theta}{180}\right)^2$$

where δ_Θ is the angle subtended by the sun in degrees. Taking $\delta_\Theta = .5$ deg., Eq. (3) gives $I_\Theta = 2.99 \times 10^{-5}$ watts/cm^2 or 299 ergs/cm^2/sec. This is a factor of 3×10^5 larger than that from the SPS. Hence, the atmospheric effect of the IR radiation from the SPS is small in comparison to the existing effect due to the solar radiation. However, the SPS will appear as a bright IR star, and as such it may pose a troublesome background for IR astronomy. The background problem would, of course, be compounded if 30 such satellites were present in the night sky.

The scattering of visible solar radiation by the SPS will also present a deleterious background for ground astronomy as discussed in the accompanying material by G. T. Davidson.

F.5 Davidson "The Effects of Ar^+ on the Magnetosphere."

Dr. Davidson was unable to attend the workshop but submitted this note which supplements the conclusions of Sections 4.3 and 4.4.

THE EFFECTS OF AR^+ IN THE MAGNETOSPHERE

G. T. Davidson
Lockheed Palo Alto Research Laboratory

The major anticipated environmental effects of Ar^+ ions have mainly to do either with disturbance of the ionosphere or with disturbance of the trapped radiation belts. These have been addressed by a recent series of reports, primarily by the Aerospace Corporation group. This note is to point out where the important unresolved problems may lie.

A large portion of the Ar^+ ions are precipitated in the ionosphere where they may stimulate airglow emission. The resulting emissions may be comparable with the airglow due to natural processes (Ref. 1). This is not usually considered serious, but it has recently been pointed out that even minor increases in the sky illumination at mid and low latitudes can interfere severely with the conduct of ground-based astronomy (Ref. 2). The natural airglow is the dominant source of interference with observation of faint celestial objects. (The contribution due to all the stars in the sky is not well known, but appears to be slightly less.) The airglow due to Ar^+ precipitation must be carefully evaluated, which entails estimation (poorly known) of the cross sections for excitation by direct impact.

The Ar^+ ions that remain in the plasmasphere would profoundly affect wave and particle processes there. The lifetimes of low energy Ar^+ ions are measured in days (Ref. 1); the effects would be expected to persist through the entire period of SPS construction activity. There is no doubt that the high energy electron content of the trapped radiation belts is strongly influenced by the cold plasma density (Ref. 3). The precise mechanism for removal of relativistic electrons is not, however, fully understood. The most popular candidate is an interaction with electromagnetic ion cyclotron waves near the plasmapause (Ref. 4). There are difficulties with that mechanism -- it has not been thoroughly tested and confirmed. The difficulties have mostly to do with how waves generated by trapped ions can resonate with trapped electrons (Ref. 5); the cold plasma approximation breaks down and only very energetic electrons can be affected by the waves. It appears that other processes must be involved in both dayside relativistic precipitation events and quiet time diffusion. After major geomagnetic storms there seem to be processes that remove 1-3 MeV electrons, both inside the plasmasphere and far outside, with lifetimes of the order of 10 days (Ref. 6).

Assuming removal of relativistic electron by interactions with ion cyclotron waves probably gives the largest possible enhancement of relativistic electron fluxes. A pressing need remains for more research on loss mechanisms for energetic electrons.

REFERENCES

1. Chiu, Y.T., J.M. Cornwall, J.G. Luhman, and M. Schulz, The Aerospace Corporation, SSL-79 (7824)-1.

2. Sky and Telescope, 57, 444, May 1979 letters by P.E. Glaser, G.T. Davidson, A.T. Young.

3. Cornwall, J.M., M. Schulz, J. Geophys. Res., 76, 7791 (1971); correction, J. Geophys. Res., 78, 6830 (1973).

4. Thorne, R.M., and C.F. Kennel, J. Geophys. Res., 76, 4446, 1971.

5. Davidson, G.T., J. Atm. Terr. Phys., 40, 1087 (1978).

6. West, H.I., Jr., and G.T. Davidson; to be published.

U.S. GOVERNMENT PRINTING OFFICE: 1980-311-119/204

UNITED STATES
DEPARTMENT OF ENERGY
WASHINGTON, D.C. 20585